CONTRIBUTIONS TO TELOMERASE ANCHOR-SITE AND TEMPLATE/PRIMER ALIGNMENT FUNCTIONS BY YEAST TERT RESIDUE E76

By

Robin Christine Brooks Bairley

Dissertation

Submitted to the Faculty of the

Graduate School of Vanderbilt University

in partial fulfillment of the requirements

for the degree of

DOCTOR OF PHILOSOPHY

in

Biological Sciences

December, 2011

Nashville, Tennessee

Approved:

Professor Todd Graham

Professor Katherine Friedman

Professor Carl Johnson

Professor Kathy Gould

Professor David Cortez

ACKNOWLEDGEMENTS

Professionally, thanks go to: (1) College of Arts and Sciences' Department of Biological Sciences for accepting me into their graduate program; (2) Drs. Cortez, Graham (Chair), Gould, Friedman (Advisor), and Johnson for serving on my Committee; (3) Dr. Singleton and all the Directors of Graduate Studies I worked with as President of the Biological Sciences Graduate Student Association; (4) Dr. Baskauf, Dr. Bruff, Dr. Stassun, and the Center for Teaching for providing opportunities to develop my teaching skills; and (5) all the undergraduates who had me as their TA during my time here at Vanderbilt as their feedback and interactions made me a much better teacher.

My time here at Vanderbilt was funded by: (1) the Department of Biological Sciences Teaching Grant; (2) Vanderbilt University Pre-doctoral Cellular Biochemical and Molecular Science Training Grant; (3) Vanderbilt University Pre-doctoral Viruses, Nucleic Acids, and Cancer Training Grant; (4) the National Institute of Health; and (5) the National Science Foundation MCB-0721595.

Personally, thanks go to: (1) Alan and Braden Bairley; (2) the Brooks and Bairley clans; (3) my lab mates Dr. Jennell Talley, Jenifer Ferguson, Charlene Hawkins, Abigail Riddle, Margaret Platts, Dr. Laura Berchard, Udo Obodo, Gina Guillaume, Jessica Miles, and Dr. Hong Ji; (4) my friends Christina Williams, Kimberly Mulligan, Sydika Banks, and Dr. Karen Riggins; (5) Jonathan Ertelt and family; (6) the graduate student members of the Alliance of Cultural Diversity in Research; and lastly (7) the graduate student members of the Biological Sciences Graduate Student Association for their unwavering support and encouragement during my time here at Vanderbilt University.

TABLE OF CONTENTS

LIST OF TABLES

LIST OF FIGURES

CHAPTER I

INTRODUCTION

There are four major sections to this Chapter, starting with a Summary of the research that led to my published work (discussed in Chapter II). The rest of Chapter I covers three topics extensively: the Discovery of Telomeres and Telomerase, Regulation of Yeast Telomerase, and finally the Enzyme Characteristics.

Summary

Nearly all of the DNA contained in a eukaryotic, linear chromosome is duplicated by the conventional DNA replication machinery. However, a combination of chemical constraints on DNA replication and nucleolytic processing results in loss of the extreme 3' ends of chromosomes (telomeres). If these ends are not replenished, progressive shortening can result in cell cycle arrest, massive genomic instability, and ultimately cell death. To circumvent this end-replication problem, cells employ the enzyme telomerase, a specialized ribonucleoprotein (Greider and Blackburn, 1985) that extends the short 3' TG- rich overhangs of the telomere. Telomerase is minimally comprised of a catalytic subunit (**TE**lomerase **R**everse **T**ranscriptase; TERT) and an intrinsic RNA molecule containing the template for reverse transcription (**TE**lomerase **R**NA **C**omponent; TERC). Telomeric DNA consists of TG-rich repetitive sequences (Chan and Blackburn, 2004) that form the basis of telomeric chromatin by providing binding sites for proteins that serve to protect and monitor telomere integrity.

In contrast to human telomeres, which contain perfect TTAGGG repeats, the 300 +/- 50 bp *Saccharomyces cerevisiae* yeast telomeres contain heterogeneous $C_{1-3}A/TG_{1-3}$ tracts with a 3' TG-rich overhang (Shampay, Szostak and Blackburn, 1984). Heterogeneity is due in part to multiple registers of alignment between the RNA template and chromosome terminus (Teixeira et al., 2004). However, yeast telomerase still abides by specific rules that govern these alignments (Förstemann and Lingner, 2001). The N-terminal TEN domain of the telomerase catalytic subunit has been suggested to interact directly with the DNA substrate (the anchor-site interaction) and may contribute to binding and proper positioning of the DNA substrate with the RNA template (Autexier and Lue, 2006). How the anchor-site interaction may contribute to the actual telomere sequence is not understood. This understanding is critical because the ability of telomeres to protect chromosomes from degradation depends upon a host of proteins that bind the DNA in a sequence-specific manner. The heterogeneity of yeast telomeres makes yeast an attractive model system to explore this question.

S. cerevisiae telomerase consists of three EST proteins (Est1, Est2 and Est3) and the RNA *TLC1* (Lendvay et al., 1996; Singer and Gottschling, 1994). Est1p and Est3p are accessory proteins essential for *in vivo* activity (Lingner et al., 1997a). Est2p and *TLC1* comprise the catalytic core and are required for *in vitro* and *in vivo* activity (Lingner et al., 1997a). Est2p is the yeast TERT component and contains functional domains for DNA binding (anchor-site), RNA interaction, and reverse transcription (Lingner et al., 1997b; Livengood, Zaug and Cech, 2002; Lue, 2005). As the reverse transcriptase component, Est2p contains the active site of telomerase. Within the active site are three absolutely conserved aspartic acid residues (D530, D670 and D671 in yeast). Mutation of

any of these three residues results in telomere shortening, senescence and lack of *in vitro* binding activity to a telomeric DNA substrate (Lingner et al., 1997b). *TLC1* serves as a scaffold with non-overlapping binding sites for Est1p, Est2p and other regulatory proteins (Livengood, Zaug and Cech, 2002; Peterson et al., 2001; Seto et al., 1999).

The heterogeneity of the yeast telomere is generated, in part, by abortive template usage. The *TLC1* RNA template (3'-^{484}ACACACACCCACACCAC^{468}-5') interacts directly with the DNA substrate. During a single round of reverse transcription, wild-type telomerase generally aligns the 3' portion of the template region with the DNA substrate and reverse transcribes through the central ^{478}ACCCACA^{472}. This "core motif" is followed by reverse transcription through ^{471}CC^{470} approximately 50% of the time and occasionally (~10% of the time) the last two nucleotides of the template (^{469}AC^{468}) are included (Förstemann and Lingner, 2001; Ji et al., 2008). Portions of the template region can be altered without extensively compromising telomerase activity, although the newly synthesized telomeric repeats reflect the changes in the template (Förstemann and Lingner, 2001; Prescott and Blackburn, 1997b; Singer and Gottschling, 1994). The change in sequence can affect the binding of regulatory proteins to the telomere, which in turn affects telomere length and/or protection. (Prescott and Blackburn, 1997b).

Extension of the DNA substrate by telomerase involves DNA-protein interactions at the anchor-site, thought to lie within the TEN domain of TERT (Hammond, Lively and Cech, 1997; Lue, 2005; Wyatt, Lobb and Beattie, 2007). The anchor-site has a role in DNA substrate recognition and repeat addition processivity (translocation of telomerase along the DNA for multiple rounds of synthesis through the template without dissociating from the DNA) (Lue and Li, 2007). In a previous study, the *est2-LT^{E76K}* mutant, located

in the Est2p TEN domain, was found to cause a 100 base pair increase in the average telomere length and to alter the sequence of the telomere repeat (Ji et al., 2008; Ji et al., 2005). As the *est2-LT*^{E76K} increases repeat addition processivity *in vitro* (Ji et al., 2008; Lue and Li, 2007) and is located in the region of the protein implicated in anchor-site function, I hypothesized that *est2-LT*^{E76K} might bring about these phenotypic effects by altering interaction of the protein with the DNA substrate.

In this thesis (Chapter II), I show that the *est2-LT*^{E76K} mutation causes increased repeat addition processivity *in vivo* and alters the preferred site of alignment between the DNA substrate and the template. To test the hypothesis that the *est2-LT*^{E76K} allele alters interaction with the DNA primer, I tested the effect of this mutation on DNA binding. To this end, I developed an *in vitro* binding assay to demonstrate that the recombinant TEN domain of Est2p binds with sequence specificity to a single-stranded TG-rich oligonucleotide. The increased strength of the protein-DNA interaction correlates with altered primer/template alignment, increased processivity, and telomere over-elongation.

The remaining sections of this Chapter discuss the history of the telomerase field, introduce topics that are the basis of my published work, and lay the groundwork for the Discussion and Future Directions (Chapter III) components of this Thesis.

Discovery of telomeres and telomerase

In this section, I will discuss foundational discoveries from the McClintock and Blackburn labs. In work done during the 1930s and 1940s, Dr. McClintock discovered that the extreme chromosome ends (telomeres) had unique properties that protected the chromosome terminus from fusion with other chromosomes. Four decades later (1980s),

the Blackburn group found the enzyme responsible for the maintenance of the telomeres (telomerase) in the ciliate *Tetrahymena*. The remainder of this section focuses on the discovery of telomerase components in yeast *Saccharomyces cerevisiae*, spearheaded by Drs. Lundblad and Gottschling in the 1990s. The functional aspects of the yeast telomerase components are addressed at the end of this section.

History of telomeres

In the portion of her 1941 paper that is the most relevant to discovery of telomeres, Dr. McClintock describes what happens when recombination between a normal chromosome and its inverted homolog occurs during meiosis (McClintock, 1941). The resulting dicentric chromosome is broken during Anaphase I. The two sister chromatids fuse at the site of breakage. In the following division, separation of the two joined centromeres to opposite poles results in a chromatin bridge and the tension generated across this bridge results in a rupture of the chromosome. Her primary investigation addressed whether this "breakage-fusion-bridge" cycle would continue indefinitely or if the broken ends would become refractory to fusion at some point. Ultimately, she found that the breakage-fusion-bridge cycle continues if the chromosome is located in the primary endosperm nuclei (the triploid tissue of the kernel). However, if a similar broken chromosome is sent to the sperm or the egg, the ends no longer fuse. Furthermore, the healing events are permanent: those special ends no longer fuse with other broken sister chromatids regardless of what tissue in the maize plant the newly healed chromosomes ultimately inhabit.

To study the repair of broken chromosomes, Dr. McClintock focused on the short arm of chromosome 9. This chromosome contains the genes, in linear order, *Yg – C – Sh – Wx*, where *Wx* is closest to the centromere. Dr. McClintock used a plant heterozygous for a normal and a rearranged chromosome 9. Recombination would result in the generation of a dicentric chromosome. In Anaphase I of meiosis, the two centromeres move to opposite ends of the cell resulting in a random break. To phenotypically see if double stranded breaks occurred in the four genes listed above, it was necessary to backcross to recessive plants. When she crossed plants carrying this dicentric chromatid to a homozygous recessive plant (*yg c sh wx*), approximately 0.7 % of the total kernels analyzed presented variegated, or heterozygous, phenotypes indicative of chromosome breaks resulting in the loss of dominant gene(s).

About her results, Dr. McClintock remarked that "it will be necessary in the future to determine the nature of these conditions by experimental methods before an understanding can be attained of the factors responsible… for healing of broken ends" (McClintock, 1941). In maize, these *de novo* events in embryo cells are known today to be due to tissue-specific differences in telomerase expression (de Lange, Blackburn and Lundblad, 2006). Telomerase, the enzyme responsible for telomere maintenance, was discovered from the instrumental work headed by Dr. Blackburn four decades after Dr. McClintock's 1941 paper.

Discovery of telomerase

By the 1980s, it was clear that the end portion of linear DNA had special non-recombinogenic properties that were important for genome stability and cellular survival.

The mechanism of replication of the extreme chromosome ends remained unclear due to a lack of suitable *in vivo* techniques. Dr. Blackburn hypothesized that an unknown terminal transferase activity was responsible for the maintenance of the extreme chromosome ends based upon the following criterion. First, a minichromosome containing the *Tetrahymena* rDNA was heterogeneous in length and new terminal sequences could be added to *Tetrahymena* rDNA minichromosomes during somatic development. Second, Dr. McClintock told Dr. Blackburn about a maize mutant that had lost the ability to heal broken chromosome ends early in the plant's development (de Lange, Blackburn and Lundblad, 2006), suggestive of the loss of a specific enzymatic activity. Most importantly, in 1982, Szostak and Blackburn showed that linear plasmids with terminal fragments of *Tetrahymena* rDNA minichromosome could be elongated after repeated rounds of replication in yeast. The DNA from these elongation events was characteristic of yeast telomeres, not ciliates (Szostak and Blackburn, 1982). The DNA sequences yeast added onto the ends of the *Tetrahymena* linear plasmid were irregular $G_{1\text{-}3}T$ yeast telomere repeats as opposed to the perfect $(TTGGGG)_n$ *Tetrahymena* telomeric repeats (Shampay, Szostak and Blackburn, 1984). Such species-specific addition was inconsistent with a self-templated (foldback) mechanism of telomere elongation and was consistent with the existence of a telomere terminal transferase.

In 1985, Greider and Blackburn published the initial finding of a specific telomere terminal transferase activity in cell-free extracts from *Tetrahymena* macronuclei (Greider and Blackburn, 1985). Briefly, they mixed a single-stranded *Tetrahymena* telomeric primer $d(TTGGGG)_4$ with crude cell free extracts, and various combinations of radiolabeled and cold dNTPs. DNA was purified from the reaction mixture and separated

on a sequencing gel. Reactions generated a discrete 6-base repeating band pattern. The only dNTPs required were dGTP and dTTP, consistent with the known telomeric sequence. A non-telomeric primer did not result in the ladder of repeats and the pattern generated was distinct from that of *E. coli* DNA polymerase I. This assay, known today as the direct *in vitro* telomerase activity (or extension) assay, demonstrated that crude extracts contain a specific telomere elongation activity that could only extend TG-rich telomeric substrates (Greider and Blackburn, 1987).

Heat denaturation as well as the addition of proteinase K inhibited the reaction, supporting the idea that an enzyme was responsible for the activity (Greider and Blackburn, 1985). Further biochemical studies were published in 1987 (Greider and Blackburn, 1987). Gel filtration chromatography eluted the enzymatic activity described above in the 200-500 kDa range. Pre-treatment of the elutions with RNase A abolished the activity, suggesting that the enzyme was a large complex containing a nucleic acid component.

As a result of the biochemical studies on the *Tetrahymena* enzyme, in 1989, the *Tetrahymena* telomerase RNA component was cloned (Greider and Blackburn, 1989). During this same time frame, telomerase activities were discovered and characterized in *Oxytricha* (1986) (Gottschling and Zakian, 1986), *Homo sapiens* (1989) (Morin, 1989), *Euplotes* (1990) (Price, 1990), and *Arabidopsis* plants (1999) (Fitzgerald et al., 1999).

The *Saccharomyces cerevisiae* telomerase complex.

As the model system used in this thesis is the yeast *S. cerevisiae*, this section will describe the initial discovery of the yeast telomerase components in two parts: the initial

discovery of each telomerase protein component and the known functions of each telomerase component.

Initial discoveries of Est1p, Est2p, Est3p, Est4p and *TLC1*

In 1989, Drs. Lundblad and Szostak devised a screen that they hoped would identify components of the yeast telomerase enzyme (Lundblad and Szostak, 1989). Because telomere shortening per se is not a phenotype that could be easily screened in large numbers, the authors designed a clever plasmid-linearization assay to identify mutants defective for telomere maintenance or function. Briefly, a yeast strain (*leu2*, *ura3*) transformed with a *LEU2* plasmid containing inverted *Tetrahymena* telomeric repeats separated by a *URA3* gene was mutagenized. Selection for growth on media lacking leucine and containing 5-fluoroorotic acid (5-FOA; selects against retention of the *URA3* gene) resulted in a low, but reproducible rate of formation of a linear plasmid with telomeric repeats on either end. Mutants were isolated that were unable to create/maintain the linear plasmid. One of these alleles demonstrated progressive telomere shortening and a senescence phenotype indicative of the inability to maintain the linear plasmid. Deletion of the gene responsible for the above phenotypes, *EST1* (**E**ver **S**horter **T**elomeres) also caused chromosome instability, a phenotype that the authors used to their advantage in a second EST screen in 1996.

EST2, *EST3* and *EST4* (subsequently found to be *CDC13*) were isolated from the second EST screen. Telomere length analysis of individual *est* mutants showed that telomeres were shortened to the same extent as *est1Δ* alone. Analysis of a strain deleted

for all four EST genes showed that the effects were not additive, suggesting these genes act in the same telomere maintenance pathway (Lendvay et al., 1996).

In the meantime, the RNA component was identified. *TLC1* RNA was discovered in 1994 by the Gottschling lab in an over-expression screen for genes that disrupt the silencing of genes located near the telomere (the telomere position effect - TPE) (Singer and Gottschling, 1994). Subsequent sequence analysis identified *TLC1* as a non-translated RNA containing a motif predicted to template *S. cerevisiae* telomeres. To test if *TLC1* was the telomerase RNA, the authors mutated the template to incorporate a *Hae III* restriction enzyme cut site, and found that newly synthesized telomeres obtained this nucleotide change. Double mutants of all the Est proteins and *TLC1* resulted in the same short telomere phenotype and cellular senescence (Lendvay et al., 1996). These data suggest the Est proteins work in the same pathway as *TLC1* for telomere length maintenance.

To summarize, there are three essential *EST* genes [see Figure 1.1; *EST4* was subsequently shown to be *CDC13* (Nugent et al., 1996)]. When disrupted, each displays the same phenotypes as a disruption of *TLC1*, suggesting they all are important for telomerase function. Numerous labs have since contributed information on the function(s) of the yeast telomerase components, which are discussed below.

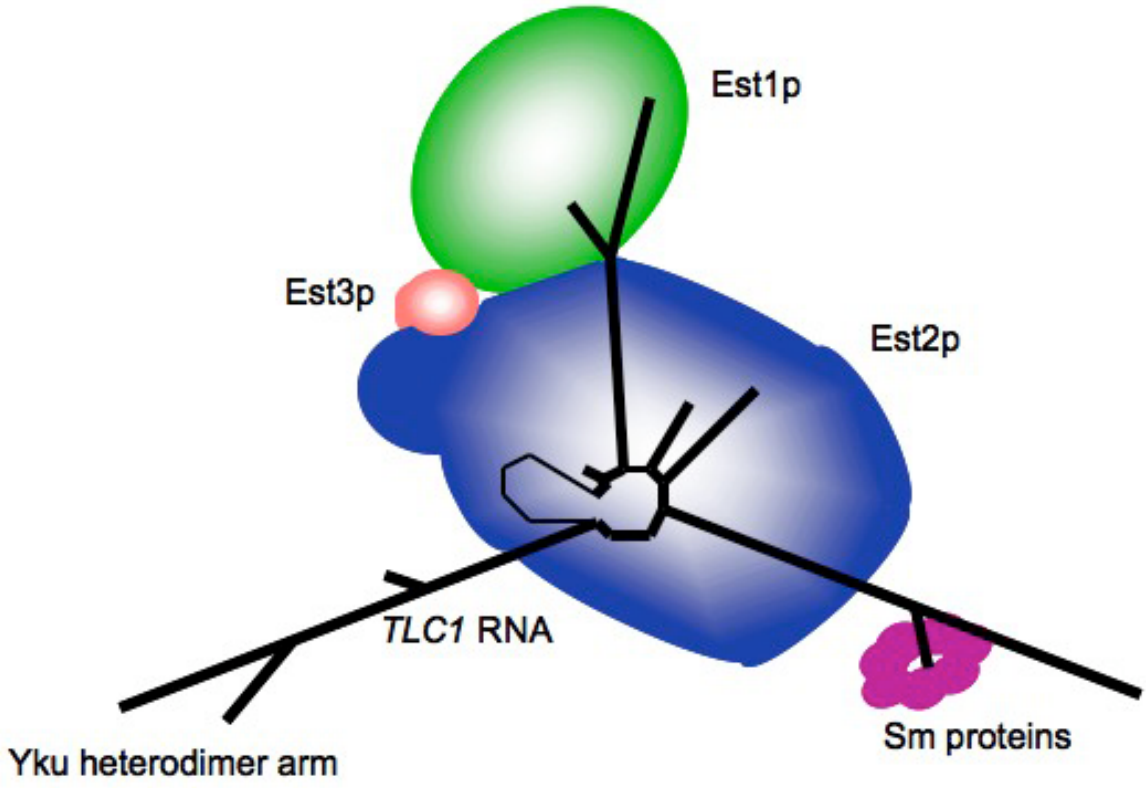

Figure 1.1: Active yeast telomerase complex components. Active yeast telomerase consists of three essential EST proteins (Est1p - green, Est2p - blue, and Est3p – light pink) and the *TLC1* RNA – solid black. Most of the RNA consists of paired stems, but the bulge and hairpin structures are not shown in this model. The single stranded template is depicted as a thin black line. *TLC1* is a scaffold with binding sites for the Sm proteins (magenta), Est1p, Est2p and yKu (not depicted). Est2p is the catalytic subunit and Est1p and Est3p are accessory proteins necessary for *in vivo* activity. Modified from (Hug and Lingner, 2006).

Characterization of each component from the time of discovery

As suggested by Figure 1, Est1p, Est2p and Est3p are integral subunits of the telomerase enzyme. Est2p synthesizes new telomeric DNA by reverse transcription of the template in *TLC1*. Est1p and Est3p are *in vivo* regulatory components. Est3p is the last known component to be recruited to the complex, possibly, activating telomerase. Cdc13p recruits the telomerase complex to the 3' single-stranded TG-rich overhang of the telomere through direct interactions with Est1p. The discovery of these main functions for each of the telomerase components is discussed below.

***CDC13* (Homologs- mammalian and plant CTC1)**

The 105 kDa Cdc13p plays multiple roles in coordinating events at the 3' terminus. Cdc13p's DNA binding domain (residues 557-694 of the 924 amino acid protein) requires a minimum of 11 nucleotides for high affinity binding to single-stranded TG-rich DNA (Ka ~ 0.37 nM) (Hughes et al., 2000b; Lin and Zakian, 1996). The DNA binding domain has an OB fold structure (Mitton-Fry et al., 2002) with a high degree of structural similarity to that of *Oxytricha*'s TEBP protein and the mammalian POT1 protein (Horvath and Schultz, 2001; Horvath et al., 1998). POT1 is part of the Shelterin complex and has important roles in the mammalian telosome for telomere end protection. Cdc13p, in a complex with Stn1p and Ten1p (CST), is an important part of the yeast telosome (covered in more detail under **Enzyme Characteristics**).

Further characterization of Est4p from the Lundblad 1996 EST screen (Lendvay et al., 1996) showed that the *est4-1* allele was a mutation of *CDC13*, hereafter referred to as *cdc13-2*^{est} (Nugent et al., 1996). Comparison of the phenotypes of *cdc13-2*^{est} and

cdc13-1^{ts} strains suggested that Cdc13p has at least two functions at the telomere. The *cdc13-1*^{ts} allele was previously found to be impaired in telomere end protection as evidenced by the rapid loss of the CA-rich strand at the non-permissive temperature (Garvik, Carson and Hartwell, 1995). The *cdc13-2*^{est} allele had none of the conditional lethality, or cell cycle arrests phenotypes associated with a *cdc13-1*^{ts} strain. Therefore, Cdc13p was suggested to have roles in telomerase function as well as end protection.

An understanding of the role played by Cdc13p in telomerase function came from genetic studies of the *cdc13-2*^{est} allele. The *est1-60* allele was isolated as a charge swap reciprocal suppressor of *cdc13-2*^{est} (Pennock, Buckley and Lundblad, 2001), suggesting a physical interaction between these two proteins. Fusion of the DNA binding domain of Cdc13p to Est1 ($Cdc13_{DBD}$-Est1) rescued telomere shortening in an *est1*Δ and *cdc13-2*^{est} backgrounds. In fact, telomeres are extensively elongated with the $Cdc13_{DBD}$-Est1 fusion protein (in the presence of functional telomerase). Furthermore, fusion of Cdc13p to Est2p (Cdc13-Est2) bypassed the requirement of Est1p (Evans and Lundblad, 1999). These data support the hypothesis that the telomerase function of Cdc13p involves recruitment of telomerase to telomeres.

End protection at the single-stranded overhang occurs by the Cdc13-Stn1-Ten1 (CST) complex. Over-expression of *TEN1* and a C-terminal truncated *STN1* can bypass the lethal phenotype of a *cdc13*Δ strain, resulting in long, heterogeneous telomeres (Petreaca et al., 2006). As expected, fusion of the Cdc13p DNA binding domain to *STN1* ($Cdc13_{DBD}$-Stn1) rescued the lethality of *cdc13*Δ, but was incapable of rescuing the telomere shortening in a *cdc13*Δ strain. However, the expression of the $Cdc13_{DBD}$-Est1 along with the $Cdc13_{DBD}$-Stn1 fusion resulted in extensive telomere lengthening

(Pennock, Buckley and Lundblad, 2001), showcasing both end protection and telomerase functions of Cdc13p. These data also support the idea that Cdc13p's only role is to recruit these other proteins to the telomeric DNA.

Phosphorylation of Cdc13p is suggested to contribute to its telomeric functions. The Teng lab published in 2006 that the Tel1p and Mec1p kinases can phosphorylate Cdc13p at serines 225, 249, and 255 (Tseng, Lin and Teng, 2006). However, the Lundblad lab published a paper in 2010 that showed that the absence of Tel1p did not alter the mobility shifts of wild-type Cdc13p phospho-isoforms (Gao et al., 2010). A yeast proteome-wide screen for kinase targets of Te1lp and Mec1p did not identify Cdc13p. The screen detected 18% of the total proteome as potential Tel1/Mec1 phosphorylated proteins and included proteins normally present at less than 1000 copies per cell (Smolka et al., 2007). Cdc13p is present at approximately 319 molecules per cell (Cherry et al., 1997), so their screen may have been sensitive enough to identify Cdc13p if indeed Cdc13p is a target.

The Blackburn lab instead proposed that Cdc13p is phosphorylated by Cdk1 (Li et al., 2009). Cdk1 (also called Cdc28) is the budding yeast cyclin-dependent kinase. Cdc13p is phosphorylated at T308 by Cdk1 *in vivo* and *in vitro*. Both Est1 and Est2 protein levels are reduced at telomeres in the $cdc13^{T308A}$ background by ChIP. However, this post-translational modification of Cdc13p is not essential as cells have short but stable telomeres in the absence of this phosphorylation.

Overall, Cdc13p binds to ssDNA to facilitate end protection and recruitment of telomerase. Recent work suggests that phosphorylated Cdc13p may play a part in the

recruitment function. The role of the CST complex for end protection is discussed in greater detail under **Enzyme Characteristics**.

EST1 (Homologs – mammalian EST1A and EST1B)

A function of the 82 kDa Est1 protein is to recruit an active telomerase complex to the telomere by interacting with Cdc13p (discussed above). Chromatin Immunoprecipitation (ChIP) studies, that address the association of telomerase components with telomeric DNA during the cell cycle, suggest that the activation of the telomerase complex is mediated (or effected) through Est1p's recruitment of Est3p. The Zakian lab showed Est1p and Cdc13p bind to telomeres preferentially in late S phase. Est2p had two peaks of interaction: G1 and late S-phase. In a *cdc13-2*^{est} background, Est2p still binds telomeres in G1 phase, but binding is reduced in late S phase. Est1p late S phase association was also reduced in the *cdc13-2*^{est} background. Furthermore, the association of Est1p with telomeres requires Est2p, and Est2p requires Est1p that is capable of interacting with *TLC1* for both proteins to associate with telomeres in late S phase (Chan, Boulé and Zakian, 2008). Est3p has recently been shown to directly interact with Est1p *in vitro* and to require Est1p for its interaction with telomeres in late S phase (Tuzon et al., 2011). All together, these data suggest that the telomerase complex is assembled off the telomere, activated by the addition of Est3p binding, and is then recruited by Cdc13p to the ssDNA overhang (see Figure 1.2).

Est1p's recruitment of telomerase to telomeres requires contributions of yKu80/70 heterodimer, Tel1p, Mre11p, and RPA (a non-specific DNA binding protein). yKu associates with double-stranded telomeric DNA throughout the cell cycle. ChIP

studies suggested that normal levels of Est1p and Est2p association with telomeres in G1 and late S phase relied on the Ku-*TLC1* interaction (Fisher, Taggart and Zakian, 2004). Using ChIP followed by real-time PCR, the Zakian lab found no Est2p association and very little association of Est1p was seen during late S phase in either a *tel1*Δ or *mre11*Δ background (Goudsouzian, Tuzon and Zakian, 2006). Loss of Rfa2, a subunit of RPA, diminished Est1p telomere binding in late S-phase whereas Cdc13p and Est2p retained normal telomere association (Schramke et al., 2004).

In summary, Est1p facilitates the assembly of Est2p and Est3p into a complex with *TLC1*. yKu Tel1p, Mre11p, and RPA contribute to Est1p's recruitment function. The Est1p-Est3p interaction is further discussed in Section 2C-ii d. In support of Est1p's activation role, the Freeman lab has shown addition of recombinant Est1p can stimulate telomerase activity *in vitro* (DeZwaan et al., 2009; DeZwann and Freeman, 2009).

TLC1 (Homologs – the other TERC components)

At first glance, the telomerase RNA components (TERC) from different organisms appear to share only the template region, which contains sequences complementary to the telomeric repeat. They differ markedly in size and, as expected for an RNA molecule, the nucleotide sequence is not easily aligned. However, secondary structure models comparing TERC from diverse species revels important structural similarities despite being unique in size. All TERCs have a template domain consisting of a pseudoknot structure, an unpaired template region and a 5' template boundary. The pseudoknot is important for the positioning of the RNA template in the catalytic pocket of TERT. All TERC templates are single-stranded and contain complementarity to approximately 1.5

telomeric repeats. The 5' boundary element is important for preventing reverse transcription past the end of the template (de Lange, Blackburn and Lundblad, 2006).

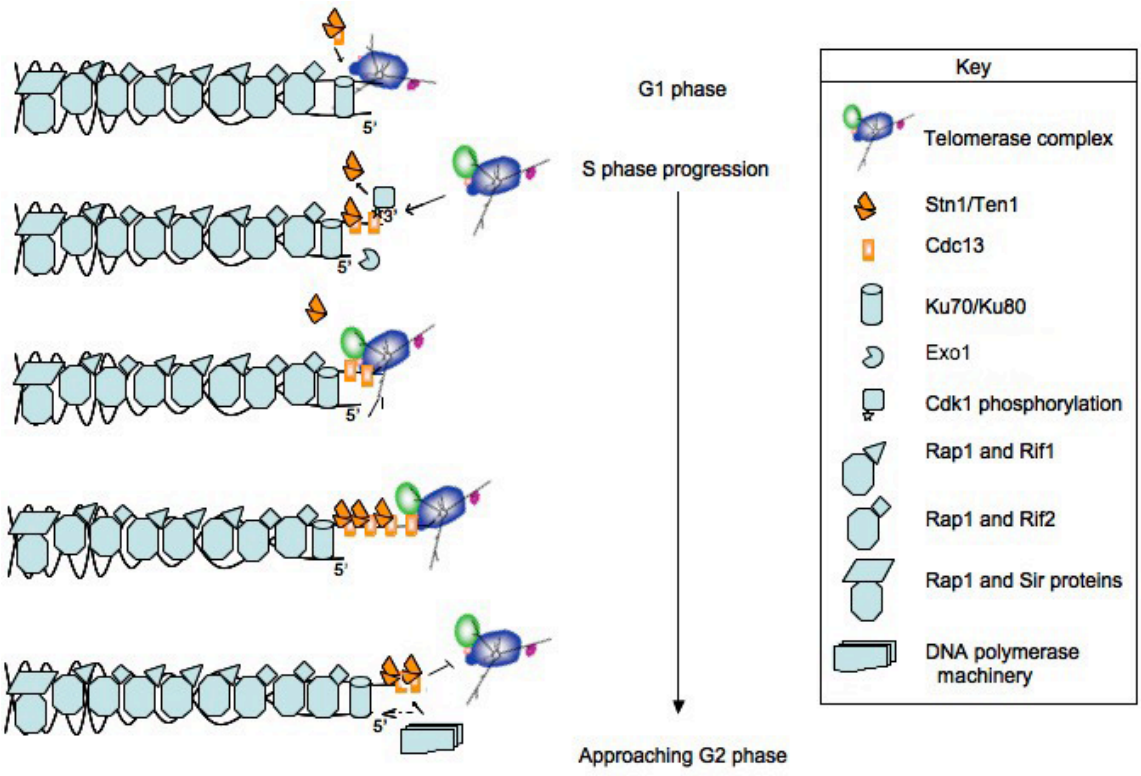

Figure 1.2: Cell cycle regulated telomere extension. In G1 phase, Rap1p and associating factors as well as the yKu heterodimer are found at the telomere. Est2p and very small amounts of Est3p are present in a *TLC1*-yKU dependent manner. By mid S-phase the known telomerase components are assembled and the complex is in its active state. Exo-nucleases (such as *EXO1*) process the 5' end (for the leading strand). Cdk1 phosphorylation of Cdc13p may facilitate the recruitment of telomerase to Cdc13p by aiding in the removal of Stn1/Ten1 for Cdc13's association with Est1p. Rif2 protein levels have decreased, and are sensed by Tel1p, marking the shortest telomeres for extension. By late S phase, telomerase has extended the 3' overhang by reverse transcription and is inhibited from further telomere extension by the CST complex (Pif1p removal of telomerase occurs on the lagging strand; not shown here) as cells approach G2 phase. The DNA replication machinery fills in the 5' gap. The CST complex protects the remaining 3' overhang and Rap1/Rif1/Rif2 protect the double stranded portion. Not all proteins involved in this process are shown for simplicity. See text for further details.

Much research has been focused on specific structures and functions of the *S. cerevisiae TLC1* RNA. After the identification of *TLC1* (Singer and Gottschling, 1994), the Blackburn lab defined the template residues of *TLC1* in a 1997 paper by making block mutations in and around the putative template (creating *Apa LI* restriction enzyme cut-sites) and assaying the *in vitro* activity of each mutant. Only those mutants that altered the residues within the sequence 3'-^{484}ACACACACCCACACCAC^{468}-5 could extend a primer with *Apa LI* sites (Prescott and Blackburn, 1997b). Within the template, there is a 3' alignment region used for RNA template base-pairing with the DNA substrate. The Lingner lab defined the 3' alignment region for wild-type *TLC1* (Förstemann and Lingner, 2001) and I have shown in my published work that a mutant of Est2p, *est2-LT^{E76K}*, alters the preferred 3' alignment site (Bairley et al., 2011). During synthesis, wild-type telomerase maintains a seven to eight base pair RNA template/DNA substrate hybrid as shown from dimethyl sulfate modification protection of *in vitro* reactions (Förstemann and Lingner, 2005). However, telomerase can utilize substrates with as little as three base pairs of homology to the template *in vivo* and *in vitro* (Lue, 2005; Stellwagen et al., 2003).

TLC1 RNA is transcribed by RNA polymerase II and a polyadenylated form is processed to produce the mature RNA. The mature *TLC1* [poly(A)$^-$] has a 5' trimethylguanosine (TMG) cap and binding sites near the 3' end for Sm proteins (residues 1127-1158). The Sm proteins are required for maturation as only the immature poly(A)$^+$ form was visible by Northern Blotting in a strain lacking the *TLC1* Sm binding sites. Mutating the Sm binding site resulted in delayed growth, barely detectible levels of *TLC1* by Northern blotting, and short telomeres. Immunoprecipitations of Smd1p (a Sm

protein) resulted in detectible telomerase activity *in vitro* (Seto et al., 2002; Seto et al., 1999), suggesting yeast telomerase associated with Smd1p has enzymatic activity. The requirement for an ribonucleoprotein (RNP) particle of some sort is evolutionarily conserved. In humans, small nucleolar ribonucleoproteins (snoRNPs) associate with the TERC and dyskerin telomerase components. Mutations in these components are involved in development of dyskeratosis congenita, a disease whose major cause is defective telomere maintenance (Kiss, 2002).

TLC1 also functions as a scaffold for protein binding. Several labs identified the pseudoknot for binding Est2p (residues 728-864) and a 5 nucleotide bulged-stem-loop (between residues 535-707) as the Est1p binding site (Chappell and Lundblad, 2004; Livengood, Zaug and Cech, 2002; Seto et al., 2002). The Gottschling and Zakian labs showed *TLC1* has a 48-nucleotide (48-nt) stem-loop, residues 273-344, for binding the yKu70/yKu80 heterodimer (Fisher, Taggart and Zakian, 2004; Peterson et al., 2001; Stellwagen et al., 2003).

TLC1, at approximately 1300 nucleotides, is much larger than other TERC components (i.e. approximately 150 nucleotides in ciliates and 500 nucleotides in vertebrates) (de Lange, Blackburn and Lundblad, 2006). Full length *TLC1* cannot be functionally produced in rabbit reticulocyte lysate (RRL). Engineered miniature forms of *TLC1*, Mini T (500) and Mini T (384), can be reconstituted in RRL. Mini T (500) and Mini T (384) retain all of the protein binding elements discussed above but telomeres are stably short. Micro T (170) only has the template and pseudoknot and is active *in vitro* when assembled with Est2p in RRL (Qiao and Cech, 2008; Zappulla, Goodrich and Cech,

2005). These data suggest that while most of *TLC1* is dispensable for *in vitro* activity, the protein binding sites and the intervening nucleotides are important for *in vivo* function.

Through the use of heterokaryons, over-expressed *TLC1* was shown to be capable of migrating from one nucleus to another, suggesting that an import and export pathway must exist (Teixeira et al., 2002). The Chartrand lab published that endogenous *TLC1* is exported through the Crm1p pathway (the main export pathway for non-coding RNAs in yeast) and imported by Mtr10p and Kap122p. Additionally, loss of any Est protein (Est1-3) or yKu resulted in cytoplasmic accumulation of endogenous *TLC1*, suggesting that stable nuclear localization requires the assembly of the telomerase complex and association with the telomere (Gallardo et al., 2008).

In conclusion, *TLC1* is documented as the first snRNA to be involved in DNA replication. Several labs show that *TLC1* is a scaffold containing separate binding sites for Est1p, Est2p, yKu, and the Sm proteins. There is no evidence that Est3p directly interacts with *TLC1*. The telomerase protein components are important for the nuclear *TLC1* trafficking.

EST2 **(Homologs – the other TERT components)**

As described above, *EST2* (encoding a 102 kDa protein) was first identified in a screen for yeast mutants that cause progressive telomere shortening (Lendvay et al., 1996). In parallel with this genetic work, purification of telomerase activity from the ciliate *Euplotes aediculatus* led to the identification of a 123 kDa protein and cloning of the corresponding gene by reverse genetic approaches. A BLAST search of protein databases showed that p123 was the most similar to *S. cerevisiae* Est2p and comparative alignments

revealed similarity with known reverse transcriptases, including the absolute conservation of three aspartic acid residues in the reverse transcriptase domain (RT) of both p123 and Est2p (Lingner et al., 1997b). An evolutionary based study showed that the RT domain motifs (named 1, 2, A, B', C, D, and E) of telomerase complexes from *Euplotes* p123, *S. cerevisiae* Est2p, *S. pombe* Trt1p and human TERT were conserved (Nakamura et al., 1997).

The RT domain has since been shown to contain a conserved IFD (**I**nsertion in **F**ingers **D**omain) motif located between A and B'(Lue, Lin and Mian, 2003) as well as a semi-conserved motif 3 located between motifs 2 and A (Xie et al., 2010). The IFD motif is required for normal telomere maintenance *in vivo* as mutants reduced association of Est2p with *TLC1*. Optimal telomerase activity and repeat addition processivity (the ability of the enzyme to synthesize multiple template repeats on the same substrate without dissociation) is disrupted with IFD mutants as well (Lue, Lin and Mian, 2003). Motif 3 was identified in human cells and was shown to be important for repeat addition processivity and effects telomerase activity (Xie et al., 2010).

An N-terminal extension domain is separated from the RT domain by a flexible linker, as suggested by modeling of human TERT (Steczkiewicz et al., 2011). With only four homologs, there was little obvious sequence homology in the N-terminal region beyond the T motif (Nakamura et al., 1997). To further explore the N-terminal extension in yeast, Dr. Friedman tested a combination of deletion and single amino acid mutations to identify three essential regions of Est2p named Region I (now called the TEN domain), II, and III (Friedman and Cech, 1999). In a later publication, she showed that over-expression of Est3p could rescue temperature-sensitive mutants in Region I (but not

Regions II or III), suggesting a function of the TEN domain is to recruit Est3p to the complex (Friedman et al., 2003).

Another function of the TEN domain is to interact with the DNA substrate through the anchor-site. Initial studies from the Lue lab showed that a recombinant protein fragment containing the yeast TEN domain (also called Region I or GQ) of Est2p tagged with MBP (MBP-Est2$^{1\text{-}160}$p) bound *TLC1* with an affinity of 5 μM. They also conducted a nucleotide binding competition experiment with the RNA-bound MBP-Est2$^{1\text{-}160}$p and various DNA substrates. All of the competitors reduced the RNA/MBP-Est2$^{1\text{-}160}$p binding by about 60%, suggesting that MBP-Est2$^{1\text{-}160}$p binds non-specifically to nucleotides as assayed by filter binding. The RNA binding activity was further shown to require the first 50 amino acids within the N-terminus of Est2p, suggesting the first 50 amino acids contributes to the non-specific nucleic acid binding (Xia et al., 2000).

Using *Tetrahymena*, the Cech lab identified a soluble portion of the TEN domain (Jacobs et al., 2005), and published the first partial crystal structure of a telomerase component with this protein fragment in 2006. To validate the structural information, several site-directed mutants were purified and analyzed for *in vitro* telomerase activity. Some of the TEN domain mutants with low *in vitro* activity were also deficient for their ability to photo-cross-link to *Tetrahymenia* telomeric DNA oligonucleotides *in vitro*. Using nitrocellulose filter binding assays, the *Tetrahymena* TEN domain bound TERC in a non-sequence specific manner. This technique did not reveal binding to single-stranded telomeric DNA (Jacobs, Podell and Cech, 2006). As discussed further in Section 4C, recent work from *Tetrahymena*, human and yeast studies have established that the TEN domain contains the anchor-site function of DNA binding.

Also within the N-terminal extension is the telomerase RNA binding domain (TRBD). TRBD is minimally comprised of the T and CP motifs (Bryan, Goodrich and Cech, 2000). In ciliates and humans, there is another more N-terminal motif (RID1) that makes important contacts with a stem loop adjacent to the template region of TERC (O'Connor, Lai and Collins, 2005). Crystal structure analysis of the TRBD from *Tetrahymena* revealed that the T motif is in the center of the molecule and forms a mostly hydrophobic pocket that is linked to the CP motif through a hydrophilic interface. The CP motif creates a shallow, but wide (20°A) pocket that is highly charged and located just below the entrance to the T motif pocket. The intervening amino acids are mostly charged residues that could make direct contacts with the stem loop of TERC as described above (Rouda and Skordalakes, 2007).

On the C-terminal side of the RT domain, is the conserved C-terminal extension (CTE) domain. As shown in *S. cerevisiae*, recombinant CTE domain can bind single- and double-stranded telomeric DNA *in vitro*. But unlike the TEN domain, the CTE has a higher affinity for double-stranded telomeric DNA. Complete loss of or mutation in conserved residues of the CTE domain reduced the stability of telomerase-DNA interactions and affected both telomerase activity and processivity as shown by *in vitro* telomerase activity assays (Hossain, Singh and Lue, 2002). However, deletion of the entire CTE domain results in short, stable telomeres and cells don't senesce (Friedman and Cech, 1999). These data suggest the CTE domain contributes to overall enzymatic activity, but is not essential.

Crystal structure analysis on full length TERT from *Tribolium* (naturally has no TEN domain) showed the TRBD, RT, and the CTE domains arranged to create a hole in

the interior of the protein that is large enough to accommodate seven to eight bases of double-stranded nucleic acids (Gillis, Schuller and Skordalakes, 2008). This number is significant as yeast telomerase prefers to maintain a RNA template/DNA substrate hybrid of similar length *in vitro* (Förstemann and Lingner, 2005), suggesting the shape of the hole could be evolutionarily conserved. The structure of TERT from *Tribolium* with the RNA-DNA heteroduplex is organized into the same ring form as the substrate free one. Interestingly, there was only a slight conformational change of the structure with the addition of the RNA-DNA substrate. The authors suggested that perhaps the substrate-free structure was trapped in the "closed" state or the enzyme could just have a "pre-formed active site" (Mitchell et al., 2010).

Spatial information on the TEN domain in the context of TERT can be obtained from a theoretical model of human TERT (minus the CTE domain) with an RNA-DNA heteroduplex (see Figure 1.3). The modeling was done by using distant homology detection; comparative structural modeling from full-length TERT (with and without the RNA/DNA substrate) crystal structures from *Tribloium*, the TEN and TRBD crystal structures from *Tetrahymena*; computational docking and elastic network models. Their model shows the TEN domain is linked to the rest of the ring-shaped protein by an unstructured region. The surface of the TEN domain is shaped like a cleft that could accommodate single-stranded nucleotides. Given the shape of the TEN domain, the authors suggested the TEN domain orientation and positioning was probably restricted in terms of movement (Steczkiewicz et al., 2011). Their modeling gives very strong support for the TEN domain acting as a stabilizer of the RNA-DNA heteroduplex during reverse transcription.

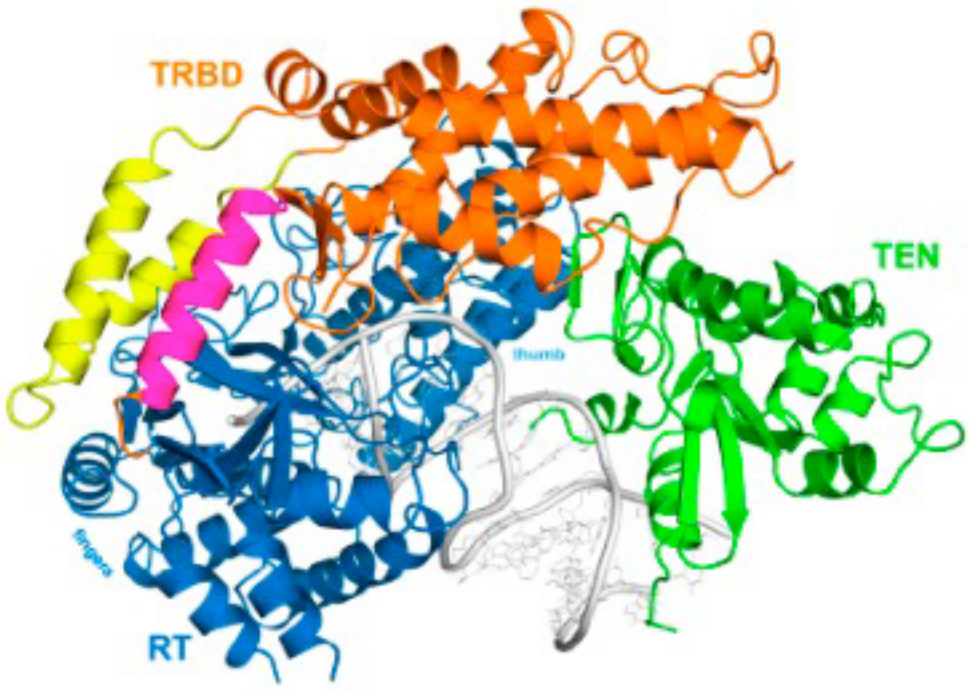

Figure 1.3: Partial model of human TERT interacting with an RNA/DNA heteroduplex (in gray). This model is generated based on homology with the *T. thermophila* and *T. castaneum* proteins for which partial crystal structures are available. TEN domain – green; TRBD – orange; last helix in TRBD plus 2 additional helices not present in species lacking the TEN domain – purple and yellow respectfully; RT – blue. The CTE (C-terminal extension) is not included in this model. Modified from (Steczkiewicz et al., 2011)

To summarize, Est2p is a reverse transcriptase and shares homology with other TERT proteins. Est2p has four main functional domains. The TEN domain interacts genetically and physically with Est3p (discussed below), and has been hypothesized to function as the anchor-site of telomerase (see **Enzyme characteristics**) for a more

detailed discussion). TRBD makes important contacts with TERC that are required for reverse transcription. The RT domain is necessary for catalytic activity and the CTE domain aids in repeat addition processivity and makes contacts with the double-stranded DNA.

EST3 (Potential homolog – TPP1)

EST3 lacks a large open reading frame (ORF) and instead has two smaller ORFs in different frames (Morris and Lundblad, 1997). Translation of the first ORF produces a 93 amino acid product that does not appear to have a function in telomerase or elsewhere. A functional 181 amino acid product is produced by a programmed translational frameshift. The Lundblad lab constructed an *EST3-fsc* allele (frame shift corrected; makes the 181 amino acid product). This allele was fully functional in its ability to complement telomere length and senescence in an *est3*Δ background. When comparing the protein levels from full-length *EST3* versus the *EST3-fsc* under the control of an *ADH1* promoter in a Gal4 fusion assay, the full-length Gal4–Est3 protein was 75–90% as abundant as the Gal4–Est3-fsc protein. In unpublished experiments, I have also observed that epitope-tagged frame-shift corrected protein is expressed at a higher level than the non-frameshift corrected protein by Western Blotting (see Figure 1.4).

The 18 kDa Est3 protein is the last known component to be recruited to the telomerase complex, suggesting an activation of telomerase function. How Est3p is recruited to the complex is still under debate. The Lundblad lab has observed that Est3p retains the ability to co-immunoprecipitate with *TLC1* when Est1p is deleted, but association is lost in an *est2*Δ background (Hughes et al., 2000a).

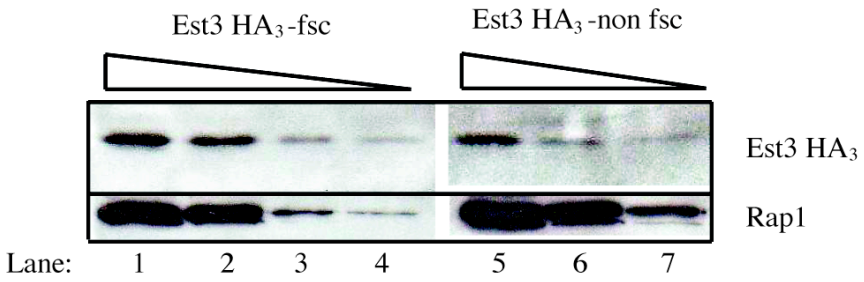

Figure 1.4: Frame shift corrected Est3p is expressed at higher levels than non-frame shift corrected Est3p. Cellular extracts were isolated from cells expressing HA-tagged Est3p [frame shift corrected (lanes 1-4) or non-frame shift corrected (lanes 5-7)]. Initial protein concentrations were normalized and four fold serial dilutions were separated in a 10% SDS-PAGE gel. The protein was wet transferred to a PVDF membrane and probed with antibodies specific to the HA epitope tag and to Rap1p (loading control).

In contrast, the Friedman lab has observed by co-immunoprecipitation experiments that Est2p and Est3p do not associate in an *est1*Δ background. Furthermore, a *TLC1* allele deleted for the region necessary for Est1p binding, *tlc1Δ 535-770*, does not associate with Est3p. Co-immunoprecipitation of epitope-tagged proteins showed that Est1 protein levels are very low in cells arrested in G1 phase, but increase in G2 phase when telomerase is active. When Est1p is over-expressed in cells blocked in G1 phase, Est3p associates with the complex in G1, suggesting that Est1 protein levels are the limiting factor for Est3p association with the complex (Osterhage, Talley and Friedman, 2006).

Using an RNA mutant deleted for the 5-nt bulge on the stem loop required for Est1p association (Chappell and Lundblad, 2004), *tlc1-47*, and the *tlc1Δ 535-770* allele the Lundblad lab came to the opposite conclusion in 2009 (Lee et al., 2010). These two results could be due to a difference in the stringency of the immunoprecipitation protocols used for the two experiments. One way to reconcile these differences is to repeat the Est3p co-immunoprecipitation of *TLC1* in G1 phase-blocked cells. If Est3p does not require Est1p to associate with *TLC1*, then association of Est3p with *TLC1* should not be altered during G1 phase.

Recently, purified recombinant Est1p and Est3p were shown to interact directly *in vitro*. Furthermore, association of Est3p with telomeres occurs largely in late S phase by ChIP, although a small amount was seen in G1 phase. In strains deleted for either Est2p or *TLC1*, Est3p no longer associates with telomeres despite being the most abundant of the Est proteins in the cell. In the absence of *EST1*, there was a small amount of Est3p binding in both phases in an *est1*Δ background by ChIP, supporting the idea that Est3p depends upon Est1p for optimal telomere association (Tuzon et al., 2011). Together, the Lundblad and Friedman papers suggest that Est1p is stimulating the association of Est3p with the telomerase complex, but may not be absolutely required under all circumstances.

Recombinant Est3p also interacts directly with a purified Est2p fragment consisting of the TEN domain (Talley et al., 2011), potentially through a predicted OB-fold (oligonucleotide/oligosaccharide) domain that is necessary for telomerase association (Lee et al., 2008). Homology-based structural predictions suggest that Est3p contains an OB-fold similar to that of the human TPP1 protein. Recombinant TPP1 (together with POT1) stimulates telomerase repeat addition processivity *in vitro,* while

recombinant Est3p stimulates telomerase activity *in vitro*, but no indication in a change in *in vitro* processivity was seen (Latrick and Cech, 2010; Talley et al., 2011). These data suggest both proteins may boost enzymatic activity of telomerase *in vivo*.

There are two additional properties of Est3p reported in the literature that are still under debate: *in vivo* dimerization and nucleotide binding. In 2006, the Zhou group published a paper demonstrating that recombinant Est3p dimerizes *in vitro*. This dimerization was suggested to be important for Est3p's *in vivo* functions as mutations disrupting *in vitro* dimerization resulted in decreased telomere length and cellular growth (Yang et al., 2006). However, the dimerization state within the cell was not directly assessed. The Dontsova lab found the *in vitro* dimerization of Est3p occurred only in the presence of Mg^{2+} ions (Malyavko et al., 2010). Also, Dr. Talley, a recent graduate from our lab, saw similar Est3p profiles during her Est3 protein purification process (J. Talley, personal communication). These data suggest that Est3p can dimerize *in vitro*, but leave the question of dimerization *in vivo* unresolved.

I have addressed *in vivo* dimerization more directly by analyzing the interaction of differentially tagged alleles of Est3p by co-immunoprecipitation (see Figure 1.5). In these strains, endogenous *EST3* is fused to one epitope tag and a differentially tagged allele is expressed from a low copy number plasmid. In all cases, regardless of the epitope tag, I saw no evidence of Est3-Est3 interaction, suggesting that Est3p dimerization does not occur *in vivo*. However, the same tagged versions of Est3p could interact with different members of the telomerase complex. Therefore, another interpretation of the *in vivo* data presented by the Zhou group is that the Est3 variants cause deficiencies in interactions with other members of the telomerase complex.

A.

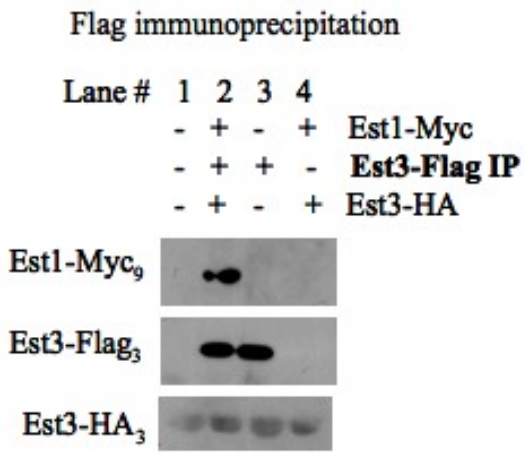
Flag immunoprecipitation
Lane # 1 2 3 4
- + - + Est1-Myc
- + + - Est3-Flag IP
- + - + Est3-HA
Est1-Myc9
Est3-Flag3
Est3-HA3

B.

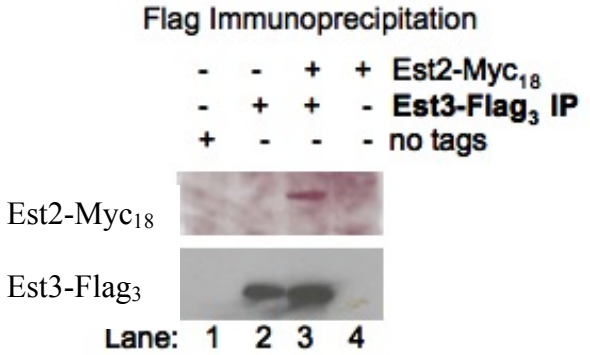
Flag Immunoprecipitation
- - + + Est2-Myc18
- + + - Est3-Flag3 IP
+ - - - no tags
Est2-Myc18
Est3-Flag3
Lane: 1 2 3 4

C.

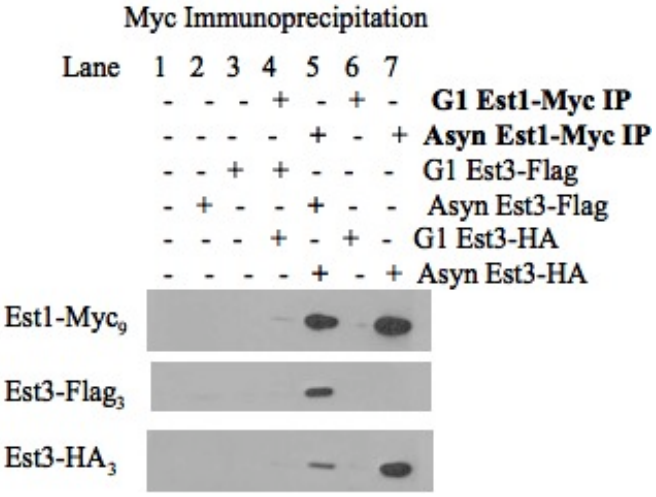
Myc Immunoprecipitation
Lane 1 2 3 4 5 6 7
- - - + - + - G1 Est1-Myc IP
- - - - + - + Asyn Est1-Myc IP
- - + + - - - G1 Est3-Flag
- + - - + - - Asyn Est3-Flag
- - - + - + - G1 Est3-HA
- - - - + - + Asyn Est3-HA
Est1-Myc9
Est3-Flag3
Est3-HA3

D.

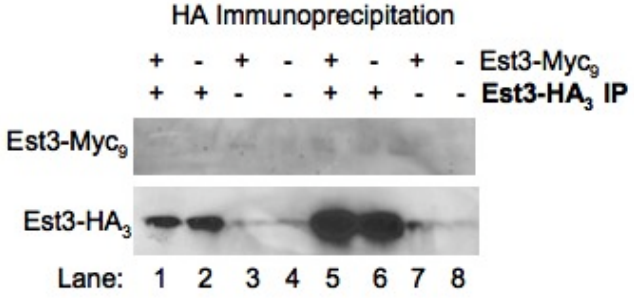
HA Immunoprecipitation
+ - + - + - + - Est3-Myc9
+ + - - + + - - Est3-HA3 IP
Est3-Myc9
Est3-HA3
Lane: 1 2 3 4 5 6 7 8

E.

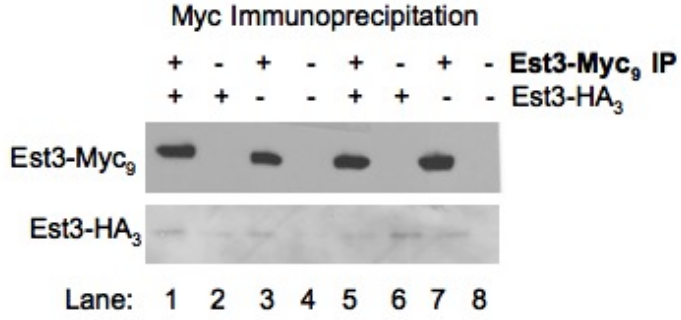
Myc Immunoprecipitation
+ - + - + - + - Est3-Myc9 IP
+ + - - + + - - Est3-HA3
Est3-Myc9
Est3-HA3
Lane: 1 2 3 4 5 6 7 8

Figure 1.5: Est3p dimerization is not detectable *in vivo*. Whole-cell extract was harvested from asynchronous cells or cells blocked in G1 phase with alpha factor and epitope-tagged proteins were immuoprecipitated as indicated. Immunoprecipitated proteins were separated in 10 or 12% SDS-PAGE gels and detected by Western Blot with epitope-tag specific antibodies. **(A)** Immunoprecipitation of Est3-$Flag_3$ allows detection of co-immunoprecipitating Est1-Myc_9 but not Est3-HA_3 (lane 2) from asynchronous cells. **(B)** Est3-$Flag_3$ interacts with Est2-Myc_{18} (lane 3) in extract harvested from asynchronous grown cells. **(C)** Est1-Myc_9 from asynchronous cells can be immunoprecipitated with both Est3-$Flag_3$ and Est3-HA_3 (lanes 5 and 7). As expected, Est1-Myc_9 levels are very low during G1 phase and no co-immunoprecipitation of Est3p can be detected (lanes 4 and 6). **(D and E)** Est3-Myc_9 does not associate with Est3-HA_3 by HA immunoprecipitation (D, lanes 1 and 5) or by Myc immunoprecipitation (E, lanes 1 and 5).

A study with recombinant *S. cerevisiae* Est3p suggested that Est3p binds weakly to DNA and RNA (Sharanov, Zvereva and Dontsova, 2006). However, the Lundblad group reported that addition of single-stranded DNA did not change the nuclear magnetic resonance chemical shifts of recombinant *S. castellii* Est3p. This result suggests that *S. castellii* Est3p does not directly recognize telomeric substrates (Lee et al., 2010). A recent publication from the Lue lab showed that recombinant Est3p from the yeast *Candida parapsilosis* could be crosslinked to telomeric DNA, but only in the presence of the TEN domain (Yen et al., 2011), suggesting that interaction with Est2p may uncover a DNA-binding function. These data suggest that Est3p nucleotide interactions may be context and species specific.

Overall, Est3p is recruited to the complex by an interaction with the TEN domain of Est2p in an Est1p-dependent manner. Est3p functions as an activator of telomerase, both *in vivo* and *in vitro*. The potential functional effects of *in vivo* dimerization and RNA and/or DNA binding have yet to be satisfactorily determined.

Regulation of yeast telomeres

Telomerase itself is not very abundant in cells. There are estimated to be approximately 71 molecules of Est1p, 37 molecules of Est2p and 84 molecules of Est3p in a haploid yeast cell (Tuzon et al., 2011). There are an estimated 29 molecules of *TLC1*, while haploid cells in late S-phase contain 64 chromosome ends (Mozdy and Cech, 2006). Telomerase extends an average of 10% of the telomeres in a given cell cycle (Teixeira et al., 2004), perhaps because the telomerase components are very low. There are three other aspects of telomere regulation that will be discussed below: formation of the 3' TG rich overhang, telomere length homeostasis and the telosome.

The TG-rich single-stranded DNA overhang

DNA substrates of telomerase have a 3' TG-rich overhang. This characteristic was first appreciated when it was shown that purified *Euplotes* telomerase has no activity on blunt-ended primers. Extension requires a 3' single-stranded overhang of at least four to six nucleotides (Lingner and Cech, 1996), but can also utilize a single-stranded primer. In yeast after lagging strand replication completes, removal of the last RNA primer was expected to leave a ~8 to 12 nucleotide 3' overhang that today is known to be extended by telomerase. The Zakian and Wellingner lab published several papers analyzing how the formation of the single-stranded $TG_{1\text{-}3}$ tails is affected by origin activation. They discovered that in late S phase, $TG_{1\text{-}3}$ tails are detectible on both ends of a small linear plasmid with terminal telomeric tracts (Wellinger, Wolf and Zakian, 1993), suggesting that natural chromosomes probably terminate on both ends with $TG_{1\text{-}3}$ tails regardless of

whether the telomeres were replicated by leading or lagging strand replication (Wellinger et al., 1996).

There is a short 3' G rich overhang (approximately 16 nucleotides in length) present at all times of the cell cycle, but that overhang becomes longer in a manner correlated with the time of DNA replication (Larrivée, LeBel and Wellinger, 2004). The length of the overhang increases during S-phase by nine to fourteen nucleotides in wild-type cells (Larrivée, LeBel and Wellinger, 2004; Wellinger, Wolf and Zakian, 1993). Processing of the single-stranded TG_{1-3} overhang did not depend upon telomerase because cells deleted for *TLC1* still had TG_{1-3} tails (Dionne and Wellinger, 1996; Wellinger et al., 1996). To demonstrate this, the Wellinger lab devised a novel in-gel hybridization assay that is now the preferred method of bulk ssDNA analysis. Genomic DNA harvested from cells with and without *TLC1* showed G rich ssDNA only from S phase blocked cells. Detection of the G rich ssDNA without functional telomerase is also observed in human cells (McElligott and Wellinger, 1997; Wright et al., 1997).

Further studies found that Rad27 and the MRX (Mre11/Rad50/Xrs2) complex are required for the formation of these overhangs, but exert their primary effect on different DNA strands. *RAD27* (the homolog of mammalian *FEN1*) is thought to be involved in the processing of Okazaki fragments. High levels of single-stranded telomeric DNA accumulate in *rad27Δ* strains, but only at one end of the DNA (presumably the end generated by lagging-strand replication). (Parenteau and Wellinger, 1999). Strains with non-functional telomerase combined with *rad27*Δ resulted in rapid cell death and a significant reduction in the detectible G- rich ssDNA as compared to *rad27*Δ cells, suggesting that telomerase and lagging strand DNA synthesis machinery both contribute

to the G-rich overhang formation (Parenteau and Wellinger, 2002). Strains depleted of Mre11p have short telomeres and decreased G-rich ssDNA throughout the cell cycle (Larrivée, LeBel and Wellinger, 2004). The MRX complex, by way of Mre11p, has sequence and structure specific endonuclease activity on both normal and *de novo* termini (Ghosal and Muniyappa, 2007).The Géli lab showed that Cdc13p, Est1p and Est2p are found at both the leading and lagging telomere ends, but only the processing of the ends by Mre11p at the leading strand is necessary for Cdc13p and telomerase to bind (Faure et al., 2010).

The negative regulator Pif1p, a 5' to 3' DNA helicase, has separate functions at the telomere (maintained in a *pif1-m1* allele) and in mitochondria (maintained in the *pif1-m2* allele) (Schulz and Zakian, 1994). The nuclear helicase function also plays a role in telomeric end processing and normal telomere length (Zhou et al., 2000). Pif1p and *pif1-m1* associate with telomeric DNA, with the highest association occurring in late S phase (Vega et al., 2007).

Nuclear Pif1p is thought to have two functions at telomeres: dissociation of the RNA template/DNA hybrid and in the creation of the 3' TG-rich overhang. For the first function, the Zakian lab observed a 30% increase of all telomere healing events on TG-rich overhangs in the absence of Pif1p (Mangahas et al., 2001). They hypothesized that Pif1p disrupted short RNA/DNA hybrids (indeed they show that this is the preferred substrate *in vitro*), perhaps by influencing the active site of telomerase. In support of this hypothesis, ChIP assays on strains over-expressing Pif1p showed decreased telomeric DNA bound by Est2p and Est1p compared to a wild-type samples (Boulé, Vega and Zakian, 2005). Normally *in vitro*, yeast telomerase already tightly bound to a DNA

substrate is incapable of adding nucleotides to a different primer (Cohn and Blackburn, 1995). The addition of recombinant Pif1p resulted in elongation of a challenge primer added after telomerase was already DNA bound, showing Pif1p is capable of telomerase removal (Boulé, Vega and Zakian, 2005).

There is some functional connection between completion of lagging-strand replication and telomere addition in which Pif1p plays a role. The CST complex (through Cdc13p and Stn1p) makes direct contacts with Pol δ, a yeast DNA polymerase that acts on the lagging strand. It is suggested that a role of the CST complex in telomerase regulation is to recruit both telomerase (through Est1p) and the lagging strand machinery (through Pol δ) (Pennock, Buckley and Lundblad, 2001). The long telomere phenotype and increased frequency of *de novo* telomere addition at double-strand breaks of a *pif1Δ* strain is dependent upon Dna2p, a helicase/nuclease required for Okazaki fragment processing (Zheng and Shen, 2011). Genetic data suggests Pif1p works together with Dna2p and Pol δ for replication fork progression by making a flap after the removal of the RNA primer. The authors suggest a model where during telomere maturation, Pif1p may displace the Okazaki fragment exposing a TG-rich strand in a non-extendible state for telomerase elongation (Budd et al., 2006). Therefore, although the CST complex is capable of recruiting telomerase, the interaction of Pif1p with Dna2p and Pol δ may act as inhibitors of telomerase to halt telomere elongation as the cell enters G2 phase.

In conclusion, the lengthening of the TG rich overhang occurs in late S-phase concurrent with the passage of the replication fork. Telomerase extends the 3’ overhangs that are processed by Rad27 (lagging strand) and the MRX complex (leading strand).

Other factors, such as the helicase Pif1p, Dna2p helicase/nuclease, and *EXO1* (a 5' to 3' nuclease not discussed here) are also involved in the G-rich 3' overhang generation.

Yeast telomere length homeostasis

Telomere length homeostasis describes the ability of yeast to maintain the bulk of telomeres at a wild-type length of 300 +/- 50 base pairs. The essential Rap1p was established as a protein-counting mechanism for telomere length regulation in the late 1990's. This was initially shown when an 80 base pair telomeric tract separated by a short linker from a single telomere was "counted" as part of the total telomere length, causing the terminal tract to shorten to approximately 220 base pairs. The 80 bp of internal telomeric repeats could be substituted with a series of Gal4-UAS sequences that would recruit Gal4-Rap1p. In this manner, the length of the telomere was shortened proportionate to the number of Rap1p molecules present (or UAS sites inserted), suggesting the amount of Rap1p molecules inversely regulates telomere length (Marcand, Brevet and Gilson, 1999; Marcand, Gilson and Shore, 1997).

There are two major possibilities for telomere maintenance: telomerase adds nucleotides to each telomere in each cell cycle to directly counteract what is lost by replication, or telomeres undergo loss for multiple generations, followed by a single more extensive elongation event. The Lingner lab showed that telomeres exist in either telomerase extendible or non-extendible states. Using a single telomere extension assay (STEX), they measured the number of nucleotides added by telomerase in a single cell cycle. This technique also allows the length of the substrate telomere to be determined.

The authors found that in wild-type cells, the frequency of telomere extension increased as a function of length – approximately 7% of telomeres 300 base pairs in length were extended versus approximately 44% of telomeres at 100 base pairs in length in a single cell cycle (Teixeira et al., 2004). When either *RIF1* or *RIF2* are deleted, telomeres become overly long (Hardy, Sussel and Shore, 1992; Wotton and Shore, 1997). STEX analysis suggested that telomeres in a *rif1*Δ or *rif2*Δ background become longer due to an increased frequency of elongation events by telomerase, although the preference for the shorter telomeres still exists (Teixeira et al., 2004). By ChIP, as telomeres naturally shorten in the absence of telomerase, there is a decrease in the amount of Rif2p and Rap1p binding at telomeres but not Rif1p, suggesting Rif2p interacts with Rap1p closer to the 3' end of the telomere (McGee et al., 2010) and perhaps Rif2p has a role in the Rap1p "counting mechanism".

Several studies published in 2007 suggested that Tel1p, first identified in a screen for temperature sensitive mutants that resulted in much shorter telomeres than wild-type (Walmsley and Petes, 1985), marks the shortest telomeres for elongation (Arnerić and Lingner, 2007; Hector et al., 2007; Sabourin, Tuzon and Zakian, 2007). In telomerase-deficient strains by ChIP that Tel1p binding to short telomeres depended upon the presence of Mre11p. The authors used a technique called Telomere-PCR to assay the length of the ChIP DNA bound by Tel1p. In this PCR assay, the isolated DNA is amplified using a primer located a little upstream of the telomere and a primer specific to a poly-C tail added to the free ends by a terminal transferase. Over successive population doublings without telomerase, the input ChIP showed a range of sizes that decreased over time as expected. The Tel1-bound DNA had a more restricted size distribution at each

time point. Sequential ChIPs for Tel1p and Est2p showed that Est2p bound the fraction of DNA pulled down by Tel1p (Hector et al., 2007). The Lingner lab showed yeast telomerase uses a processive mode of synthesis for rapid elongation of short telomeres (<125 base pairs) in a Tel1p dependent fashion (Chang, Arnerić and Lingner, 2007). This is an important finding for the yeast telomerase field because until this publication, it was thought that yeast telomerase always behaved non-processively *in vivo*.

Normal length yeast telomeres are replicated in late S-phase due to late firing of telomere-proximal replication origins (McCarroll and Fangman, 1988). The Gilson lab showed that an artificially shortened telomere was elongated by telomerase only in S phase (Marcand et al., 2000). The Shore lab further investigated the replication timing of short telomeres in 2007. Using an inducible telomere shortening assay, they found that if a telomere became abruptly shortened, that telomere was replicate early in S phase due to the early firing of DNA replication origins in subtelomeric regions. This early telomere replication correlated with increased telomere length and telomerase activity (Bianchi and Shore, 2007).

A recent 2011 publication suggests yKu also mediates telomere replication timing in cells. Yeast cells without the Ku70 and Ku80 heterodimer have dramatically shortened telomeres (Shore and Bianchi, 2009) with extensive ssDNA throughout the cell cycle (Gravel et al., 1998). In cells deleted for yKu, telomeres replicated earlier than their counterparts in wild-type cells. This early replication occurred as far as 40 Kb from the telomere, suggesting there could be an upstream target of Ku. The authors suggest this target, or perhaps interacting partner, is Rif1p, as the *rif1*Δ *yku70*Δ does not rescue the early replication defects seen in a *yku70*Δ (Lian et al., 2011). These data suggest that

telomere length can affect the activity of nearby replication origins and provides a potential link between telomere replication timing and telomerase action.

In 2010, the Zakian lab extended the Shore 2007 study by showing reduced levels of Rif2p and members of the MRX complex were important regulators of short telomere elongation (McGee et al., 2010). Rif2p (and Rif1p) are Rap1p interacting factors that compete for binding to Rap1p's C-terminus (Hardy, Sussel and Shore, 1992; Wotton and Shore, 1997). Southern Blotting on DNA from a *rif1*Δ *rif2*Δ strain showed longer telomeres than either single mutant alone (Wotton and Shore, 1997), suggesting Rif1p and Rif2p perform partially redundant functions at telomeres. The Zakian lab used the Gilson lab's FLP recombinase system to induce short telomeres (approximately 100 base pairs in length) on chromosomes VI-R or VII-L (Marcand et al., 2000). By ChIP, the authors showed the shortened telomeres had a significant increase in the amount of each MRX component. As expected, Rap1p and Rif2p binding was reduced at short telomeres. Most interestingly, Tel1p preferential binding to the induced short telomeres was lost in a *rif2*Δ background. These data suggest a model in which Tel1p recruitment responds to Rif2 protein levels. When Rif2p (and Rap1p) levels drop as the telomere naturally shortens, the telomere is then bound by Tel1p to facilitate telomerase extension. In support of this finding, the Sugimoto lab found the amount of Tel1p binding at an induced double-strand DNA break was decreased to that of a vector control when Rif2p, but not Rif1p, was artificially tethered adjacent to the dsDNA break (Hirano, Fukunaga and Sugimoto, 2009).

Genes that modulate the RNA abundance of the telomerase components also control telomere length. Disruption of *RNT1* (RNase III - a double-stranded RNA-

specific endoribonuclease) resulted in increased expression of Est1, Est2, Est3, and *TLC1* RNAs with a corresponding increase in telomerase activity and subsequent telomere elongation (Larose et al., 2007). Along with RNase III, genes that specifically modulate *TLC1* RNA abundance, like the Paf1C complex, affect telomere length as demonstrated by the Cech lab in 2008 (Mozdy, Podell and Cech, 2008).

In summary, telomere length homeostasis is maintained through a feedback mechanism that responds to telomere length. As telomeres shorten, they can be replicated earlier in S-phase than other telomeres. One possibility is the early replication of the short telomeres allows telomerase ample time to get these telomeres to the appropriate length for avoidance of a cell cycle checkpoint. Important positive and negative protein regulators facilitate telomere length homeostasis.

The telosome and end protection

In a cell with linear chromosomes, the cell is challenged to distinguish normal chromosome ends from broken ends in need of repair. The telosome (telomeric DNA and associated proteins) represents the biological solution to this challenge. If the telosome is absent or nonfunctional, cells recognize telomeres as double stranded breaks. These unstable ends tend to heal by fusing or recombining with other chromosomes in the cell (Orr-Weaver, Szostak and Rothenstein, 1981). Therefore, the telosome must be capable of preventing normal chromosome ends from triggering DNA damage response pathways.

The telosome is a telomere cap complex formed by the association of sequence-specific telomeric ssDNA and dsDNA binding proteins for protection and recruitment of

telomerase. In mammalian cells, the telosome is referred to as shelterin (TRF1, TRF2, TIN2, RAP1, TPP1 and POT1). TRF1 and TRF2 bind to the dsDNA. TIN2 links TRF1/2 to a heterodimer consisting of TPP1 and POT1. POT1 interacts with the ssDNA. In contrast to the budding yeast Rap1p, mammalian RAP1 associates with TRF2 and does not have an affinity for DNA (de Lange, 2005). The shelterin TIN2-TPP1 components recruit telomerase to the telomere in human cells (Abreu et al., 2010). In budding yeast, the telosome is minimally made up of Rap1p (with Rif1p and Rif2p interacting factors) and the CST (Cdc13p, Stn1p, Ten1p) complex. The yeast Rap1p interacts with the dsDNA and Rif1p/Rif2p associate directly with Rap1p. Cdc13p binds to ssDNA whereas Stn1p and Ten1p interact directly with Cdc13p (Price et al., 2010). Cdc13p and Est1p recruit telomerase to the yeast telomere (Evans and Lundblad, 1999; Taggart, Teng and Zakian, 2002) (see Figure 1.6). There is a mammalian CST complex, but mammalian CST plays both telomeric and non-telomeric roles (Price et al., 2010), and will not be discussed further here.

The Stn1 component of the yeast CST complex was found as a suppressor of the *cdc13-1*^{ts} allele (Grandin, Reed and Charbonneau, 1997). *TEN1* was discovered as a protein that could rescue the temperature-sensitivity of the *stn1-13* allele. (Grandin, Damon and Charbonneau, 2001). Disruption of *TEN1* or *STN1* causes a Rad9-dependent cell cycle arrests. Ten1p, Stn1p, and Cdc13p all interact with one another as assayed by Co-IP and yeast 2-hybrid analysis (Grandin, Damon and Charbonneau, 2001; Grandin, Reed and Charbonneau, 1997). An allele of *CDC13*, *cdc13-5*, increased TG-rich ssDNA that is eliminated by over-expression of *STN1* (Chandra et al., 2001). The order of the CST loading at telomeres is not known at this time.

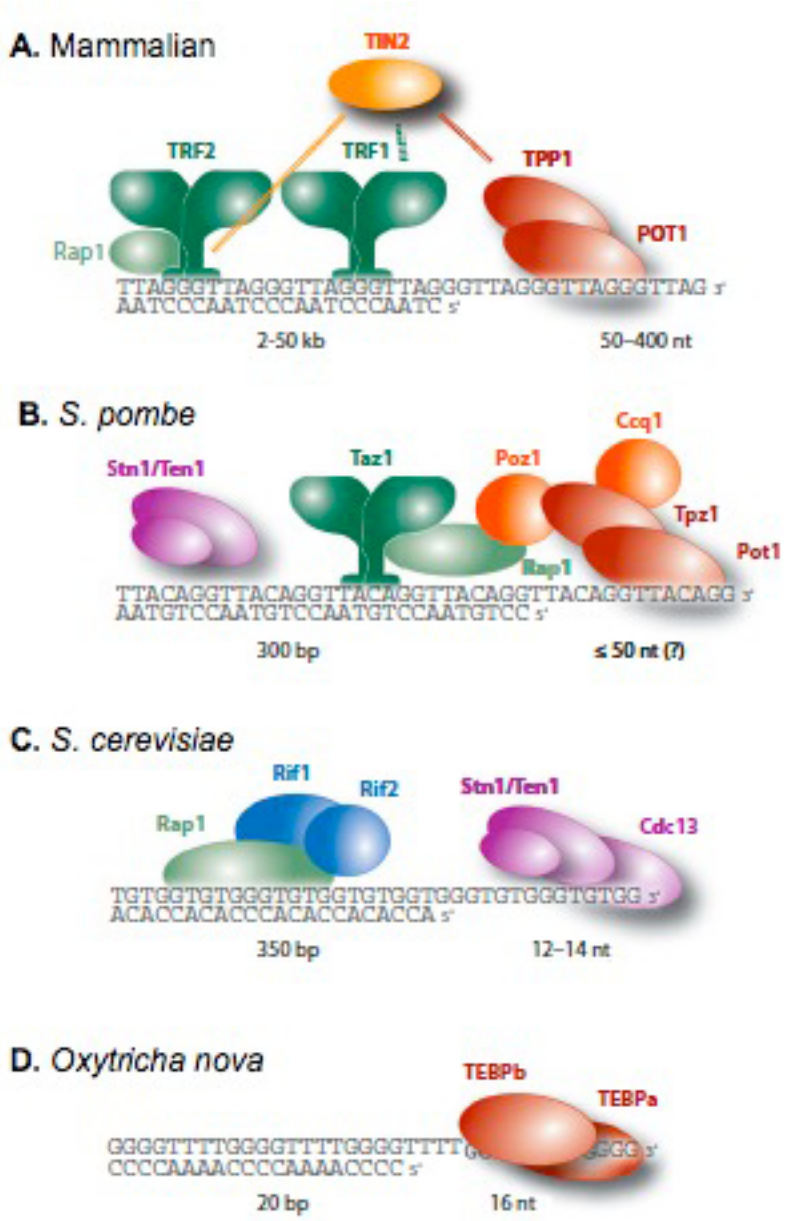

Figure 1.6: The telosome protein complexes and DNA sequences are species-specific. Homologs are shown in the same color. The approximate lengths of the dsDNA and ssDNA portions of the telomeres are indicated. **(A)** Mammaian shelterin is comprised of Rap1, TRF1/2, TIN2, TPP1, and POT1. The mammalian CST complex is not shown. **(B)** The telosome protein complex in *S. pombe* (fission yeast) has both mammalian and *S. cerevisiae* homologs. **(C)** *S. cerevisiae* telosome is comprised of Rap1, Rif1, and Rif2 at the double-stranded portion whereas the CST complex (Cdc13/Stn1/Ten1) interacts with the single-stranded overhang. **(D)** The ciliate *Oxytricha* telosome is comprised of TEBPa and b. Image modified from (Palm and de Lange, 2008).

The telosome protein components protect telomeres from DNA damage signaling pathways. Cell cycle arrests in response to DNA damage sensing rely on the activity of the ATM (Tel1p in yeast) and ATR (Mec1p in yeast) kinases to trigger DNA repair response pathways (de Lange, 2009). RPA, a non-specific ssDNA binding protein that activates Mec1p (Vodenicharov and Wellinger, 2006), is part of the *MEC1* kinase DNA damage response pathway. While RPA is found at yeast telomeres, RPA binds to double stranded breaks eight-fold higher than the telomere single stranded ends as assayed by ChIP. In conjunction with this observation, Mec1p binding is not detected at telomeres (whereas Cdc13p is), but Mec1p molecules are present at high levels at double stranded breaks (McGee et al., 2010). These data suggest that the CST complex represses the Mec1-RPA pathway.

Tel1p has a primary role in facilitating telomere elongation by telomerase. A recent paper by the Zakian lab showed that at induced short telomeres (approximately 100 base pairs in length), there is increased binding of the MRX complex (McGee et al., 2010). Tel1p requires the C-terminus of Xrs2p to bind to telomeres (Sabourin, Tuzon and Zakian, 2007), suggesting that Tel1p is targeted to telomeres by the MRX complex. It has been shown with *in vitro* studies that the Tel1p-Xrs2p interaction is prevented by Rif2p interaction with the C-terminus of Xrs2p (Hirano, Fukunaga and Sugimoto, 2009). In a *rif2Δ* background, Tel1p no longer bound preferentially to the shortest telomeres (McGee et al., 2010). These data suggest that as telomeres naturally shorten, and Rif2p binding decreases and lifts the inhibitory block on the MRX complex allowing MRX to recruit Tel1p to mark telomeres for elongation by telomerase. Interestingly, the MRX

complex is what targets Tel1p to double stranded breaks and interacts with exo-nucleases for generation of the single-stranded DNA overhang at double stranded breaks (Hirano and Sugimoto, 2007). The generation of the single stranded overhang at telomeres is cell cycle regulated (Larrivée, LeBel and Wellinger, 2004) and is coated with Cdc13p in S phase, not RPA (McGee et al., 2010). The Tel1p double strand break pathway is only activated when Mec1p is compromised (Nakada et al., 2003). Therefore, Tel1p double stranded break action is also blocked by the telosome and Tel1p's primary role is in telomerase recruitment.

Enzyme characteristics

This last section of the Introduction Chapter will cover characteristics of the telomerase enzyme. It starts with an overview of yeast telomere sequence patterns and an introduction to long telomere mutants of *EST2* that alter the telomeric sequence. End protection mediated by the telomere discussed. Lastly, this section will focus on the enzymatic mode of telomere synthesis: processivity, and how the anchor-site mediates this phenomenon.

Yeast telomeric sequence patterns

Unlike human and ciliates, yeast telomerase uses its template to incorporate heterogeneous telomere sequences (Shampay, Szostak and Blackburn, 1984). The importance of the templating region of the telomerase RNA subunit was first shown in *Tetrahymena* by the Blackburn lab in 1990. Modification of any of the *Tetrahymena* RNA template residues resulted in the corresponding change incorporated into the *in vivo*

synthesized telomeres (Yu and Blackburn, 1990). This effect occurs in yeast as well. For example, Singer and Gottschling showed that mutation of the template residues to *Hae III* restriction sites were incorporated in the newly synthesized telomeres (Singer and Gottschling, 1994).

In 1993, the Haber lab noted that a common 11 or 13 base pair sequence was typically seen in yeast telomeres despite the heterogeneity (Kramer and Haber, 1993). The Lingner lab refined the pattern into a model of wild-type telomerase template usage by using mutations in the template and analyzing the resulting telomere sequences to make inferences about template usage *in vivo* (Förstemann and Lingner, 2001). As a reminder, the *TLC1* template is 3' – ^{484}ACACACACCCACACCAC^{468}. Assuming a DNA substrate ending in 5' TGGTG, their model suggested that wild-type telomerase preferred to make contacts with the DNA through residues ^{483}C through ^{479}C (60% of all alignments). Only 19% of alignments occurred with the extreme 3' ^{484}AC^{483} residues.

The most common template nucleotides used for telomeric synthesis were ^{478}ACCCACA^{472}, generating a telomeric sequence of 5'-TGGGTGT-3' that is termed the "core motif." About 53% of the time, the ^{471}CC^{470} was incorporated into the telomere immediately following this core motif (5' – TGGGTGT**GG**). However, the extreme 5' ^{469}AC^{468} was rarely used for synthesis (10% of the time) and never for alignment (see Figure 1.7). These data were confirmed with a 2008 Friedman lab paper comparing the wild-type pattern of telomere sequences to those generated by two long-telomere mutants: *est2-LT^{E76K}* and *est2-up34* (Ji et al., 2008). The *est2-LT^{E76K}* (glutamic acid residue 76 to lysine) telomerase elongates telomeres approximately 100 base pairs over

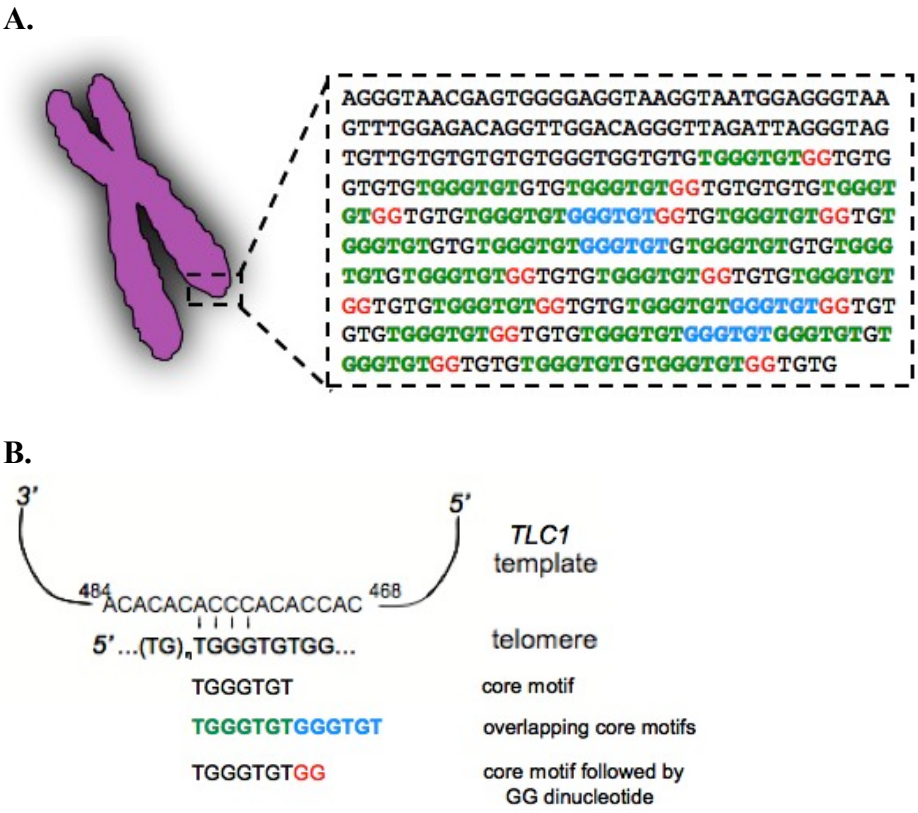

Figure 1.7: Yeast telomere sequence patterns. **(A)** Example yeast telomere with the telomere sequence patterns highlighted. **(B)** The *TLC1* RNA template aligning with a telomeric DNA substrate. Core motifs are synthesized from the ^{478}ACCCACA^{472} portion of the template. Green text – core motifs. For cases in which two core motifs overlap, the second core motif is shown in blue. Inter-core regions are the nucleotides between core motifs. Inter-core regions can be characterized by size (number of nucleotides) or by sequence. Some core motifs are followed by a GG dinucleotide (red) arising from synthesis of ^{471}CC^{470} in the RNA template.

wild-type The telomere over-elongation phenotype is independent of *RAD52,* but requires

Tel1p (Ji et al., 2005). The *est2-up34* (aspartic acid residue 460 to asparagines)

telomerase causes a similar telomere length increase dependent upon *PIF1* (Eugster et al., 2006).

Both *est2-LT^{E76K}* and *est2-up34* alter the telomere sequences (Ji et al., 2008). Both mutant enzymes significantly increase the incorporation of the GG dinucleotide following a core motif from 53% to approximately 66%. The number of TG dinucleotides synthesized between core motifs was also higher in telomeres synthesized by the *est2-LT^{E76K}* and *est2-up34* telomerases as compared to wild-type (Ji et al., 2008). My published data suggest that the reason for the increased number of nucleotides between core motifs (the inter-core region) is a change in the 3' alignment of the RNA template with the DNA substrates with *est2-LT^{E76K}* telomerase (Bairley et al., 2011).

The contributions of TERT to the catalytic core

This thesis chapter already gave general information on both Est2p and *TLC1* RNA in terms of their discovery and main roles in the telomerase complex. This portion focuses on processivity and the anchor-site.

Processivity

There are two types of processivity: nucleotide addition processivity (type I) and repeat addition processivity (type II). Nucleotide addition processivity consists of the addition of single nucleotides from the template for a single round. Repeat addition processivity is the ability of the enzyme to translocate and repeat the nucleotide addition processivity for multiple rounds, thereby generating multiple "template repeats" (Lue, 2004) (see Figure 1.8). Repeat addition processivity is a unique feature of telomerase that allows the

enzyme to add upwards of 100 base pairs of telomeric DNA (depending on the species and situation) in a single binding reaction.

S. cerevisiae telomerase is predominantly non-processive as compared to other telomerases (such as from human and *Tetrahymena*) (Cohn and Blackburn, 1995). *S. cerevisiae* telomerase displays single turnover kinetics *in vitro*, meaning that telomerase remains associated with the elongated primer once the end of the template has been reached (Prescott and Blackburn, 1997a). However, when presented with a non-yeast telomeric primer, such as the *Oxytricha* telomeric sequence, yeast is capable of limited repeat addition processivity (Lue, 2005; Lue and Li, 2007). *In vivo*, wild-type yeast telomerase does not have pronounced repeat addition processivity over multiple rounds of a cell cycle when assayed with two differing templates (Bairley et al., 2011; Chang, Arnerić and Lingner, 2007), but displays a significant increase in processivity on short telomeres (<125 base pairs) during a single cell cycle (Chang, Arnerić and Lingner, 2007).

Both the TERT (previously discussed in Section 2) and TERC components of the catalytic core effect processivity. Within TERC, the template plays a major role in processivity. Mutations in certain yeast and *Tetrahymena* template residues have been shown to alter nucleotide addition processivity (both species) and repeat addition processivity (*Tetrahymena) in vitro* and *in vitro* (Chang, Arnerić and Lingner, 2007; Förstemann and Lingner, 2001; Gilley, Lee and Blackburn, 1995; Prescott and Blackburn, 1997b). A short RNA-DNA hybrid can decrease nucleotide addition processivity (Bosoy and Lue, 2004; Lue, 2005), and the 5' end of the DNA substrate

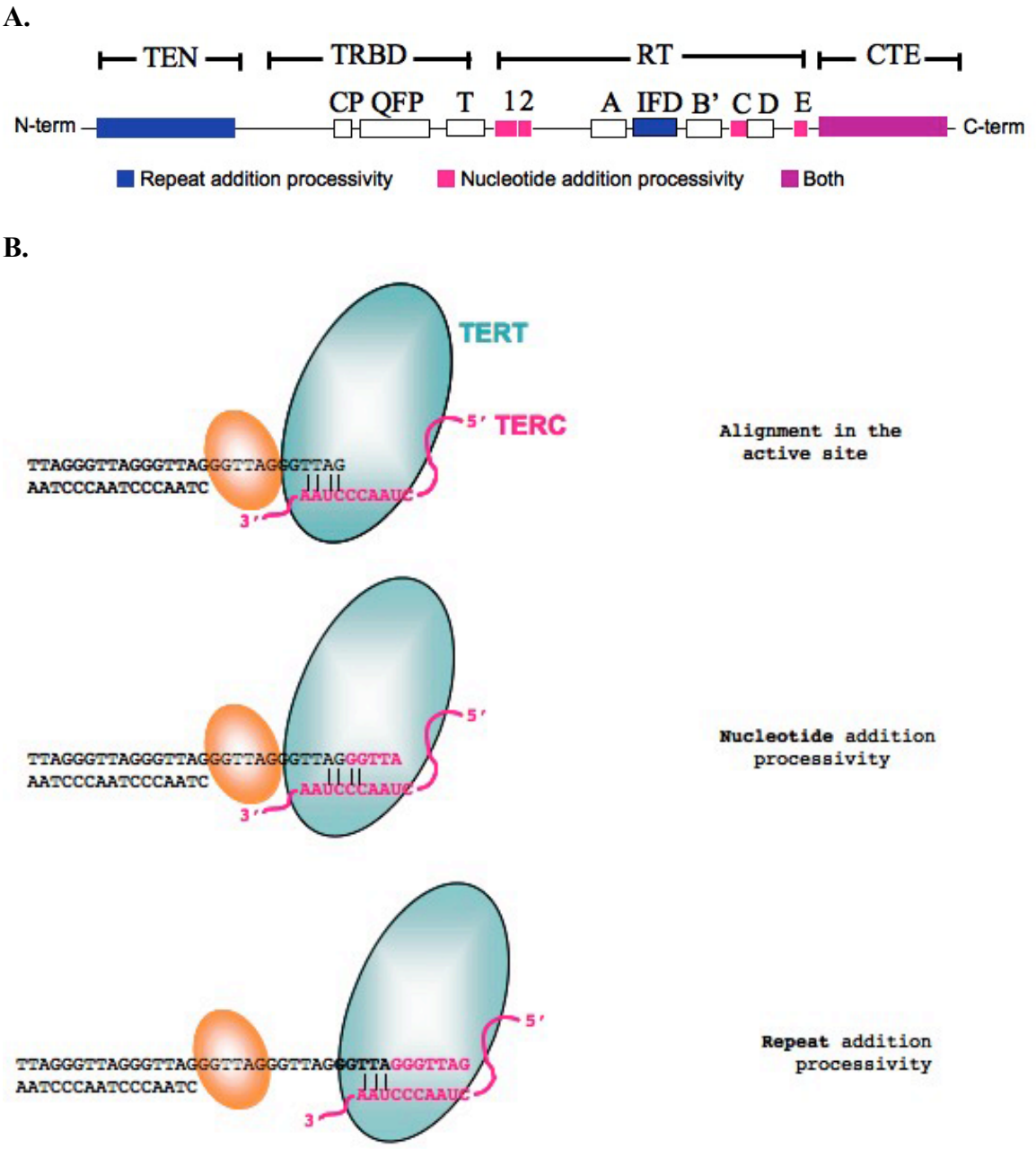

Figure 1.8: Nucleotide and repeat addition processivity. **(A)** Conserved domains in *TERT* that contribute to repeat addition processivity (blue), nucleotide addition processivity (pink) or both types of processivity (magenta). TRBD – Telomerase RNA binding domain; RT – reverse transcriptase domain; CTE – C-terminal extension. **(B)** Human telomerase (blue) recruited to the telomere by POT1-TPP1-TIN2 (orange) aligns the 3' end of a DNA substrate (solid bars) in the active site with the *TERC* template (purple text; top panel). The other portions of TERC are not depicted for simplicity. Nucleotide addition proceeds with the addition of individual nucleotides (purple text; middle panel). Repeat addition occurs when the same telomerase enzyme translocates, the RNA template re-aligns (solid bars) with the newly synthesized DNA (black bold text), and initiates another round of reverse transcription (purple text; bottom panel).

affects repeat addition processivity (Finger and Bryan, 2008; Jacobs, Podell and Cech, 2006; Lee and Blackburn, 1993). The structural integrity of the 5' template boundary, the 3' flanking regions surrounding the template as well as the conserved pseudoknot are important for both types of processivity (Lue, 2004).

In vitro, the minimum components required for yeast are the Est2p and *TLC1* RNA (Lingner et al., 1997a). Some recent studies have shown that addition of recombinant Est1p or Est3p stimulates overall telomerase activity, but a direct role in repeat addition processivity has not been addressed (DeZwann and Freeman, 2009; Lee et al., 2010; Talley et al., 2011). Components of the telosome also influence processivity *in vitro*. The Freeman lab showed that recombinant Cdc13p alone increased telomerase activity independent of interactions with Est1p (DeZwaan et al., 2009; DeZwann and Freeman, 2009). However, when in a complex with Stn1p and Ten1p, *in vitro* telomerase activity was inhibited (DeZwaan et al., 2009). The Cech lab showed in 2010 that addition of TPP1-POT1 increased repeat addition processivity by inhibiting the primer dissociation from telomerase while simultaneously increasing the efficiency of the telomerase translocation step (Latrick and Cech, 2010).

Overall, repeat addition processivity is limited in yeast. Recombinant Est1p, Est3p and the CST complex affect overall telomerase activity *in vitro*. Multiple regions of TERC and TERT contribute to processivity, including the anchor-site (see below).

Anchor-site

The anchor-site of telomerase is located in the TEN domain of TERT and is thought to maintain important contacts with the 5' end of the DNA substrate for repeat addition

processivity (Autexier and Lue, 2006). The first study to suggest that the 5' end of telomeric DNA could be making important contacts with TERT was in 1993. In *Tetrahymena*, the telomere is comprised of perfect $(TTGGGG)_n$ repeats. When the 5' ends of 12 nucleotide primers (with a common –TTGGGG 3' end) were non-telomeric in nature, the ability of the *Tetrahymena* enzyme to processively add -TT or -TTG to the 3' end was substantially reduced as compared to a 5'-GGGGTT control primer (Lee and Blackburn, 1993). Studies by the Greider lab with human telomerase showed an increase in processivity *in vitro* as the number of DNA substrate base pairs complementary to the template increased (Chen and Greider, 2003). These data suggest that the spatial arrangement of the anchor-site is close in proximity to the active site of telomerase, supporting the hypothesis that the TEN domain functions as an important heteroduplex stabilizer (Steczkiewicz et al., 2011). This idea is not without merit as a recent paper by the Bryan lab suggests that the human TEN domain may mediate positioning of the 3' end of the primer in the active site (Jurczyluk et al., 2010).

Binding of the TEN domain to DNA substrates has since been assayed in *Tetrahymena*, human and yeast systems in the presence and absence of the RNA. Telomeric primers have been shown to photo-cross-link to the TEN domain in an RNA dependent manner (Jacobs, Podell and Cech, 2006; Lue, 2005; Romi et al., 2007). In *S. cerevisiae*, the TEN domain is capable of interacting with full-length *TLC1* RNA and increasing amounts of DNA compete with the RNA for protein binding *in vitro* (Xia et al., 2000). *In vitro*, the N-terminal portion of Est2 and specific residues in the *Tetrahymena* TEN can be photo-cross-linked to a telomeric primer (Jacobs, Podell and Cech, 2006; Lue, 2005). The Bryan lab developed an *in vitro* assay in 2008 to study DNA

binding of *Tetrahymena* telomerase reconstituted in rabbit reticulocyte lysate (RRL) (Finger and Bryan, 2008). Purified ^{35}S labeled full length TERT, reconstituted in the presence of the TERC, was shown to directly bind to 5' biotinylated 18 nucleotide telomeric DNA primer with high affinity, K_d of ~9 nM. The affinity was reduced to ~ 29 nM without TERC. RRL $TERT^{\Delta TEN}$ reduced the affinity to 31 nM (in the presence of the RNA) and the TEN domain alone was found to have an affinity for DNA at 550 +/- 250 nM using a photo-cross-linking assay.

DNA binding assays without the RNA have been utilized for the human (Finger and Bryan, 2008; Sealey et al., 2010; Wyatt, Lobb and Beattie, 2007; Wyatt et al., 2009) and yeast TEN domains (Bairley et al., 2011). Like the other model organisms mentioned previously, mutations thought to disrupt the *S. cerevisiae* anchor-site interaction impaired catalytic function and processivity on specific primers *in vitro* (Lue and Li, 2007). My published work identified a mutation within the *S. cerevisiae* TEN domain (*est2-LT*^{E76K}) that increases the relative strength of the $Est2^{TEN}$-DNA binding (Bairley et al., 2011). Overall, the studies on the anchor-site of telomerase show the TEN domain contributes to several catalytic functions that include the anchor-site DNA binding as well as RNA-DNA interactions.

SIGNIFICANCE

Telomerase was first characterized in 1985 and the yeast telomerase components were discovered in the 1990s. Since their discovery, many labs have contributed knowledge on the functions of the telomerase components. There are numerous ways in which telomere

synthesis is regulated to include cell cycle assemble of the telomerase complex, binding of capping proteins, as well as protein factors that both positively and negatively regulation telomerase. In yeast, telomeres are comprised of heterogeneous $C_{1-3}A/TG_{1-3}$ repeats with a short TG rich 3' overhang unlike the perfect templated repeats that are seen in other model systems like *Tetrahymena* and mammalian cells (de Lange, Blackburn and Lundblad, 2006). Although the yeast telomerase is a mostly non-processive enzyme *in vivo* and *in vitro* (Lue, 2004), Cdc13p, Est1p and Est3p can increase the basal level of enzymatic activity *in vitro* (DeZwaan et al., 2009; DeZwann and Freeman, 2009; Talley et al., 2011).

There are several human diseases directly correlated to deficiencies in the telomerase complex such as dyskeratosis congenita. Dyskeratosis congenita is an inherited disease involving systematic bone marrow failure as well as epiderminal abnormalities such as nail dystrophy and abnormal pigmentation. Research has shown that the X-linked form of the disease is caused by mutations of the gene encoding dyskerin (*DKC1*), a component of the human telomerase complex. The autosomal dominant form of the disease is due to mutations in human *TERT* or *TERC* that result in telomerase deficiency through haploinsufficiency (Vulliamy and Dokal, 2008). Very recently, an autosomal recessive form was shown to arises from mutations in *TCAB1* (Telomerase Cajal body protein 1). This protein controls telomerase localization to Cajal bodies and delivers *TERC* to telomeres in S phase (Zhong et al., 2011). Patients with either form of the disease present with severely decreased telomere lengths (usually less than first percentile) and the catalytic activity and/or abundance of telomerase is decreased (Vulliamy and Dokal, 2008; Zhong et al., 2011).

One possible treatment for these patients could be to simply over-express telomerase from their own hematopoietic stem cells *in vitro* and then transplant these cells into the bone marrow to rescue the short telomere lengths and decrease the likelihood of transplant rejection. But, over-expression of telomerase does not rescue the appropriate phenotypes for most model systems. For example, the Weissman group found that over-expression of mouse *TERT* did not rescue the long-term transplantation survival of hematopoietic stem cells, despite a slight increase in telomere lengths (Allisopp et al., 2003). A recent paper from the Artandi lab does lend some promise for future therapeutic guides. They stably over-expressed wild-type telomerase (or DCK1 or TCAB1) from patient-derived dyskeratosis congenital fibroblasts, creating disease specific induced pluipotent stem cells (iPCS) with long telomeres. These iPCS started out morphologically similar to human embryonic stem cells, were positive for pluripotency, and differentiated properly. If these iPCS are reprogrammed with the disease specific DKC1, TCAB1, or telomerase mutants, the mutant iPCS cells presented the same disease morphological defects as the original patient (Batista et al., 2011). These data suggest reprogrammed iPCS stably over-expressing a wild-type version of the appropriate gene could be a future treatment for these patients.

Another possible approach to restoring telomerase function for dyskeratosis congenita patients could be to over-elongate telomeres of the starting hematopoietic stem cells, and then transplant them into the bone marrow. Over-expression of *TERT* to increase cell survival has been tested with mouse embryonic stem cells (mECS) with promising results: increased telomerase activity enhanced the self-renewal of *TERT* over-expressing ESCs and improved resistance to apoptosis. Importantly, differentiation

toward hematopoietic lineages was more efficient than normal mECS cells without over-expressed *TERT* (Armstrong et al., 2005). Interestingly, telomeres were not drastically over-elongated in the mECS cells over-expressing *TERT*. The long telomere length threshold and other factors, such as capping of telomeres to protect from degradation are therefore important for normal cytological phenotypes.

Demonstration of this phenomenon is seen in yeast cells. Rif1p and Rif2p inhibit exo-nucleolytic processing at telomeres by the MRX complex (Bonetti et al., 2010). Yeast deleted for either *RIF1* or *RIF2* result in over-elongated telomeres (Hardy, Sussel and Shore, 1992; Wotton and Shore, 1997) at 227 and 130 base pairs over wild type length respectfully (Bairley et al., 2011). However, analysis from sporulated cells lacking functional telomerase and were *rif1Δ*, *rif2Δ* or *rif1Δ rif2Δ*, resulted in premature senescence in comparison to, the sporulated *est2Δ RIF1 RIF2* cells. These Rif deficient *est2Δ* cells were quickly targeted for a telomerase alternative lengthening pathway for cell survival even though the rate of telomere shortening was the same as the *est2Δ* cells (Chang, Dittmar and Rothstein, 2011). These data suggest that loss of either Rif1p or Rif2p triggers a DNA damage checkpoint earlier than just telomerase deficient cells. The downstream effect of Rif1p and Rif2p on cellular senescence could be telomerase independent. I have unpublished data showing telomerase positive *rif1Δ rif2Δ* yeast strains could maintain their long telomeres over 375+ generations, yet the cells became very sick and had a slow growing phenotype over time (see Figure 1.9; and data not shown). This suggests that longer telomeres maintained by telomerase in a background where the capping functions are disrupted are still detrimental to cell growth.

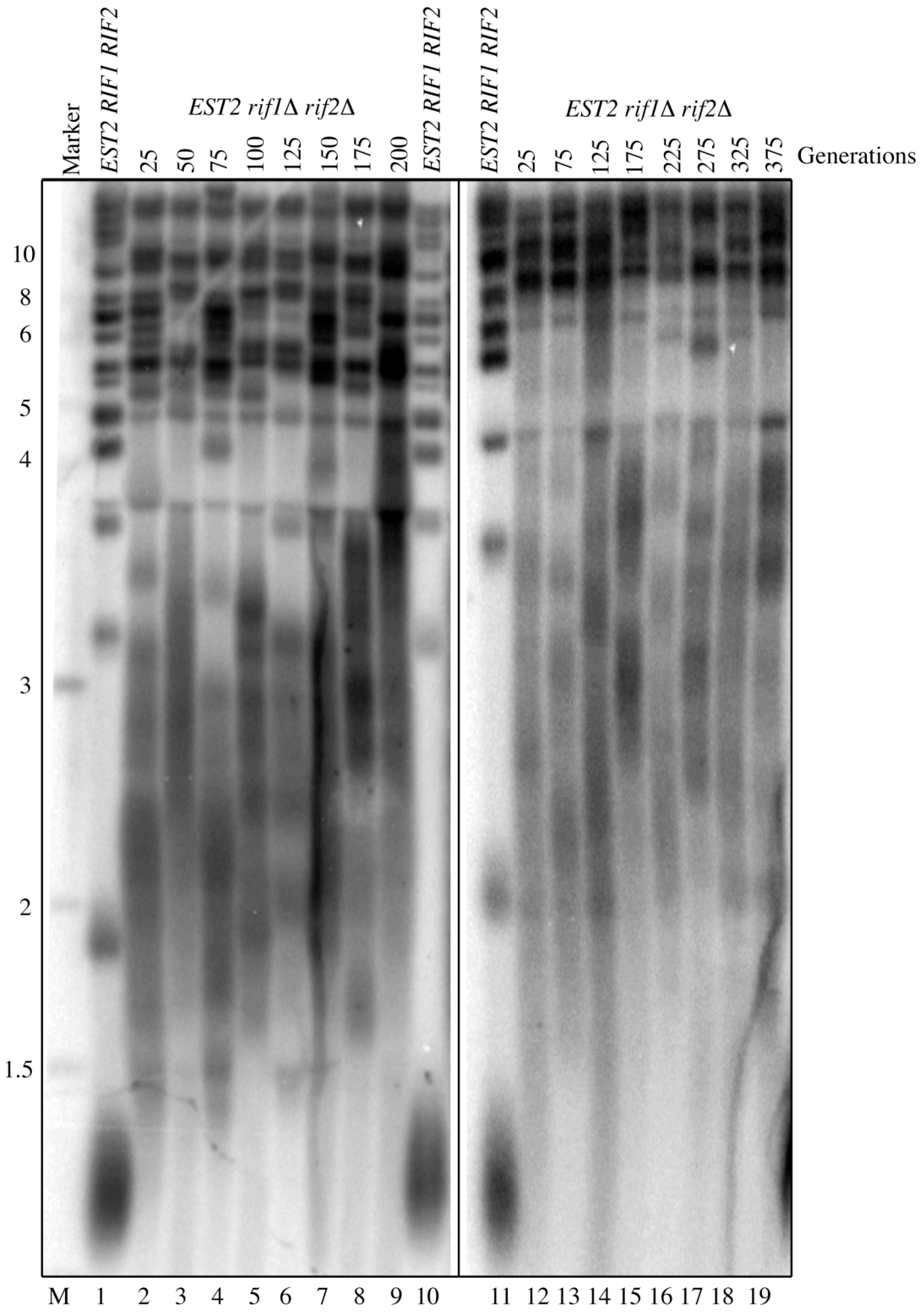
Marker
EST2 RIF1 RIF2
EST2 rif1Δ rif2Δ
25
50
75
100
125
150
175
200
EST2 RIF1 RIF2
EST2 RIF1 RIF2
EST2 rif1Δ rif2Δ
25
75
125
175
225
275
325
375
Generations
10
8
6
5
4
3
2
1.5
M 1 2 3 4 5 6 7 8 9 10 11 12 13 14 15 16 17 18 19

Figure 1.9: Telomere length analysis on an *EST2 rif1Δ rif2Δ* strain. Each lane represents DNA from a representative colony of an *EST2 rif1Δ rif2Δ* strain that was grown on rich-media for the indicated successive restreaks for approximately 375 generations (lanes 2-9; 12-19). The colony in lane 2 is the parent to the colonies represented in lanes 3 thru 10. The colony in lane 12 is the parent to the colonies represented in lanes 13 thru 19. DNA was isolated, digested with *XhoI*, and separated by electrophoresis. Denatured DNA was wet transferred to a nitrocellulose membrane and probed with a radiolabeled telomeric fragment. The marker is indicated in kilo base pairs. An *EST2 RIF1 RIF2* strain is included for comparison (lanes 1, 10, 11). Although the telomeres were severely over-elongated, by the 375th generation, the colonies were small and slow growing (data not shown). Experiment performed with Charlene Hawkins.

Collectively, these data from mammalian and yeast demonstrate that simply over-extending telomeres will not fix all the deleterious consequences for cells. The majority of the telomere and telomerase field is exploring defects in telomerase that result in shorter telomeres. The analysis of long telomeres is an untapped avenue of importance as labs and therapeutic companies continue to target telomerase for the reversal of cancer, aging, and diseases such as dyskeratosis congenita and aplastic anemia that are associated with telomere shortening. My published work (Bairley et al., 2011) (see Chapter II) adds to this body of knowledge by showing that a mutation in the TEN domain of the yeast TERT component, resulting in over-elongated telomeres, is an important regulator of the anchor-site DNA binding function as well as RNA template-DNA substrate alignments. Future studies addressing the global consequences of the altered telomere sequences and longer telomeres are outlined in Chapter III.

CHAPTER II

A MUTATION IN THE CATALYTIC SUBUNIT OF YEAST TELOMERASE ALTERS PRIMER/TEMPLATE ALIGNMENT WHILE PROMOTING PROCESSIVITY AND PROTEIN/DNA BINDING.

Introduction

Chemical constraints of DNA replication prevent complete duplication of linear eukaryotic chromosomes (i.e. end-replication problem). In most eukaryotic organisms, chromosome shortening is counteracted by the enzyme telomerase, a ribonucleoprotein complex that uses a portion of its intrinsic RNA molecule as a template for nucleotide addition to the end of the chromosome (Greider and Blackburn, 1985). Telomeres consist of a variable number of double-stranded G-rich repeats, terminating in a short 3' overhang (Shampay, Szostak and Blackburn, 1984). The TG-rich telomere forms the basis of the telosome by providing binding sites for proteins that protect the chromosome terminus from nucleolytic digestion and inappropriate DNA repair.

The telomerase enzyme is minimally composed of a catalytic subunit (Telomerase Reverse Transcriptase; TERT) and an RNA containing a short template region complementary to the telomeric repeat. Base pairing between the telomerase RNA and the single-stranded 3' telomeric overhang allows nucleotide addition to the chromosome terminus by reverse transcription of template nucleotides (de Lange, Blackburn and Lundblad, 2006). The yeast *Saccharomyces cerevisiae* TERT is encoded by the *EST2* gene (Lendvay et al., 1996; Lingner et al., 1997b) and the RNA moiety is encoded by *TLC1* (Lendvay et al., 1996; Singer and Gottschling, 1994). These components constitute the catalytic core of the enzyme and are required for *in vitro* and *in vivo* activity (Lingner

et al., 1997a). Like other TERT homologs, Est2p contains a catalytic domain that is conserved with reverse transcriptases of retroviruses and non-LTR retrotransposons (Lingner et al., 1997b; Nakamura et al., 1997).

Telomerase displays two types of processivity during telomere synthesis. Type I (nucleotide addition) processivity refers to the propensity of the enzyme to synthesize a full repeat extending to the end of the RNA template region. In contrast, Type II (repeat addition) processivity describes the ability of telomerase to reposition the 3' end of a newly synthesized repeat within the active site for a second round of reverse transcription (Greider, 1991; Lue, 2004). Repeat addition processivity of both human and *Tetrahymena* telomerase is affected by sequences at the 5' end of the primer (Finger and Bryan, 2008; Jacobs, Podell and Cech, 2006; Lee and Blackburn, 1993). Multiple experiments have suggested that a region of telomerase outside of the active site mediates an "anchor-site" interaction with these upstream primer nucleotides that is important for the ability of telomerase to undergo reiterative copying of the RNA template (Autexier and Lue, 2006).

Assays of telomerase activity implicate an N-terminal domain of TERT [called Telomerase Essential N-terminus (TEN), GQ, or Region I (Friedman and Cech, 1999; Jacobs, Podell and Cech, 2006; O'Connor, Lai and Collins, 2005; Xia et al., 2000)] in anchor-site function (Lue, 2004; Lue, 2005; Moriarty et al., 2005). Mutations within the *Tetrahymena* TEN domain decrease interaction with the DNA primer (Jacobs, Podell and Cech, 2006) and the primer can be photo-cross-linked to a fragment containing the *Tetrahymena* and *S. cerevisiae* TEN domains (Lue, 2005; Romi et al., 2007). Direct binding assays have demonstrated that the isolated TEN domain from human and *Tetrahymena* binds telomeric DNA (Finger and Bryan, 2008; Sealey et al., 2010; Wyatt,

Lobb and Beattie, 2007; Wyatt et al., 2009). In *S. cerevisiae*, a fragment of Est2p containing the TEN domain interacts with full-length *TLC1* RNA and increasing amounts of DNA compete with the RNA for protein binding *in vitro* (Xia et al., 2000). Mutations thought to disrupt the *S. cerevisiae* anchor-site interaction impair catalytic function and processivity on specific primers *in vitro* (Lue and Li, 2007). The TEN domain of human TERT may also mediate positioning of the 3' end of the primer in the active site in a manner independent of the anchor-site interaction defined above (Jurczyluk et al., 2010).

In contrast to human telomeres, which contain perfect 5'-TTAGGG repeats, *S. cerevisiae* telomeres contain 300 base pairs (+/- 50) of heterogeneous $C_{1-3}A/TG_{1-3}$ tracts (Shampay, Szostak and Blackburn, 1984). Heterogeneity arises in part due to łow nucleotide addition processivity. Synthesis often terminates before the 5' end of the template, resulting in the generation of variable primer sequences for the next round of synthesis (Förstemann and Lingner, 2001). In addition, yeast telomerase tolerates multiple registers of primer/template alignment (Förstemann and Lingner, 2001; Teixeira et al., 2004). Although the general phenomena that generate telomere heterogeneity have been described, how the catalytic core modulates telomere sequence is less well understood.

We have previously described mutants in the TEN domain of Est2p (the *est2-LT* alleles) that alter the sequence of the telomeric repeat, but were unable to determine the mechanism that gives rise to this change. Interestingly, while these mutations increase telomere length by about 30% (~100 base pairs), this telomere over-elongation does not appear to be directly related to the change in telomere sequence (Ji et al., 2008). The *est2-LT* mutations do not affect nucleotide addition processivity *in vitro* (Ji et al., 2005), but

the *est2-LT*^{E76K} allele increases repeat addition processivity under specific primer extension conditions (Lue and Li, 2007).

Here, we investigate the telomere sequence alteration and processivity phenotypes of the *est2-LT*^{E76K} allele. Analysis of both *de novo* telomere addition and endogenous telomere sequences supports the hypothesis that this mutation alters telomere sequences by affecting the alignment of the DNA primer with the telomerase RNA template. We also employ expression of two distinguishable *TLC1* template alleles to show that the *est2-LT*^{E76K} mutation slightly increases processivity of telomerase *in vivo*, similar to the effect previously reported *in vitro*. Recombinant Est2p TEN domain (residues 1-161) associates with a single-stranded oligonucleotide containing the yeast telomere sequence. Mutations previously suggested to disrupt anchor-site interaction eliminate DNA binding in this assay and introduction of the E76K mutation into the purified TEN domain increases its ability to bind telomeric DNA. These results support the idea that the anchor-site interaction in yeast contributes to repeat addition processivity and suggest a novel role in guiding alignment of the DNA primer with the RNA template.

Results

Telomere over-elongation does not correlate with a specific change in telomere sequence.

Our previous work showed that mutations in *EST2* that cause telomere lengthening are associated with changes in the telomere sequence (Ji et al., 2008). Both *est2-LT*^{E76K} and *est2-up34* [D460N; located within the reverse transcriptase domain (Eugster et al., 2006)] cause the same telomere sequence changes despite requiring different genetic

pathways for over-elongation (Ji et al., 2008). Based on these data, it remained possible that telomere sequence changes observed in these *est2* mutant strains are an indirect consequence of disrupted telomere length homeostasis.

Although the yeast telomere sequence is heterogeneous, a heptamer motif (5'-TGGGTGT-3') complementary to the central portion of the *TLC1* template (underlined; 3'-ACACAC<u>ACCCACA</u>CCAC -5') can be used to define individual repeats (Förstemann and Lingner, 2001). In some cases, "core motifs" occur in groups of two or more where the last T of the first motif corresponds to the first T of the next motif (TGGGTG**<u>T</u>**GGGTGT; called an "overlap"). In other cases, core motifs are separated by $(TG)_n$ or $GG(TG)_n$ sequences of variable length. Rare variations of the spacer sequence (<10% of repeats) also occur. Since telomeres in both wild-type and mutant strains contain core motifs, we have analyzed two properties of "inter-core regions" that lie between core motifs. First, the frequency of core motif overlap is calculated as the number of inter-core regions that consist of overlaps divided by the total number of inter-core regions (Ji et al., 2008). Second, the frequency with which the GG dinucleotide occurs within the telomeric sequence is calculated as the number of inter-core regions containing the GG dinucleotide divided by the total number of core motifs (Ji et al., 2008). By analyzing the sequence of an *ADE2*-marked telomere lacking subtelomeric repeats in the GA426 *EST2* strain, we previously showed that 53% of core motifs are followed by a GG dinucleotide, while 29% of the inter-core regions are overlaps. In contrast, GA426 *est2-LT*^{E76K} has telomeres in which 67% of core motifs are followed by a GG dinucleotide and only 18% of the inter-core regions are overlaps (Ji et al., 2008). As described in Materials and Methods, sequence calculations are confined to those

telomeric repeats synthesized during clonal growth from a single cell, thus representing the sequence generated after introduction of the mutant allele.

We first verified that sequence phenotypes are reproducible by analyzing different chromosome ends and wild-type strain backgrounds. To address chromosome arm specificity, we analyzed telomere sequences from chromosome XV-L. As shown in Figure 2.1A, the overlap and GG-dinucleotide frequencies are extremely similar to those at the *ADE2*-marked telomere. To address strain specificity, telomeres from chromosome XV-L were cloned and sequenced from three additional *EST2* strains. Telomere sequence patterns were very similar between these strains with GG dinucleotide incorporation of 47 - 55% and overlap generation of 26 - 29% (Figure 2.1A). Telomeres from a UCC5706 *est2-LT*^{E76K} strain show an indistinguishable sequence pattern from those obtained in the GA426 *est2-LT*^{E76K} background (Figure 2.1A). Together, these results suggest that the observed telomere sequence differences between *EST2* and *est2-LT*^{E76K} strains are not chromosome arm- or strain-dependent. Given that cloning and sequencing of individual telomeres is time and cost intensive, these data also demonstrate that analysis of approximately 80 core motifs per strain gives a reliable and reproducible measure of the telomeric sequence pattern.

Having established the robustness of this assay, we tested whether other strains with over-elongated telomeres cause similar telomere sequence phenotypes using the *ADE2*-marked chromosome V-R from strain GA426. Six different mutant strains were analyzed: *rif1Δ, rif2Δ, pif1Δ, pif1-m2, elg1Δ,* and *ssn8Δ*. The Rif1/2 and Pif1 proteins have well characterized roles in the negative regulation of telomere length.

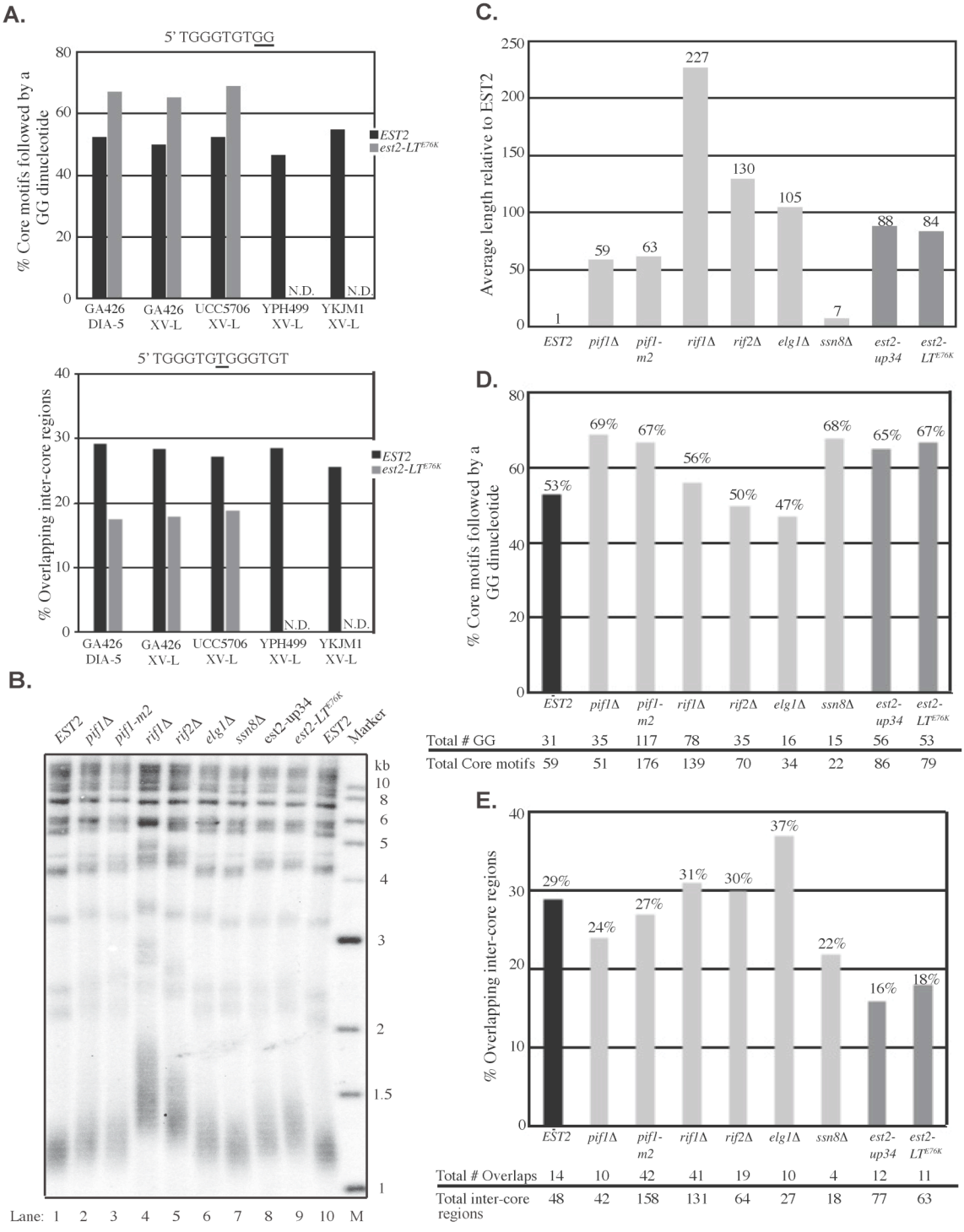
A.
5' TGGGTGTGG
% Core motifs followed by a GG dinucleotide
EST2
est2-LT^E76K
N.D.
GA426 DIA-5
GA426 XV-L
UCC5706 XV-L
YPH499 XV-L
YKJM1 XV-L
5' TGGGTGTGGGTGT
% Overlapping inter-core regions
B.
EST2
pif1Δ
pif1-m2
rif1Δ
rif2Δ
elg1Δ
ssn8Δ
est2-up34
est2-LT^E76K
Marker
kb
Lane: 1 2 3 4 5 6 7 8 9 10 M
C.
Average length relative to EST2
1
59
63
227
130
105
7
88
84
D.
% Core motifs followed by a GG dinucleotide
53%
69%
67%
56%
50%
47%
68%
65%
67%
Total # GG 31 35 117 78 35 16 15 56 53
Total Core motifs 59 51 176 139 70 34 22 86 79
E.
% Overlapping inter-core regions
29%
24%
27%
31%
30%
37%
22%
16%
18%
Total # Overlaps 14 10 42 41 19 10 4 12 11
Total inter-core regions 48 42 158 131 64 27 18 77 63

Figure 2.1: Disruption of negative telomere length regulation does not result in a specific telomere sequence phenotype. The indicated strains were grown for a minimum of 75 generations before cloning of telomeres by ligation-mediated PCR from the *ADE2* marked chromosome V-R (DIA-5) or from chromosome XV-L. Chromosome V-R data for the *EST2*, *est2-up34*, and *est2-LT*^{E76K} GA426 strains were previously published (Ji *et al*., 2008) and are included for comparison. **(A)** Telomere sequence characteristics of the indicated chromosome ends expressing either *EST2* (black bar) or *est2-LT*^{E76K} (gray bar). N.D.: not determined. **(B)** GA426 telomere length of GA426 strains determined by Southern blotting. Genomic DNA from the indicated strains was cleaved with *Xho*I, Southern blotted, and probed with a radiolabeled telomeric fragment. Marker sizes are in kilobases (kb). **(C)** Average length of 9 – 21 cloned telomeres used to generate data in D and E. Telomere length is normalized to the GA426 *EST2* strain. Black bar -*EST2*; dark gray bars - *est2-up34* and *est2-LT*^{E76K}; light gray bars - six additional mutants. **(D)** Percent of core motifs followed by a GG dinucleotide in telomeres from the indicated GA426 strains. Primary data for each strain are indicated (bottom). Grayscale categories are the same as in (C). **(E)** Percent of inter-core regions in the same telomeres analyzed in (D). Primary data for each strain are indicated (bottom). Grayscale categories are the same as in (C and D).

Rif1p and Rif2p negatively regulate telomere length through interactions with Rap1p (Hardy, Sussel and Shore, 1992; Wotton and Shore, 1997). Telomere lengthening by the *est2-up34* mutation requires the function of Pif1p (Eugster et al., 2006). This DNA helicase negatively regulates telomere length by dissociating telomerase from the chromosome terminus (Boulé, Vega and Zakian, 2005; Zhou et al., 2000) and has a second function in the maintenance of mitochondrial DNA (Lahaye et al., 1991). To avoid complications of this pleiotrophic phenotype, we analyzed telomere sequences in GA426 strains containing either *pif1*Δ or *pif1-m2*, an allele that retains mitochondrial function but lacks most telomere function (Schulz and Zakian, 1994). *ELG1* and *SSN8* were described as negative regulators of telomere length in a genome-wide telomere maintenance screen (Askree et al., 2004). *ELG1* plays a role in genome stability (Ben-

Aroya et al., 2003) and transcriptional silencing (Smolikov, Mazor and Krauskopf, 2004). *SSN8* encodes a cyclin homolog with 35% identity to human cyclin C, but its role in telomere length regulation is unclear (Kuchin, Yeghiayan and Carlson, 1995).

All strains except *ssn8Δ* caused telomere over-elongation to an extent similar or greater than that observed in the *est2-LT^{E76K}* and *est2-up34* strains [measured by Southern blot (Figure 2.1C) and average length of cloned telomeres (Figure 2.1 D)]. In this light, it is interesting that only *ssn8Δ* has a telomere sequence phenotype similar to that of *est2-LT^{E76K}* (Figure 2,1D, E; 22% overlaps and 68% GG dinucleotides) while the other mutant strains either resemble *EST2* (*rif1Δ, rif2Δ*), have an intermediate phenotype (*pif1Δ, pif1-m2*), or display a telomeric sequence pattern not previously observed (*elg1Δ*). Taken together, these data suggest the *est2-LT^{E76K}* sequence phenotypes are not a general consequence of overly long telomeres.

Mutation of Est2p E76 to lysine alters the alignment of telomerase with the telomeric primer.

The heterogeneity of yeast telomeres has been proposed to arise through a combination of poor processivity and multiple sites of primer/template alignment (Förstemann and Lingner, 2001). Using an allele of *TLC1* that contains a mutation near the 5' end of the template region (^{469}A to U), we found that the rate at which the complementary A is incorporated into the telomere by *est2-LT^{E76K}* telomerase is indistinguishable from that of *EST2* telomerase (Ji et al., 2008). These results suggest that altered nucleotide-addition processivity alone is unlikely to explain the differences in telomere sequence, albeit subtle changes in telomerase processivity at nucleotides proximal to the core motif have not been ruled out.

We hypothesized that the *est2-LT*^{E76K} mutation instead alters the position at which the telomerase template aligns with the DNA substrate. Since terminal primers generated during normal telomere replication can have different 3' termini, determining the site at which the 3' end of the primer aligns with the *TLC1* template during the next round of addition is difficult. Instead, we took advantage of a strain that allows extension of a known telomeric seed by telomerase *in vivo* (Diede and Gottschling, 1999). In this *de novo* telomere assay, the non-essential terminus of chromosome VII-L is modified to contain the *ADE2* gene, an 81 base pair telomeric "seed" sequence, and a telomere-proximal HO endonuclease cleavage site (Figure 2.2A). A *LYS2* marker integrated distal to the HO cleavage site allows selection for cells that retain the chromosome terminus prior to induction of the HO endonuclease.

EST2 and *est2-LT*^{E76K} strains were grown as described in Materials and Methods. The *de novo* telomeres present at the 4-hour time point were amplified from the *ADE2*-marked telomere by ligation-mediated PCR, cloned and sequenced. Consistent with the telomere length measured by Southern blot (Figure 2.2 B), the average *de novo* telomere synthesized by *EST2* is 154 base pairs compared to the average *de novo* telomere of 263 base pairs synthesized by *est2-LT*^{E76K} telomerase. The HO endonuclease generates a 4 base 3' overhang ending in 5'-TGTT-3' (Kostriken et al., 1983). With one exception, telomere addition was initiated on this site and not within the telomeric seed sequence. Because only a single T remains at the junction of *de novo* telomere addition, the terminal T must be removed prior to telomerase action. For the remaining 5'-TGT-3' sequence, it is unclear which nucleotides were present in the overhang and which were added by

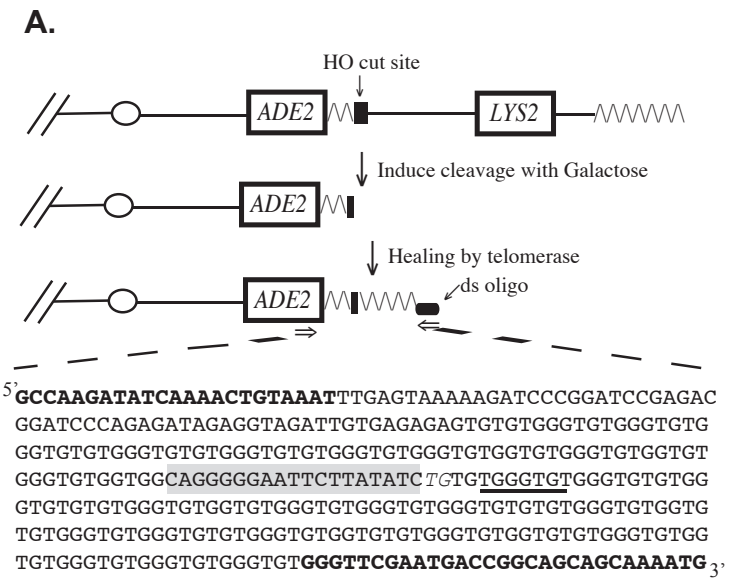

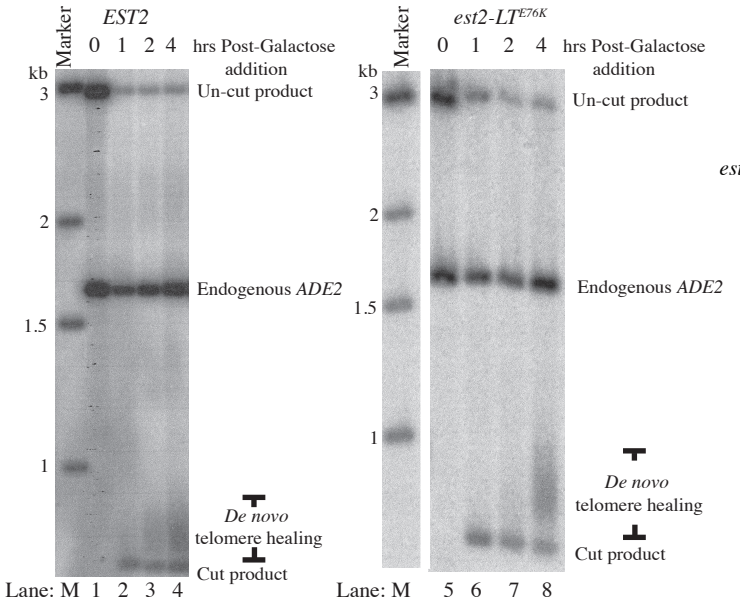

C.

Exceptional de novo healing events

Synthesized nucleotides	Telomerase	Freq
TTCTTATAC*TG*TTGGGTGT	*est2-LT*^{E76K}	1/16
TTCTTATAC*TG*TGTGGTGTGTGTGGGTGT	*est2-LT*^{E76K}	1/16
TTCTTATAC*TG*TGTGTGGTGTGTGGGTGT	*EST2*	1/17
TTCTTATAC*TG*TGTGGTGTGTGTGGGTGT	*EST2*	1/17
TTCTTATAC*TG*GTGTGGGTGT	*EST2*	1/17

D.

EST2 :	6	4	2	1	0	1	(of 17)
est2-LT^{E76K} :	1	5	7	1	0	0	(of 16)

E.

Alignments	#TG	enzyme preference
3′ - ACACACACCCACACCAC -5′ *TLC1* GGAATTCTTATAC*TG*TGGGTGT...	add 0 TG	*EST2*
3′ - ACACACACCCACACCAC GGAATTCTTATAC*TG*TGTGTGGGTGT...	add 2 TG	*est2-LT*^{E76K}

Figure 2.2: The *est2-LT*^{E76K} mutation alters the alignment of telomerase with a short telomeric primer. **(A)** Illustration of the *de novo* telomere addition system developed by Diede and Gottschling, 1999. The left arm of chromosome VII is modified by addition (from centromere to telomere) of an *ADE2* gene, 81 base pairs of telomere sequence, an HO endonuclease cleavage site, and the *LYS2* gene. Upon addition of galactose, expression of the HO endonuclease is induced and cleavage exposes a single-stranded overhang. *De novo* telomeres are isolated by ligation-mediated PCR utilizing primers specific to the ligated oligonucleotide and to the *ADE2* gene (bold). An example telomere synthesized by *est2-LT*^{E76K} is shown. The 5'-TG-3' sequence assumed to facilitate primer/template alignment is italicized and the remainder of the HO endonuclease recognition site is highlighted in gray. The first core motif of the *de novo* telomere is underlined. **(B)** Time course of *de novo* telomere addition by *EST2* (Lanes 1-4) and *est2-LT*^{E76K} (Lanes 5-8) telomerase. Cells were harvested immediately prior to HO induction (0 hrs) or 1, 2, and 4 hours after galactose addition as indicated. Marker sizes are in kilobases (lane M). Positions of the un-cut product (no HO endonuclease cleavage) and endogenous *ADE2* fragment are indicated. Cleavage by HO endonuclease releases a short fragment (cut product) that is elongated by telomerase (*de novo* telomere healing). **(C)** Exceptional *de novo* telomere addition events. Sequences added to the 5'-TG-3' primer within the HO endonuclease cleavage site are shown in a 5' to 3' orientation. The first core motif is underlined and the TG sequence generated by HO endonuclease cleavage is italicized. **(D)** Number of TG dinucleotide sequences synthesized between the 5'-TG-3' HO cleavage site and the first core motif by *EST2* or *est2-LT*^{E76K} telomerase. Total *de novo* telomeres analyzed were 17 (*EST2*) and 16 (*est2-LT*^{E76K}). **(E)** Model of the preferred alignment for *EST2* and *est2-LT*^{E76K} telomerase with the primer remaining after HO endonuclease cleavage (indicated in gray italics). Newly synthesized sequence extends to the right. The first core motif is underlined.

telomerase during *de novo* telomere synthesis. For simplicity, we assume that synthesis initiated on a primer ending in 5'-TG-3' (Figure 2.2 A, italics). Analysis was conducted on 17 *EST2* telomeres and 16 *est2-LT*^{E76K} telomeres. With few exceptions (three in the *EST2* strain and two in the *est2-LT*^{E76K} strain; Figure 2.2 C), telomerase synthesized 0 - 5 TG dinucleotides before the first core motif (5'-TG$_{0\text{-}5}$TGGGTGT; Figure 2.2 D). Addition of 0 - 2 TG dinucleotides is most simply explained as a single

annealing event, followed by synthesis through the central region of the template (Figure 2.2 E). Addition of 3 or more TG dinucleotides requires more than one round of annealing and synthesis, making the specific site of primer/template annealing unclear. Several anomalous cases were observed in which a GG dinucleotide interrupted the TG repeats or in which the TT dinucleotide present in the HO cleavage site was retained (Figure 2.2 C). These events did not appear to differ in type or frequency between the *EST2* and *est2-LT*^{E76K} strains and were not analyzed further.

Among those telomeres in which 0 - 2 TG dinucleotides were added prior to the first core motif, there is a striking difference between the *EST2* and *est2-LT*^{E76K} strains. As shown in Figure 2.2 D, 35% of the telomeres synthesized in the *EST2* strain contained a core motif immediately adjacent to the 5'-TG-3' primer (0 TG), while the *est2-LT*^{E76K} strain exhibited this pattern in only 6% of *de novo* telomeres. Incorporation of 1 TG dinucleotide was approximately equal in the two strains. In contrast, 44% of *est2-LT*^{E76K} telomeres contained 2 TG dinucleotides prior to the first core motif, while the same pattern was observed in only 12% of telomeres synthesized in the *EST2* strain (Figure 2.2 D). These differences are statistically significant (Chi-square, p=0.04) and suggest the *est2-LT*^{E76K} mutation alters the preferred sites at which telomerase aligns with a short TG primer. *EST2* telomerase prefers to align with template nucleotides ^{481}CAC^{479} (immediately 3' of the core motif template) whereas *est2-LT*^{E76K} prefers to align at a more 3' position of the template with nucleotides ^{484}ACA^{482} (Figure 2.2 E).

Improved primer/template complementarity eliminates the difference in telomere sequences from *EST2* and *est2-LT^{E76K}* strains.

Because the activity of telomerase in the *de novo* telomere-healing assay may not fully recapitulate the behavior of the enzyme during normal telomere replication, we sought to verify the results shown in Figure 2.2 by analyzing the pattern of telomere addition at normal chromosome ends. As described above, analysis within endogenous telomeres is difficult because the nature of the 3' telomeric primer is ambiguous. Potential exceptions to this generalization are repeats in which a GG dinucleotide is incorporated following the core motif. We and others have shown that the GG dinucleotides arise exclusively from reverse transcription of template nucleotides ^{471}CC^{470} by *EST2* (Förstemann and Lingner, 2001) and est2-*LT^{E76K}* (Ji et al., 2008). Also, *est2-LT^{E76K}* telomerase incorporates the nucleotide complementary to *TLC1* position A^{469} at the same rate as the *EST2* enzyme (Ji et al., 2008). Following a GG dinucleotide, a maximum of one TG dinucleotide can be added by reverse transcription at the 5' end of the RNA template. Additional TG dinucleotides must arise through alignment of the primer terminus with the 3' end of the RNA template (Figure 2.3 A, top). We therefore reasoned that differences in primer alignment contributed by the *est2-LT^{E76K}* mutation might be detected in endogenous telomeres as a difference in the number of TG dinucleotides incorporated between each GG dinucleotide and the subsequent core motif.

In the divergent 3' end-portions of telomeres synthesized by *EST2* with *TLC1*, the GG dinucleotide and adjacent core motif are separated by 1-3 TG dinucleotides, although rare instances of 0 or 4 TG repeats are observed (Figure 2.3 A). The exact position at which the 3' end of the primer aligns with the template is unknown since the first TG

sequence may be derived from copying of the 5' template nucleotides (^{469}AC^{468}) or from realignment of a GG-terminated primer at the 3' end of the template (Figure 2.3 A, top). Despite this ambiguity, it appears that *EST2* telomerase utilizes several different alignment registers, with the most common alignment being that depicted in Figure 2.3 A. In contrast, the divergent 3' end-portions of telomeres synthesized in an *est2-LT^{E76K} TLC1* strain are more homogeneous, with 83% of GG dinucleotides followed by 1 - 2 TG repeats (Figure 2.3 A). The differences in TG repeat distribution between the two strains is statistically significant (Chi-square, p=0.0029). These results at endogenous telomeres are consistent with the conclusion from the *de novo* telomere addition assay that alignment between primer and template is changed by the *est2-LT^{E76K}* mutation.

If differences in primer/template alignment contribute to the telomere sequence changes observed at endogenous telomeres in the *est2-LT^{E76K}* strain, then a mutation in the *TLC1* template that increases complementarity between the DNA primer and the 3' end of the RNA template might overcome, or be epistatic to, any difference in alignment caused by the *est2-LT^{E76K}* mutation. We took advantage of a *TLC1* allele previously created and characterized by the Lingner lab (*tlc1-KF10*) (Förstemann and Lingner, 2001). This allele alters template nucleotides ^{484}ACA^{482} to CAC. As a result, a telomeric primer that terminates in 5'-TGGGTGTGG(TG)-3' can base pair perfectly with 4 (or 6) of the 3' nucleotides of the *TLC1* template (Figure 2.3 B, top).

By Southern blot, expression of *tlc1-KF10* increases telomere length in both the *EST2* and *est2-LT^{E76K}* strains (Figure 2.3 C). The increase in telomere length for the *EST2*

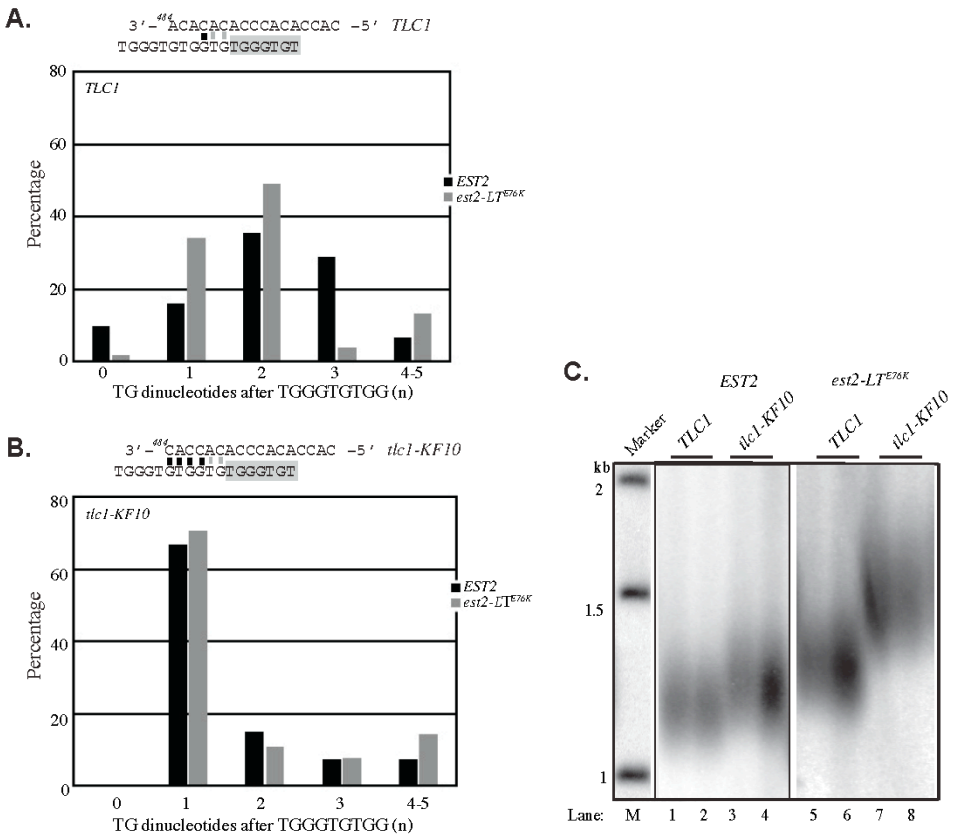

Figure 2.3: A mutation in the *TLC1* template eliminates sequence pattern differences. **(A)** Top: Alignment of a telomeric primer ending in 5'- TGGGTGTGG with the *TLC1* template to generate a single TG dinucleotide prior to the following core motif. The black horizontal line indicates the position of complementarity. Complementarity may continue through the following two template positions (gray bars) if synthesis in the previous round extends to the end of the *TLC1* template (see text for detail). Newly synthesized nucleotides are highlighted in gray. Bottom: Percentage of core motifs associated with a GG dinucleotide (5'TGGGTGTGG) that is followed by the indicated number of TG dinucleotides prior to the subsequent core motif. Black bars - *EST2* telomeres; gray bars - *est2-LT*^{E76K} telomeres. **(B)** Same as (A) except the template used is from the *tlc1-KF10* allele. **(C)** Southern blot of telomere length in GA426 *tlc1::KAN* strains expressing *EST2* (lanes 1-4) or *est2-LT*^{E76K} (lanes 5-8) from the endogenous locus and complemented with plasmids expressing *TLC1* (lanes 1, 2, 5, 6) or *tlc1-KF10* (3, 4, 7, 8). Marker sizes are in kilobases (kb).

tlc1-KF10 strain has also been reported by the Lingner group (Förstemann and Lingner, 2001) and likely results from the reduced number of predicted Rap1p binding sites within this altered telomere sequence. When using this template, *EST2* telomerase almost always synthesizes a GGTG inter-core region (TGGGTGTGGTGTGGGTGT), consistent with the alignment predicted for this template mutant (Figure 2.3 B). Telomeres in the *est2-LT^{E76K} tlc1-KF10* strain show a nearly identical pattern (Chi-square, p=0.6372). The ability of the improved base pairing interaction between the DNA primer and the *tlc1-KF10* RNA template to eliminate the observed difference between *EST2* and *est2-LT^{E76K}* telomeres is consistent with the proposal that altered primer/template alignment underlies sequence changes within the *est2-LT^{E76K}* telomeres. However, because the *tlc1-KF10* allele also affects the sequence of telomeres synthesized by *EST2* telomerase, we cannot exclude the possibility that an unrelated defect of the *est2-LT^{E76K}* allele is masked under these conditions.

The E76 to lysine mutation in Est2p increases the repeat-addition processivity of telomerase *in vivo*.

Yeast telomerase generally has low repeat addition processivity except at telomeres shorter than 125 base pairs (Chang, Arnerić and Lingner, 2007). The *est2-LT^{E76K}* mutation has been reported to moderately increase repeat-addition processivity of telomerase *in vitro* (Lue and Li, 2007). However, the relevance of this observation for the behavior of telomerase *in vivo* has been unclear. To test whether the mutant enzyme also demonstrates increased processivity in cells, we co-expressed a wild-type and a mutant *TLC1* allele in GA426 *EST2* and GA426 *est2-LT^{E76K}* strains, cloned and sequenced the newly synthesized telomeric DNA, and analyzed the pattern of interspersion of the two

repeat types. The *tlc1-tm* allele contains a highly altered template sequence (3'-ACACCUAAACCACACACAC-5'; Figure 2.4 A), but has a minor effect on telomere length when expressed alone (Chang, Arnerić and Lingner, 2007). Importantly, when *TLC1* and *tlc1-tm* are co-expressed and telomere addition is monitored during a single S phase, a fraction of the shortest telomeres that undergo processive elongation contain strings of mutant repeats, indicating that *tlc1-tm* can be used processively by the *EST2* enzyme (Chang, Arnerić and Lingner, 2007).

PCR amplification of the *ADE2*-marked chromosome V-R telomere confirmed that co-expression of *TLC1* and *tlc1-tm* does not alter the long-telomere phenotype of *est2-LT*^{E76K} (Figure 2.4 A). The lengths of identical and divergent portions of each cloned telomere are shown in Figure 2.4 B. The average total length of telomeres from the *est2-LT*^{E76K} strain was 63 base pairs longer than *EST2* telomeres, with an average of 15 base pairs more divergent telomeric sequence per telomere than in the *EST2* strain (Figure 2.4 B).

An *EST2 tlc1-tm* strain generates a telomeric consensus repeat of $(TG_{0-4}TGG)_n$ (Chang, Arnerić and Lingner, 2007). The *tlc1-tm* sequences are distinguishable from those templated by *TLC1* due to the frequent incorporation of the GG dinucleotide without an intervening GGG sequence and by the occasional synthesis of an ATTTGG repeat (Chang, Arnerić and Lingner, 2007). The number of consecutive *tlc1-tm* repeats was defined as the number of consecutive GG motifs in the absence of an intervening core motif. *TLC1* repeats were defined by the number of consecutive core motifs (5' TGGGTGT). Because the *TLC1* template can also be used to synthesize GG dinucleotides, we made the assumption that any GG dinucleotide immediately following

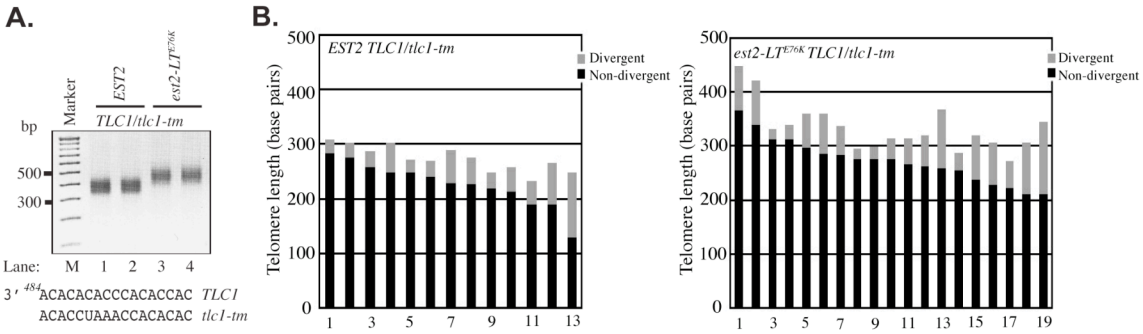

C.

Examples from *EST2 TLC1/tlc1-tm* strain

12. GTGGGTGTGGTGTGGTGTGTGTGGGTGTGGGTGTGGTGTGGGTGTGGTG
13. GTGGGTGTGTGTTTGGGTTTGGGTGTGTGTGGGTGTGGTGTGTGGGTGTGGGTGTGGTGGGTGTGGTGTGTGTGGGTGTGGTGTGTGTGGGTGTGGTGGATTTGGTGTGGTGTGTGTGGGTGTGTGT

Examples from *est2-LT*^{E76K} *TLC1/tlc1-tm* strain

1. TGTGGTGTGTGGGTGTGGTGTGTGGGTGTGGTGGTGTGTGGTGGTGTGTGTGGGTGTGGTGTGGGTGTGGTGTGTGTGTGGGTGTGGTGTGTGTGGGTGTGGGTGT
18. TGTGGTGTGTGGGTGTGGTGTGTGTGGGTGTGTGTGGGTGTGTGGGTGTGGGTGTGGTGTGTGGGGTGTGGGTGTGGTGTGTGGGTGTGGGTGGATTTGGTGTGTGTGGG

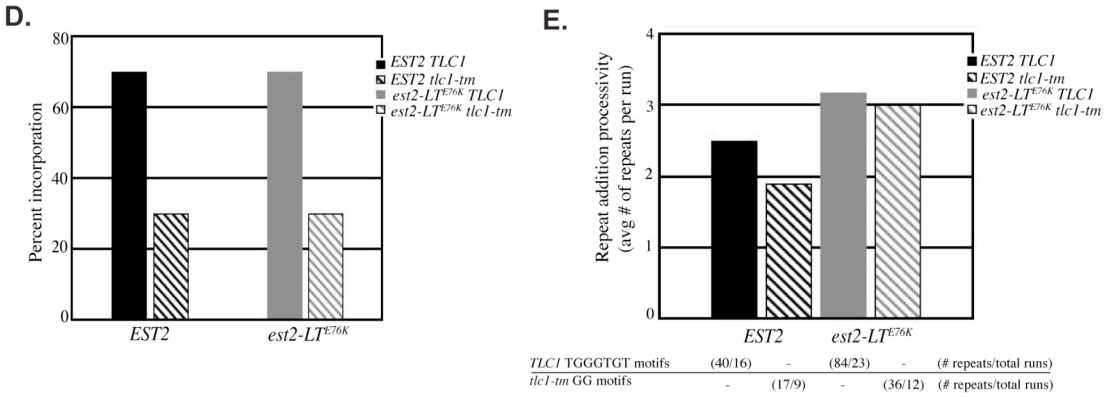

Figure 2.4: The *est2-LT*^{E76K} telomerase demonstrates increased processivity *in vivo*. **(A)** Ligation-mediated telomere PCR of the *ADE2*-marked chromosome V-R was used to amplify telomeres from asynchronous cultures of *EST2* and *est2-LT*^{E76K} GA426 strains expressing both *TLC1* and *tlc1-tm* RNAs. PCR products were separated by agarose gel electrophoresis. Marker sizes are in base pairs (bp). The template sequences of *TLC1* and *tlc1-tm* are shown (bottom). **(B)** Length of 13 *EST2 TLC1*/*tlc1-tm* and 19 *est2-LT*^{E76K} *TLC1*/*tlc1-tm* cloned telomeres. Black bars, non-divergent TG sequences; gray bars, divergent TG sequences. **(C)** Two representative telomeric sequences from *EST2* (telomeres 12 and 13) and *est2-LT*^{E76K} (telomeres 1 and 18) strains. Numbers correspond to the telomeres shown in (B). Black text, a small portion of the non-divergent sequence; red text, sequence inferred to derive from the *TLC1* template with core motifs underlined; blue text, sequence inferred to derive from the *tlc1-tm* template. **(D)** The percent of total telomeric repeats synthesized from the *TLC1* (solid bar) or *tlc1-tm* (hatched bar) template is indicated. Strains expressed wild-type *EST2* (black) or *est2-LT*^{E76K} (gray). **(E)** The average number of consecutive repeats derived from a single template (*TLC1* or *tlc1-tm*) is graphed for strains expressing *EST2* or *est2-LT*^{E76K}. Consecutive repeats of the same type are defined as a "run." The average run length was obtained from the total number of either *TLC1* or *tlc1-tm* repeats divided by the total number of runs for each template (data are indicated below each sample in the graph). Samples are labeled as in (D).

a wild-type core motif was synthesized by *TLC1* (see the example sequences in Figure 2.4 C).

Analysis was conducted on the divergent portions of 13 telomeres from an *EST2* *TLC1*/*tlc1-tm* strain and 19 telomeres from an *est2-LT*^{E76K} *TLC1*/*tlc1-tm* strain (Figure 2.4 B). *EST2* telomerase incorporates both *TLC1* and *tlc1-tm* repeats, although the majority of the repeats are derived from *TLC1* (70.2%; Figure 2.4 D). This value is identical to that previously reported for telomere addition during a single cell-cycle in the presence of both RNAs (Chang, Arnerić and Lingner, 2007). In our assay, *EST2* telomeres contain an average of 2.5 *TLC1* repeats and 1.9 *tlc1-tm* repeats per run (where a run is defined as a series of repeats of a single type). The *est2-LT*^{E76K} telomerase does not alter the relative use of the wild-type *TLC1* template (70.0%; Figure 2.4 D). However, *est2-LT*^{E76K}

telomerase generates longer run lengths than *EST2* telomerase, with an average of 3.2 consecutive *TLC1* core motifs and 3.0 consecutive *tlc1-tm* GG dinucleotide repeats (Figure 2.4 E). These data suggest that *est2-LT^{E76K}* telomerase has slightly increased repeat addition processivity compared to the *EST2* enzyme *in vivo*.

Glutamic acid 76 enhances DNA binding by the Est2p TEN domain

Given that repeat addition processivity is moderately increased by the *est2-LT^{E76K}* mutation (Figure 2.4), we speculated that glutamic acid 76 might influence the strength of DNA interaction by the TEN domain anchor-site. Crosslinking studies *in vivo* have implicated this N-terminal domain of Est2p in interactions with the telomeric primer (Lue, 2005) and the recombinant TEN domain has been previously shown to have a non-sequence specific nucleic acid binding activity (Xia et al., 2000) . To test whether the E76K mutation affects the ability of the TEN domain to interact with TG-rich single-stranded DNA, a biotin pull-down assay, similar to that utilized to characterize the human TEN domain-DNA interaction (Wyatt, Lobb and Beattie, 2007), was developed.

The first 161 amino acids of Est2p were N-terminally tagged with MBP (MBP-Est2p^{TEN}) and both wild-type and mutant variants were sequentially purified from BL21 *E. coli* cells by amylose affinity and size-exclusion chromatography (see Materials and Methods; Figure 2.5 A). A four-fold molar excess of MBP-Est2p^{TEN} was incubated with 5' biotinylated TG-rich, AC-rich or random-sequence single-stranded DNA TG-rich oligonucleotides (TG16 and TG28 respectively) compared to the AC16 control (t-test, p=0.0004). Interaction of MBP-Est2p^{TEN} with an oligonucleotide of random-sequence (Random) was not enriched over the AC16 background (Figure 2.5 B, D). There is no

statistical difference in binding by MBP-Est2p^{TEN} to the two TG oligonucleotides of different length (t-test, p=0.73). RNase treatment prior to DNA incubation does not alter protein-DNA binding (Lanes 11 and 12; Figure 2.5 B). Together, these data show that the TEN domain of yeast TERT interacts with a single-stranded TG-rich oligonucleotide of at least 16 base pairs in length in the absence of the *TLC1* RNA.

Est2p containing a mutation of R151A maintains normal levels of association with *TLC1* RNA, but is defective in telomere length maintenance and *in vitro* repeat addition processivity (Lue and Li, 2007), consistent with an anchor-site defect. The R151A mutation was introduced into the pET MBP-Est2p^{TEN} vector by site-directed mutagenesis and purified as described above (Figure 2.5 A). The interaction of MBP-Est2 R151Ap^{TEN} with the TG16 oligonucleotide is not enriched above the AC16 background and shows significantly less binding than MBP-Est2p^{TEN} (Figure 2.5 C; t-test, p=0.02), supporting the specificity of the assay. The E76K mutation was introduced into the pET MBP-Est2p^{TEN} vector by site-directed mutagenesis and recombinant protein was produced (Figure 2.5 A). Importantly, the interaction of MBP-Est2 E76Kp^{TEN} with the TG28 oligonucleotide is significantly greater than that of MBP-Est2^{TEN} (t-test, p=0.013). Collectively, these data confirm that the TEN domain of yeast Est2p functions as an anchor-site for yeast telomerase and show that mutation of E76K enhances this anchor-site interaction.

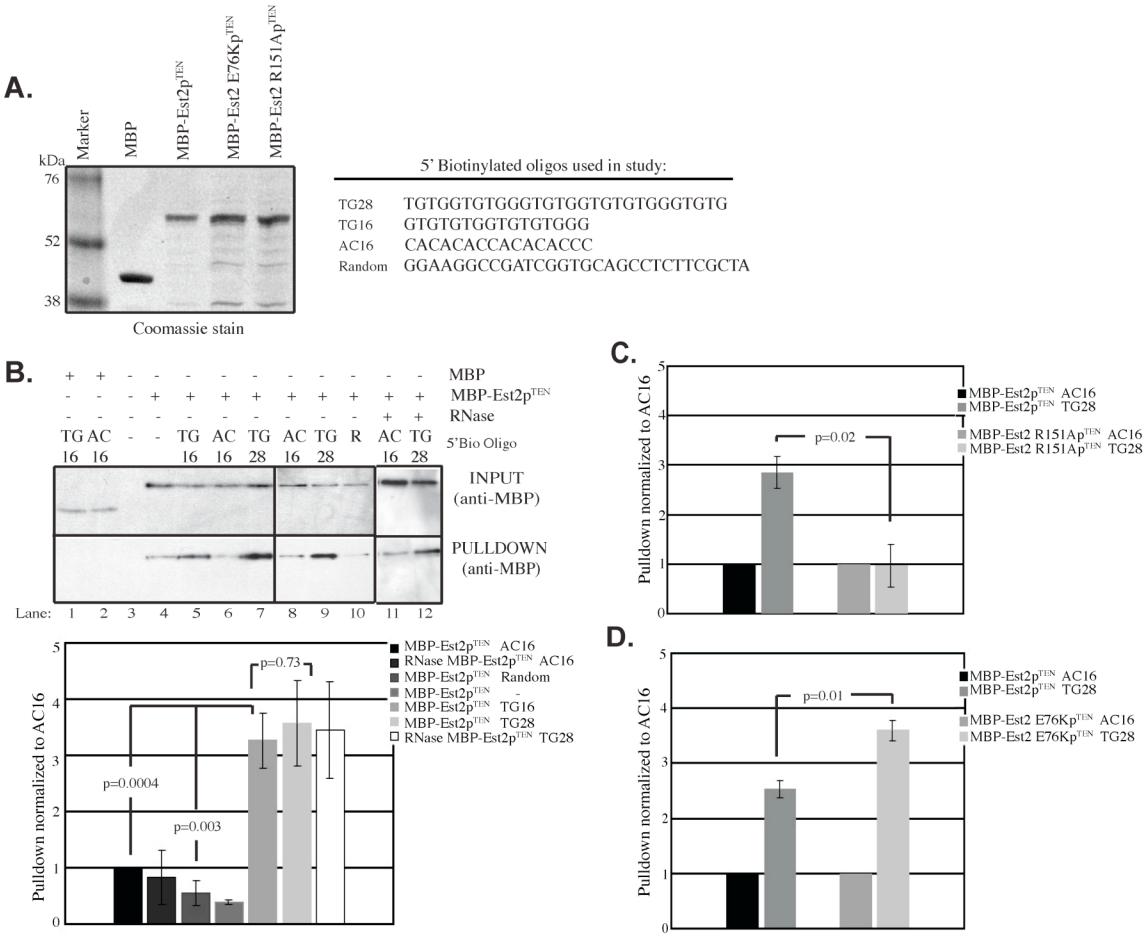
A.
Marker
MBP
MBP-Est2p^TEN
MBP-Est2 E76Kp^TEN
MBP-Est2 R151Ap^TEN
kDa
76
52
38
Coomassie stain
5' Biotinylated oligos used in study:
TG28 TGTGGTGTGGGTGTGGTGTGTGGGTGTG
TG16 GTGTGTGGTGTGTGGG
AC16 CACACACCACACACCC
Random GGAAGGCCGATCGGTGCAGCCTCTTCGCTA
B.
MBP
MBP-Est2p^TEN
RNase
5'Bio Oligo
TG16 AC16 - - TG16 AC16 TG28 AC16 TG28 R AC16 TG28
INPUT (anti-MBP)
PULLDOWN (anti-MBP)
Lane: 1 2 3 4 5 6 7 8 9 10 11 12
Pulldown normalized to AC16
p=0.0004
p=0.003
p=0.73
MBP-Est2p^TEN AC16
RNase MBP-Est2p^TEN AC16
MBP-Est2p^TEN Random
MBP-Est2p^TEN -
MBP-Est2p^TEN TG16
MBP-Est2p^TEN TG28
RNase MBP-Est2p^TEN TG28
C.
Pulldown normalized to AC16
p=0.02
MBP-Est2p^TEN AC16
MBP-Est2p^TEN TG28
MBP-Est2 R151Ap^TEN AC16
MBP-Est2 R151Ap^TEN TG28
D.
Pulldown normalized to AC16
p=0.01
MBP-Est2p^TEN AC16
MBP-Est2p^TEN TG28
MBP-Est2 E76Kp^TEN AC16
MBP-Est2 E76Kp^TEN TG28

Figure 2.5: Binding of recombinant MBP-Est2p^{TEN} to TG-rich DNA is enhanced by the E76K mutation. **(A)** Left: Coomassie-stained gel of maltose-binding protein (MBP), MBP-Est2p^{TEN}, MBP-Est2 E76Kp^{TEN}, and MBP-Est2 R151Ap^{TEN}. MBP-Est2p variants were expressed in *E. coli* and purified by amylose affinity and size exclusion chromatography. Right: Single-stranded 5'-biotinylated DNA oligonucleotides utilized for the binding assay. **(B)** Purification of MBP-Est2p^{TEN} with the TG16 and TG28 oligonucleotides is enhanced over the AC16 and random-sequence (R) oligonucleotides. Top: Input samples (INPUT) and samples following binding of the biotin-labeled primers to streptavidin beads (PULLDOWN) were separated by polyacrylamide gel electrophoresis, Western blotted and probed with anti-MBP antibody. Binding reactions contained MBP alone or MBP-Est2p^{TEN} as indicated. Lane 4 is a binding reaction in the absence of biotinylated oligonucleotide. Lanes 11 and 12 are binding reactions of RNase-treated MBP-Est2p^{TEN}. Bottom: The average binding efficiency of MBP-Est2p^{TEN} to the indicated oligonucleotide is shown from at least 4 replicates. Values are normalized to that of the AC16 oligonucleotide. Error bars represent standard error of the mean. **(C)** Association of the MBP-Est2 R151Ap^{TEN} protein with the TG28 oligonucleotide is not above background. Binding was determined and quantified as in (B) from at least 3 replicates. **(D)** MBP-Est2 E76Kp^{TEN} significantly enhances binding to the TG28 oligonucleotide as compared to MBP-Est2p^{TEN}. The average binding efficiency is calculated as in (B) from at least 4 replicates.

CONCLUSIONS

Here we demonstrate that the isolated yeast Est2p TEN domain is sufficient to bind telomeric DNA in a sequence-specific manner. A mutation in this domain (glutamic acid 76 to lysine; E76K) increases the strength of the interaction (Figure 2.5). Because this mutant supports robust telomere elongation, it affords a unique opportunity to characterize the functional importance of the anchor-site interaction. We show that the *est2-LT^{E76K}* mutation alters the spectrum of sites at which the telomerase template aligns with the chromosome terminus (Figures 2.2, 2.3), suggesting that residues within the TEN domain may influence positioning of the primer within the enzyme active site. This

mutation also slightly increases the processivity of yeast telomerase *in vivo* (Figure 2.4), a phenotype previously only reported *in vitro*. A more extensive discussion on what these findings mean to the field as well as future studies is in Chapter III. This work was funded by the National Science Foundation grant MCB-0721595 to KLF.

MATERIALS AND METHODS

Strains and plasmids

See Table 2.1 for the strains/plasmids and Table 2.2 for the primers used in this work. YKJM1 (Banerjee et al., 2008) and YPH499 (Schulz and Zakian, 1994) were gifts from K. Myung and V. Zakian respectively. YKF500 (GA426 *est2-LT*^{E76K}) has been previously described (Ji et al., 2008). Two-step gene replacement was used to generate strain YKF511 (GA426 *est2-up34*). Gene disruptions of *RIF1*, *RIF2*, *PIF1* (YKF600 – YKF602, respectively), *ELG1* (YKF604) and *SSN8* (YKF605) were obtained by amplification of the *Kan*^{R} gene and flanking DNA from the appropriate gene knockout strain (Open Biosystems). PCR products were transformed into GA426 and creation of the correct strains was verified by PCR. To make GA426 *pif1-m2* (YKF603), the *pif1-m2* allele was integrated by two-step gene replacement using plasmid pVS31. The *est2-LT*^{E76K} mutant was integrated as described (Ji et al., 2008) into UCC5706 previously transformed with a *RAD52 TRP1 CEN* plasmid to create YKF512. After integration of the mutant allele, colonies were screened for loss of the *RAD52 TRP1* plasmid. To create strains expressing *EST2* or *est2-LT*^{E76K} with either *TLC1* or *tlc1-KF10*, the endogenous *TLC1* gene was disrupted by *Kan*^{R} in strains GA426 and YKF500. Plasmids pKF5 (*TLC1*) or

pKF10 (*tlc1-KF10*) (gifts of J. Lingner) were transformed and *RAD52* was subsequently disrupted by transformation with a *rad52::LEU2* fragment (Friedman and Cech, 1999). To make *EST2* or *est2-LT*^{E76K} strains expressing *tlc1-tm*, the pLIB17 plasmid (Förstemann et al., 2003) was digested with *Hind*III and *Hpa*I resulting in 2.3 kb fragment that was ligated into pRS306 (*URA3*) (Sikorski and Hieter, 1989) to make pRS306 *tlc1-tm*. pRS306 *tlc1-tm* was digested with *Nru*I and transformed into GA426 and YKF500 to create YKF610 and YKF611 respectfully. The TEN domain mutants (E76K and R151A) were made by site-directed PCR mutagenesis as described (Landt, Grunert and Hahn, 1990) from pET Duet MBP-EST2^{TEN} (pKF1201) (Talley et al., 2011) to make pKF1202 and pKF1203 respectively. The point mutants were confirmed by PCR and sequencing.

Telomere DNA cloning and sequence analysis

Telomeric DNA was cloned as previously described with minor modifications (Kramer and Haber, 1993). All primer sequences are list in Table 2.2. Genomic DNA was extracted by glass bead lysis. RNase treated DNA samples (~20 to 40 ug) were blunted by treatment with 4.5 units of T4 DNA polymerase (NEB) in the presence of 1 mM dNTPs at 12°C. The samples were ethanol precipitated and 40 ng of a double-stranded oligonucleotide (created by annealing primers ds oligo 1 and ds oligo 2; Table 2.2) was incubated with the genomic DNA and 20 units of T4 DNA ligase (NEB) overnight at 17°C. Ligation products were ethanol precipitated and telomeres were amplified using one primer specific to the double-stranded oligonucleotide (ds oligo 1 or ds oligo 2) and another primer designed to anneal internal to the telomere on the chromosome of interest.

Table 2.1: Strains and plasmids used in (Bairley et al., 2011).

Strains or plasmids	Genotype	Source
GA426	*MATa ade2 trp1 can1 his3-11 ura3-52 DIA V-I*	(Förstemann, Hoss and Lingner, 2000)
YKF500	GA426 *est2-LT^{E76K}*	(Ji et al., 2008)
YKF511	GA426 *est2-up34*	(Bairley et al., 2011)
YKF600	GA426 *rif1::Kan^{R}*	(Bairley et al., 2011)
YKF601	GA426 *rif2:: Kan^{R}*	(Bairley et al., 2011)
YKF602	GA426 *pif1:: Kan^{R}*	(Bairley et al., 2011)
YKF603	GA426 *pif1-m2*	(Bairley et al., 2011)
YKF604	GA426 *elg1:: Kan^{R}*	(Bairley et al., 2011)
YKF605	GA426 *ssn8:: Kan^{R}*	(Bairley et al., 2011)
YKJM1[a]	*MATa ura3-52 leu2-Δ1 trp1-Δ63 his3-Δ200 lys2ΔBgl hom3-10 ade2Δ1 ade8 YEL069::URA3*	(Banerjee et al., 2008)
YPH499	*MATa ura3-52 lys2-801 ade2-801 trp1-Δ1 his3-Δ200 leu2-Δ1*	(Schulz and Zakian, 1994)
UCC5706	*MATa-inc ura3-52 lys2-801 ade2-101 trp1-Δ63 his3-Δ200 leu2-Δ1::LEU2-GALHO VII-L::ADE2-TG-HO stie-LYS2 rad52::hisG*	(Diede and Gottschling, 1999)
YKF512	UCC5706 *est2-LT^{E76K}*	(Bairley et al., 2011)
YKF606	GA426 *EST2 tlc1::Kan^{R}* pKF5	(Bairley et al., 2011)
YKF607	GA426 *EST2 tlc1::Kan^{R}* pKF10	(Bairley et al., 2011)
YKF608	GA426 *est2-LT^{E76K} tlc1::Kan^{R}* pKF5	(Bairley et al., 2011)
YKF609	GA426 *est2-LT^{E76K} tlc1::Kan^{R}* pKF10	(Bairley et al., 2011)
YKF610	GA426 *EST2 tlc1::TLC1 tlc1-tm*	(Bairley et al., 2011)
YKF611	GA426 *est2-LT^{E76K} tlc1::TLC1 tlc1-tm*	(Bairley et al., 2011)
pKF5	*CEN TLC1 ΔNcoI (^{455}G→A) TRP*	(Förstemann and Lingner, 2001)
pKF10	*CEN TLC1 ΔNcoI (^{455}G→A + ^{484}ACA^{482}→CAC) TRP*	(Förstemann and Lingner, 2001; Förstemann et al., 2003)
pLIB17	*CEN tlc1-tm ΔNcoI (^{455}G→A + ^{480}ACACCCACAC^{471}→CUAAACCACA) TRP*	(Förstemann *et al*., 2003)
pRS306 tlc1-tm	*INT tlc1-tm URA*	(Bairley et al., 2011)
pKF1201	pET Duet-1 *MBP-EST2^{TEN}*	Talley, J and Friedman, K; submitted
pKF1202	pET Duet-1 *MBP-Est2 E76K^{TEN}*	(Bairley et al., 2011)
pKF1203	pET Duet-1 *MBP-Est2 R151A^{TEN}*	(Bairley et al., 2011)

[a] Previously published as RDKY3615

Table 2.2: Primers used in (Bairley et al., 2011).

Name	Primer sequence
RIF1::Kan^R	CGTCAACGTTATTACAGGAT CGATTTCTAGTGTGTCATCG
RIF2::Kan^R	CGCTTACAGATATGTACAGA AATAGAGACAAGCCAGGTGG
PIF1::Kan^R	GTAGTTTTGTGATGCTGTTCAG GTGAGTTAGTCTCCTTTGGC
ELG1::Kan^R	GACGCCAAACGCGTAACGTTAGCGGTG CGCTGTTTTGAAATATGCACTATGAGG
SSN8::Kan^R	GAAAATTAGGGTTCATACAGGAGTAG GCATTATAACGGTACCTATTCTCAATATG
TLC1::Kan^R	GATGTAACAAGCATATGCAATTATTTGGTTTCCC GGTGGCATCTATAAGAGCTCTATCTGGCTGCTAAGC
est2-E76K	CCTGTTGACGGGCAAGCTTTACAACAACGTAC GTACGTTGTTGTAAAGCTTGCCCGTCAACAGG
est2-R151A	CTCAAATCGTGGGTAATGCATGTAACGAACCTCATC GATGAGGTTCGTTACATGCATTACCCACGATTTGAG
pET Duet MBP	GGTTATGCGTTCAAGTATGAAAACGGCAAGTACG CGGTGAGCGTGGGTCTCGCGGTATCATTGCAGCAC
ds oligo 1	GGGTTCGAATGACCGGCAGCAGCAAAATG
ds oligo 2	CATTTTGCTGCTGCCGGTCATTCGAACCC
DIA5-1	GTGAGCGGATAACAATTTCACACAGTCTAGATGTCCGAATT GATCCCAGAGTAG
XV-L	GTGAGTACCAGATGATGGAT
Inv 5'ADE2	CAAGATATCAAAACTGTAAAT
Bio-TG28*	B - TGTGGTGTGGGTGTGGTGTGTGGGTGTG
Bio-TG16*	B - GTGTGTGGTGTGTGGG
Bio-AC16*	B - CACACACCACACACCC
Bio-Random*	B - GGAAGGCCGATCGGTGCAGCCTCTTCGCTA

All primers sequences are written 5' to 3'. * B refers to the 5' biotinylation.

The internal primer for the GA426 strains (primer DIA5-1) anneals to the *ADE2* gene integrated at chromosome V-R (Förstemann, Hoss and Lingner, 2000). The internal primer utilized in strains UCC5706, YKJM1, and YPH499 is specific to chromosome XV-L (primer XV-L). PCR products were separated in 1.8% agarose gels and the

telomeric smear was purified from the gel (Qiagen). Products were ligated into pGEM T Easy vector (Promega) and transformed in DH5α *E. coli*. Inserts were sequenced by GENEWIZ (South Plains, New Jersey) using the primer M13R. Analysis of telomeric sequence data was performed as described (Ji et al., 2008) using JMP software unless otherwise noted in the text.

De novo telomere formation

Telomere formation events occurring at the site of HO cleavage were generated as previously described (Diede and Gottschling, 1999) with minor modifications. Fresh colonies from UCC5706 strains were grown in media lacking lysine and used to inoculate a 100 mL culture of YEP + 2.5% Raffinose and grown to an OD_{600} of approximately 0.5. Cultures were blocked with nocodazole (10 μg/mL) for 4 hours or until >90% of the cells had a single large bud. A 15 mL sample was isolated as the "pre-healing control." The pellet from an additional 15 mL sample was washed twice with cold ddH_2O, resuspended in 100 mL of pre-warmed YEP + 3% galactose to allow release from the nocodozole block, and harvested after incubation for six hours. The pellet derived from the remaining culture was washed twice as described above and resuspended in 100 mL of pre-warmed YEP + 3% galactose with nocodazole (10 μg/mL). 15 mL samples were removed every 2 hours over a 6-hour time period. The *de novo* telomeres were cloned and sequenced as described above with internal primer Inv 5'ADE2 (Diede and Gottschling, 1999). FACS analysis confirmed the nocodazole block efficiency (data not shown).

Protein purification and biotin pull-down assay

Wild-type or mutant variants of MBP-tagged Est2 TEN domain (residues 1-161; pKF1201 - pKF1203) were expressed in BL21 *E. coli*. The protein was induced with 500 mM IPTG followed by growth for 16 to 20 hours in LB media supplemented with ampicilian (50 mg/ml) at 17°C. Cells were lysed by emulsification in Gel Filtration buffer (20 mM Tris-HCl [pH 7.5], 200mM sodium chloride, 1mM EDTA [pH 8], 10% glycerol) plus protease inhibitors (one Roche Complete Protease Inhibitor Tablet per 10 mL). The MBP-tagged protein was isolated from the resulting supernatant with Amylose Resin (NEB). The resin was washed with Wash buffer A (20mM Tris-HCl [pH 7.4], 500mM sodium chloride, 1mM EDTA [pH 8], one Roche Complete Protease Inhibitor Tablet per 10 mL) and eluted with Elution buffer B (20mM Tris-HCl [pH 7.4], 500mM sodium chloride, 1mM EDTA [pH 8], 5mM Maltose, one Roche Complete Protease Inhibitor Tablet per 10 mL). The eluate was concentrated and purified by size-exclusion chromatography. Protein concentrations were verified by a Nanodrop spectrometer. For the pull-down assay, 19.2 fmoles of MBP tagged proteins (with or without 5 μg RNase) were incubated with 5 fmoles 5' biotinylated oligo (Table 2.2) on ice for 30 mins in 75 μL of Gel Filtration buffer. Steptavidin UltraLink Resin (Pierce) was equilibrated with 4 washes of 1 mL each Equilibration Solution (Gel Filtration buffer plus one Roche Complete Protease Inhibitor Tablet per 10 mL, 0.1% Tween, 0.01% 1M DTT) and 5 μL equilibrated resin (resuspended in half the original volume) was incubated with each sample for 45 mins at 4°C with gentle agitation. Bound resin was washed 2X 10 mins with 500 μL cold Wash Solution (Wash buffer A plus one Roche Complete Protease Inhibitor Tablet per 10 mL, 0.1% Tween, 0.01% 1M DTT) at 4°C, heated in SDS

Reducing buffer (Bio-Rad) at 100°C for 4 minutes and the supernatant was separated in a 10% BioRad SDS-PAGE gel for 1 hour at 200 V. The proteins were wet transferred to PVDF membrane (Amersham) at 30 V for 2.5 hours and blocked overnight at 4°C in a PBST/milk solution (1X PBS, 0.05% Tween, 5% dried milk). MBP protein was detected using a horseradish peroxidase (HRP)-conjugated anti-MBP monoclonal antibody from NEB at a 1:50,000 dilution. After washing the membrane with a PBST solution (1X PBS, 0.05% Tween,), the ECL Plus Western Blotting Detection System and Hyperfilm ECL (GE Healthcare) was utilized. The sequences of 5' biotinylated oligonucleotides TG28, TG16, AC16, and Random are listed in Table 2.2.

Southern analysis of telomere length

Southern blot analysis of endogenous telomeres was done as previously described (Friedman et al., 2003). For Southern blot analysis of *de novo* telomere formation in strains UCC5706 and YKF512, genomic DNA was digested with *SpeI* and the blot was probed with a fragment of *ADE2* as previously described (Diede and Gottschling, 1999).

CHAPTER III

DISCUSSION AND FUTURE DIRECTIONS

The purposes of the two sections of this Chapter are to build upon what is already known in the field and to suggest several avenues of approach scientists could take to continue my line of research. The Discussion highlights what my work means to the field. The Future Directions represent experimental approaches to address the un-answered questions beyond the scope of my published manuscript.

Discussion

My published research (see Chapter II) shows that the highly reproducible telomeric sequence pattern synthesized by *est2-LT*^{E76K} telomerase is not a general phenotype caused by loss of negative telomerase regulation. Rather, mutation of Est2p residue E76 to lysine restricts the DNA primer-RNA template alignment possibilities *in vivo* both during *de novo* telomere formation and during synthesis of endogenous telomeres. A mutation of the template that increases the number of bases of perfect complementarity between the DNA primer and RNA template is epistatic to the *est2-LT*^{E76K} allele, consistent with the hypothesis that the TEN domain is most important for alignment when complementarity is low. My work also showed a new way to analyze anchor-site function based on the gain-of-function E76K mutation that retains cell viability to allow *in vivo* analysis. Mutation of residue E76 to lysine also results in moderate increases of repeat addition processivity *in vivo* and DNA binding *in vitro* suggesting an enhancement of the anchor-site interaction.

Specificity of *est2-LT* telomere sequence patterns

Until the publication of the telomeric sequence changes created by the *est2-LT* mutants in 2008, the only previously reported changes in telomeric sequence occurred as a result of nucleotide changes in the RNA template. Interestingly, mutations in different functional domains of *EST2*, both resulting in increased telomere length, produced similar telomere sequence pattern changes (Ji et al., 2008). These data left open the possibility that any loss of a negative telomere length regulator would result in a hallmark "*est2-LT*^{E76K}" sequence phenotype. However, six other mutants that act in either the same genetic pathway as the *est2-LT*^{E76K} (*rif1Δ* and *rif2Δ*) or *est2-up34* (*pif1*Δ and *pif1-m2*) or indirectly affect telomere length (*elg1*Δ and *ssn8*Δ) did not give the same *est2-LT* phenotypes (Figure 2.1). These data suggest that while many genes negatively influence the telomere length, the associated telomere sequences are variable.

These results allude to the complexity of telomere end protection and the influence that the sequence of the telomere may have on telomeric heterochromatin. In yeast, end protection of the single-stranded G-rich overhang is mediated through the CST (Cdc13p/Stn1p/Ten1p) complex (Price et al., 2010). Rap1p and its associating factors Rif1p and Rif2p bind to the double-strand portion of the telomere and inhibit the MRX complex access to telomeres and non-homologous end joining (NHEJ) (Bonetti et al., 2010). Rap1p is also part of the telomeric heterochromatin along with the Sir protein family (Rusche, Kirchmaier and Rine, 2003). Changes to the heterochromatin can alter the transcription of genes located adjacent to the telomere (Liu, Mao and Lustig, 1994). Most of the mutants analyzed in my study elevate the levels of telomeric gene silencing

(Eugster et al., 2006; Ji et al., 2008; Smolikov, Mazor and Krauskopf, 2004; Wotton and Shore, 1997), presumably because longer telomeres provide more binding sites for Rap1p that can in turn recruit the Sir complex important for transcriptional silencing. In contrast, the *est2-LT*^{E76K} mutation does not alter silencing (Eugster et al., 2006; Ji et al., 2008), suggesting that the longer telomeres in this strain may not bind increased levels of Rap1p. Indeed, chromatin immunoprecipitation experiments suggest that Rap1p associates with *est2-LT*^{E76K} telomeres at a lower density (per nucleotide) than wild-type telomeres *in vivo*.

The reduction in Rap1p binding at *est2-LT*^{E76K} telomeres is not directly related to the telomere sequence changes caused by *est2-LT*^{E76K} telomerase. The telomere sequence pattern derived from *est2-up34* telomerase (has a similar over-elongated telomere phenotype as *est2-LT*^{E76K}) produces comparable telomere sequence phenotypes as *est2-LT*^{E76K} telomeres, yet more Rap1p is bound to the *est2-up34* telomeres by ChIP (Ji et al., 2008). Isolation of the telosome and subsequent analysis of the integrity and composition of the telomeric heterochromatin in the *est2-LT*^{E76K} background would be an interesting undertaking to address how the telomere sequence plays a role in chromatin formation.

RNA/DNA sequence alignments

When a double-strand break occurs, the MRX (Mre11/Rad50/Xrs2) complex, Tel1p and Sae2p are recruited to the site. When cyclin-dependent kinase (CDK) activity is high, resection occurs and RPA binds to the single-stranded DNA to recruit other associating factors to initiate strand invasion (Garber, Vidanes and Toczyski, 2005). In the Diede and Gottschling *de novo* healing assay (in which an HO endonuclease induces a double-strand

break at a site adjacent to an 81 base pair TG seed), after end processing by the MRX complex, telomerase can be recruited by Cdc13p to heal the broken ends (Negrini et al., 2007). During normal telomere synthesis it can be difficult to infer the sequence of the 3' end portion of a DNA substrate that was present at the time of initial telomerase binding and alignment. Restricting the sequence of the available 3' ends for telomerase to bind using this *de novo* healing assay was thus able to highlight the preferred alignment for *EST2* and *est2-LT*^{E76K} telomerases (Figure 2.2).

Introduction of the *tlc1-KF10* allele allowed us to force *EST2* and *est2-LT*^{E76K} to align in a single, highly preferred site on the template. The increased pairing with the extreme 3' end of the template resulted in highly similar TG dinucleotide distribution for both enzymes (Figure 2.3). The observation that the *est2-LT*^{E76K} allele generates telomere sequences similar to those of the *EST2* enzyme in the presence of *tlc1-KF10* is consistent with the hypothesis that the E76K mutation influences template alignment when base pairing interactions are limited. However, we cannot rule out the possibility that because the *tlc1-KF10* allele also affects the sequence of telomeres synthesized by *EST2* telomerase, an unrelated effect of the *est2-LT*^{E76K} allele is masked under these conditions.

It is of interest to note that both the *EST2 tlc1-KF10* and *est2-LT*^{E76K} *tlc1-KF10* telomerases make longer and more heterogeneous telomeres (Figure 2.3 C). This could be directly due to the restriction of RNA alignment to the extreme 3' end of the template from the *tlc1-KF10* allele. If true, then it could be argued that the extreme 3' alignment preference by *est2-LT*^{E76K} telomerase is the cause of the *est2-LT*^{E76K} long telomere phenotype. This argument alone would not explain why *est2-LT*^{E76K} *tlc1-KF10* makes the telomeres even longer than *EST2 tlc1-KF10* alone as discussed in more detail below.

In the *tlc1-KF10* background, the 5'-TGGGTGTGTGG sequence commonly incorporated in the telomere (Figure 2.3), contains two mismatches with the consensus Rap1p binding sequence (Wang and Zakian, 1990). As the propensity to create this Rap1p sequence is dramatically increased with the *tlc1-KF10* template as compared to the *TLC1* template, the over-lengthening telomere phenotype seen in the *tlc1-KF10* background could be due to a reduction in high affinity Rap1p binding sites. With the *TLC1* template, *EST2* and *est2-LT*^{E76K} synthesized telomeres have indistinguishable amounts of Rap1p bound *in vivo* and *in vitro* (Ji et al., 2008). I have shown that the telomere sequence change synthesized by *est2-LT*^{E76K} is not a hallmark of general loss of negative telomere length regulation (Figure 2.1). Therefore, I favor a model in which both the restrictions in alignment with the DNA substrate and moderate increase in repeat addition processivity (discussed under **Processivity**) regulate the telomere length phenotype.

I also feel the change in the preferred alignment is one of the main reasons for the telomere sequence changes caused by *est2-LT*^{E76K} telomerase. An alternative explanation for the generation of the telomere sequence changes is that perhaps the *est2-LT*^{E76K} enzyme is more inclined to "slip" during nucleotide addition and it is this slippage through the 3' ^{481}CAC^{479} portion of the template that results in an increased number of TG nucleotides in the inter-core regions between core motifs (Figures 2.2 and 2.3). This alternative is not likely *in vivo* as there are some cases where the TG dinucleotide incorporation before the first core motif on the HO induced double stranded break are too large to explain by alignment alone (cases of 3 TG's or more; see Figure 2.2). These

cases do not differ significantly in number between the two strains, showing that *in vivo* nucleotide addition "slippage" in the context of this assay is unchanged.

Also, *in vitro*, *est2-LT*^{E76K} telomerase does not display abortive slippage or poor nucleotide addition processivity on the normal 15-mer yeast telomeric primer (Ji et al., 2005). I have extended this primer-extension analysis on multiple yeast telomeric primers of varying length and sequence and saw no difference in nucleotide addition between the *EST2* and *est2-LT*^{E76K} enzymes (Bairley, R. and Friedman, K., unpublished data). On a non-yeast primer where *est2-LT*^{E76K} telomerase exhibited a modest increase in repeat addition processivity *in vitro* over *EST2*, *est2-LT*^{E76K} telomerase showed similar nucleotide processivity in the first repeat as *EST2* telomerase (Lue and Li, 2007). Alignment of the template with the non-yeast primer for synthesis of the second repeat was not tested so the contribution of alignment is not known under these conditions. These data suggest that, overall decreased nucleotide addition processivity is not an intrinsic property of the *est2-LT*^{E76K} telomerase enzyme.

It could also be argued that increased nucleolytic degradation through a previously synthesized core motif contributes to the increased number of TG dinucleotides seen in the inter-core region of *est2-LT*^{E76K} generated telomeres. There is no evidence of increased ssDNA as analyzed in a native gel (Ji et al., 2005). The MRX complex (Mre11/Rad50/Xrs2) in yeast possesses both single and double stranded 3' to 5' exonuclease activity as well as the 5' to 3' resection of double stranded breaks (Diede and Gottschling, 2001). There is no evidence to refute the argument that increased exonuclease activity results in slightly longer overhangs in the *est2-LT*^{E76K} background (undetectable in native gels) and thereby contributes to the sequence pattern. The cells

from an the *est2-LT*^{E76K} stain are able to divide normally, suggesting end protection from Cdc13p is intact as there is not a significant level of adherent nucleolytic activity to trigger a Rad9p cell cycle arrest in either the *de novo* healing assay or on normal telomere ends by *est2-LT*^{E76K}. This interpretation is complicated by data showing that in a *yku*Δ background, where there is extensive single stranded DNA that persists throughout the cell cycle, at permissive temp, the long overhangs do not trigger a checkpoint arrest, presumably because the overhangs are bound by Cdc13 rather than RPA (Fisher and Zakian, 2005). A closer look at the potential role of nucleolytic degradation is therefore warranted and discussed in the Future Directions section of this Chapter.

Processivity

The Lingner lab proposed that telomerase behaves processively for rapid elongation of telomeres shorter than 125 base pairs. This rapid elongation mechanism was shown to be Tel1p dependent (Chang, Arnerić and Lingner, 2007). As *est2-LT*^{E76K}'s increased telomere length phenotype is also Tel1p dependent and experiments from the Lue lab had demonstrated increased repeat addition processivity by *est2-LT*^{E76K} telomerase *in vitro*, I addressed the repeat addition processivity of the *est2-LT*^{E76K} telomerase *in vivo*. While the wild-type protein behaved as expected during multiple cell cycles, *est2-LT*^{E76K} telomerase has a moderate increase in repeat addition processivity over that of wild-type (Figure 2.4).

Because the telomere lengthening phenotype conferred by *est2-LT*^{E76K} and the rapid elongation by wild-type telomerase at shorter than 125 base pair telomeres in a single cell cycle both depend upon Tel1p, I speculated that the increased *in vivo*

processivity played a role in the over-lengthened *est2-LT*^{E76K} telomeres. Loss of Tel1p results in an inability of telomerase to recognize the shortest telomeres for elongation (Arnerić and Lingner, 2007; Hector et al., 2007; Sabourin, Tuzon and Zakian, 2007), presumably a major reason for telomere shortening in a *tel1Δ* background. As *est2-LT*^{E76K} *tel1Δ* telomeres are as short a *tel1Δ* stain (Ji et al., 2005), the same loss of telomere targeting must occur. When Dr. Ji analyzed telomeres generated in a single cell cycle, the frequency and the amount of telomere addition by *est2-LT*^{E76K} was not different than wild-type. There was also no difference in the preference of elongation of the shortest telomeres (Ji et al., 2008), unlike what is seen when Rif1p or Rif2p is deleted (Teixeira et al., 2004). In the *rif1Δ* and *rif2Δ* backgrounds, the amount of nucleotides added to telomeres and the frequency of elongation at telomeres shorter than 120 base pairs was increased in a single cell cycle (Teixeira et al., 2004). Therefore, the potential role of repeat addition processivity in the long telomere phenotype of *est2-LT*^{E76K} may be more easily distinguished by using the two-template single cell cycle extension (2T-STEX) assay.

Anchor-site

The increased telomere length and repeat addition processivity resulting from the E76 to lysine mutation in the TEN domain led us to test if there was also a change in the DNA binding of this mutant protein through the anchor-site. The anchor-site of human telomerase, both in the context of full-length protein and an N-terminal domain of 350 residues in length, has been shown with an *in vitro* DNA pull-down assay to weakly bind a telomeric oligonucleotide (Sealey et al., 2010; Wyatt, Lobb and Beattie, 2007; Wyatt et

al., 2009). I developed a similar DNA pull-down assay for the yeast TEN domain and found that, in an RNA-independent manner, both MBP-Est2p^{TEN} and MBP-Est2^{TEN} containing the E76K mutation associate with TG-rich DNA above the level observed for a CA-rich or random sequence. The protein-DNA interaction is enhanced by the E76K mutation. Another TERT mutant previously shown to be defective in anchor-site functions, R151A, was introduced into this system and tested. Mutation of R151A reduced binding to the TG-rich DNA substrate to background levels (Figure 2.5), confirming that one function of the TEN domain of the yeast TERT protein is DNA binding.

Although the purified TEN domain is sufficient to bind DNA, other regions of TERT must also contribute to primer interactions. When the TEN domain was deleted from *Tetrahymena* TERT, a one-third reduction in the amount of DNA photo-cross-linking efficiency occurred (Jacobs, Podell and Cech, 2006). The residues surrounding the TEN domain are also likely to play a role. Studies with the human TEN domain (amino acids 1-196) found that a Q169A mutation disrupted binding to single-stranded DNA in the context of residues 1-196. However, when a fragment spanning amino acids 1-300 were used, Q169A no longer completely disrupted binding (Wyatt et al., 2009).

Also, not all mutants within the TEN-domain result in full disruption of the likely anchor-site functions. For example, like the yeast TEN domain E76 residue, a mutation of L14 to alanine (located just beneath the DNA binding groove but still on the same face) in the TEN domain of *Tetrahymena* was shown with a photo-cross-linking assay to have a moderate increase in DNA binding activity over wild-type but unlike our result, this L14A mutation resulted in defective repeat addition processivity. The authors measured

the kinetics of DNA release and extension of a challenge primer and found the challenge primer was not extended (Zaug, Podell and Cech, 2008). The observed decreased repeat processivity *in vitro* suggests that *Tetrahymena* L14A causes the enzyme to be unable to translocate during synthesis, an aspect that is reminiscent to the actions of wild-type yeast telomerase *in vitro*. In yeast, the N-terminal 50 amino acids accounted for the majority of the non-specific nucleic acid binding (Xia et al., 2000), so perhaps the *Tetrahymena* L14 residue is influencing DNA binding in a similar manner.

The overall role of residue E76

My published data shows mutation of E76 to lysine enhances telomere length, repeat addition processivity, and DNA binding and also alters the RNA template/DNA substrate preferred alignment (Bairley et al., 2011). E76K is the first TEN domain mutant allele to show an enhancement of three of the main TERT functions that are suggested to require the TEN domain. The alignment change and corresponding increase in the TG nucleotides making up the inter-core region suggest *est2-LT*^{E76K} telomerase favors instances of increased RNA/DNA hybrids for subsequent telomere synthesis. The mechanism of action in influencing alignment, DNA binding and processivity could be indirect based upon structural modeling. Structural modeling of the yeast TEN domain places residue E76 on the opposite face of the cleft where the DNA substrate is predicted to directly contact the TEN domain (Lue and Li, 2007), suggesting an indirect role for residue E76. The structural model of human TERT shows the TEN domain linked to the rest of the ring shaped protein through an unstructured linker region between the TEN domain and the telomerase RNA binding domain (TRBD) (Steczkiewicz et al., 2011).

These data allude to the possibility that E76 could indirectly influence DNA binding and processivity by altering with the way the TEN domain interacts with the RT-TRBD domains of TERT. I instead postulate the E76K mutation has a direct impact based upon my *in vivo* and protein binding data (Figures 2.4 – 2.5) and that perhaps the structural models are incorrect. A full-length yeast TERT model or crystal structure with the RNA/DNA heteroduplex is an important step in clarifying this model.

We were unable to obtain a DNA binding affinity for the TEN domain using fluorescence anisotropy (data not shown), which is similar to what has been reported for both the *Tetrahymena* and human TEN domains using filter binding and electrophoretic mobility shift assays (Jacobs, Podell and Cech, 2006; Moriarty et al., 2005; Sealey et al., 2010). However, this was not altogether unexpected as a weak or rapid exchange between the DNA and the anchor-site would aid in translocation of the DNA substrate during telomeric synthesis. A recent publication on the human TEN domain gave evidence of a separation-of-function allele which did not affect the anchor-site DNA binding function, but instead altered the RNA-DNA alignment (Jurczyluk et al., 2010). In yeast, the E76 residue in the TEN domain is impacting both anchor-site functions. Experiments further examining this interaction, such as nuclear magnetic resonance on the TEN domain with and without a DNA substrate, will improve the knowledge of anchor-site operations.

Future directions

The work described in Chapter II confirms that the TEN domain of Est2 contains an anchor-site that interacts with the DNA primer. The gain-of-function *est2-LT*^{E76K} allele allowed for the first time to show that the strength of that interaction affects telomere

sequence by influencing the alignment of telomerase with the DNA primer. Enzyme processivity is also affected. However, there are still several unanswered questions that were beyond the scope of my published manuscript that need to be addressed. This section of Chapter III highlights those questions and experimental approaches in five categories: specificity of the telomere sequence phenotype, processivity, anchor-site interactions, alignment and other possible E76K phenotypes.

Specificity of the telomere sequence changes

Differences in the mode of synthesis between *est2-up34* and *est2-LT^{E76K}*

Dr. Ji's 2008 paper showed no difference in the telomere sequence phenotypes between the two *EST2* long telomere mutants *est2-LT^{E76K}* and *est2-up34* (Ji et al., 2008). The telomere lengthening aspect, however, depends upon two different pathways. The *est2-up34* telomere lengthening depends upon the negative regulator *PIF1*, whereas *est2-LT^{E76K}* depends upon *TEL1*, a positive regulator, and *RAP1* (Eugster et al., 2006; Ji et al., 2005). These data suggest the hypothesis that the mode of telomere synthesis between the two mutants is different. I have unpublished data to support that the two mutations cause the sequence alteration through different mechanisms.

To examine synthesis mechanisms, I worked with an undergraduate from Barry University testing the ability of both mutant telomerases to utilize different *tlc1* template mutants published by Förstemann and Lingner in 2001. The most interesting result came from use of the *tlc1-KF11* allele. This allele alters template residues ^{473}**CAC**^{471} to ^{473}ACA^{471}, (the *TLC1* template is 3'- ^{484}ACACACACCCA**CAC**CAC^{468}) resulting in a new core motif, TGGGTTG, no GG dinucleotides, and a new inter-core region called

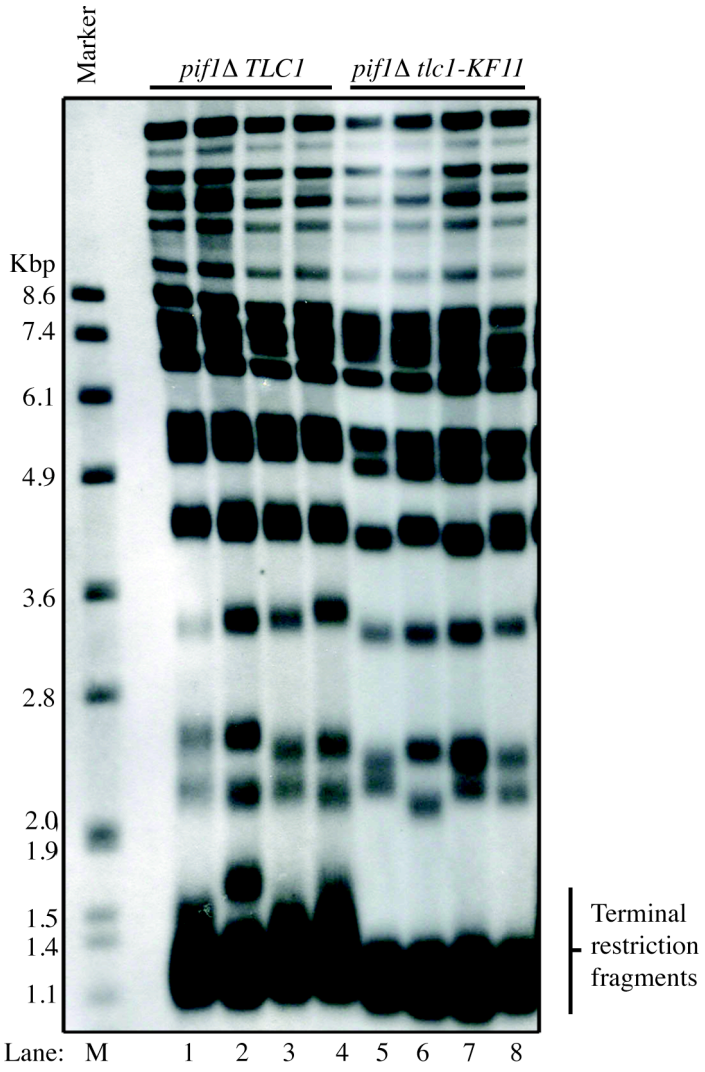

Figure 3.1: *pif1Δ tlc1-KF11* telomeres are shorter than *pif1Δ TLC1* telomeres. Genomic DNA from 4 separate colonies of GA426 *pif1Δ* (lanes 1-4) and GA426 *pif1Δ tlc1-KF11* (lanes 5-8) was isolated, digested with *Xho I*, and separated by electrophoresis. Denatured DNA was hybridized to a telomeric radiolabeled probe and visualized. The marker (Roche DNA molecular weight marker VII – DIG labeled) is indicated in kilo base pairs (lane M). The telomeres (terminal restriction fragments) are indicated. Data generated by Gina Guillaume.

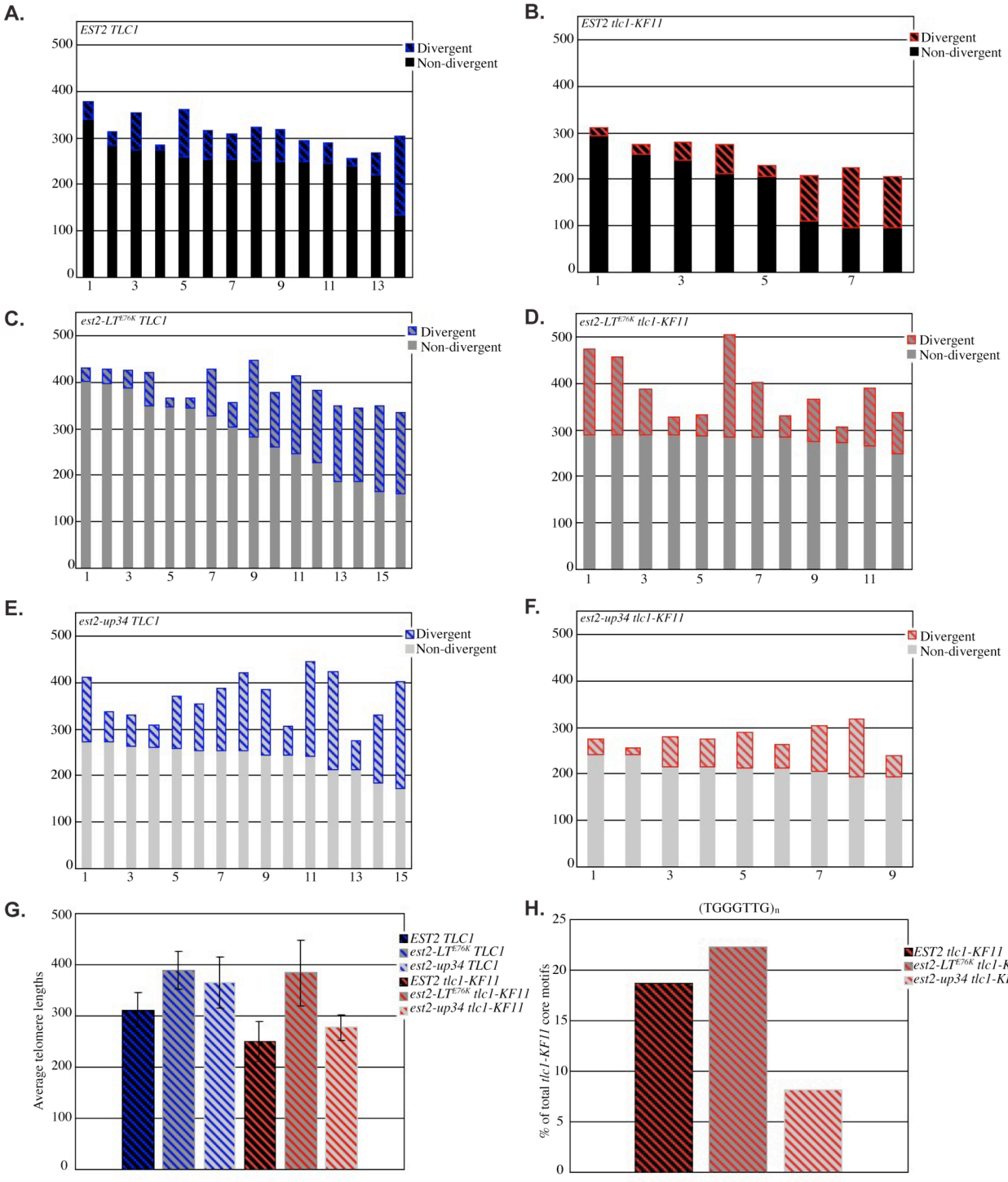
A.
EST2 TLC1
Divergent
Non-divergent
B.
EST2 tlc1-KF11
Divergent
Non-divergent
C.
est2-LT^E76K TLC1
Divergent
Non-divergent
D.
est2-LT^E76K tlc1-KF11
Divergent
Non-divergent
E.
est2-up34 TLC1
Divergent
Non-divergent
F.
est2-up34 tlc1-KF11
Divergent
Non-divergent
G.
Average telomere lengths
EST2 TLC1
est2-LT^E76K TLC1
est2-up34 TLC1
EST2 tlc1-KF11
est2-LT^E76K tlc1-KF11
est2-up34 tlc1-KF11
H.
(TGGGTTG)n
% of total tlc1-KF11 core motifs
EST2 tlc1-KF11
est2-LT^E76K tlc1-KF11
est2-up34 tlc1-KF11

Figure 3.2: The *est2-up34* telomerase utilizes *tlc1-KF11* differently than *EST2* and *est2-LT^{E76K}* telomerases. The *tlc1-KF11* template mutant alters residues ^{473}CAC^{471} to ^{473}ACA^{471}. **(A-F)** Total telomeres in sample set. Telomeres from (A-B) GA426 *EST2* – black; (C-D) GA426 *est2-LT^{E76K}* – gray; and (E-F) GA426 *est2-up34* – light gray. Strains were cloned and sequenced as previously described. The lengths of *TLC1* divergent (blue hash marks), *tlc1-KF11* divergent (red hash marks) and non-divergent (solid colors) telomeric repeats are shown. **(G)** Average total telomere length from the telomeres in A-F. Sequences synthesized by *TLC1* (blue hash marks) and *tlc1-KF11* (red hash marks) are shown for *EST2* – black; *est2-LT^{E76K}* – gray; and *est2-up34* – light gray. Error bars are standard deviation. **(H)** Percent of adjacent *tlc1-KF11* core motifs $(TGGGTTG)_n$ from total *tlc1-KF11* core motifs for each strain. Bar colors are as in (G).

adjacent core motifs $(TGGGTTG)_n$ (Förstemann and Lingner, 2001). The first piece of evidence came from a telomere Southern with *pif1*Δ strains. Telomerase is defective in utilizing the *tlc1-KF11* allele in a *pif1*Δ strain as telomeres are shorter compared to telomeres in a *pif1*Δ *TLC1* background (see Figure 3.1). Second, *est2-up34* utilizes the *tlc1-KF11* allele differently than *EST2* and *est2-LT^{E76K}* telomerases (see Figure 3.2). The *EST2* and *est2-LT^{E76K}* telomeres are relatively similar in length in both *TLC1* backgrounds (compare Figures 3.2A-3.2D, and 3.2G). Telomeres from the *est2-up34 tlc1-KF11* strain are much shorter than telomeres from the *est2-up34 TLC1* strain (compare Figures 3.2E-3.2F, and 3.2G). Analysis of adjacent *tlc1-KF11* core motifs $(TGGGTTG)_n$ from the divergent telomere sequences shows that *est2-up34 tlc1-KF11* telomeres have 10 fold fewer adjacent *tlc1-KF11* core motifs than *EST2 tlc1-KF11* and *est2-LT^{E76K} tlc1-KF11* telomeres (Figure 3.2H).

These data lend strong support to the idea that the two *EST2* long telomere mutants *est2-LT^{E76K}* and *est2-up34* are in fact different in terms of their mode of telomere synthesis. Given the shorter telomeres in the *pif1*Δ *tlc1-KF11* background, I hypothesize

the mechanism of *est2-up34* synthesis requires *PIF1*. To test this hypothesis, the telomeres in the *pif1*Δ *tlc1-KF11* background should be sequenced and analyzed for the frequency of adjacent *tlc1-KF11* core motifs. I predict they will be similar to the telomeres from the *est2-up34 tlc1-KF11* strain. Further, a double mutant, *est2-up34 pif1*Δ should be tested with *TLC1* or *tlc1-KF11* for telomere length and sequence patterns. These additional experiments should provide additional evidence supporting my hypothesis.

Importance of phosphorylation in the telomere sequence patterning

Because the telomere lengthening by *est2-LT*^{E76K} is dependent upon the presence of Tel1p (Ji et al., 2005), I wanted to see if the sequence phenotype was also dependent upon Tel1p. I made GA426 *tel1*Δ and GA426 *est2-LT*^{E76K} *tel1*Δ strains and restreaked 13 times (approximately 325 generations). The 13th restreak was outgrown in liquid culture for 125 generations, and the telomeres from the marked arm of chromosome V-R were isolated and analyzed. Unfortunately, neither strain produced telomeres with long enough divergent sequences to analyze (data not shown). However, it is published that Cdc13p can be phosphorylated by Tel1p or Mec1p (at serine residues S249 and S255) (Tseng, Lin and Teng, 2006), although these modifications are not required for Cdc13p function (Gao et al., 2010). Cdc13p is also phosphorylated by Clb-Cdc28 (the yeast S-phase Cdk) at threonine residue T308 (Li et al., 2009), and loss of this modification causes telomere shortening. I think it would be interesting to further investigate whether the long telomere and/or the telomere sequence phenotypes are dependent upon phosphorylated Cdc13p.

To test this, GA426 and GA426 *est2-LT^{E76K}* strains would be introduced with a series of mutants: *cdc13^{T308A}* and *cdc13$^{S249A, S255A, T308A}$*. The Blackburn lab has already shown that *cdc13$^{S249A, S255A, T308A}$* does not result in synergistic telomere shortening as compared to the individual mutants alone (Li et al., 2009). Southern Blotting will assay an epistasis analysis of telomere length. If the *est2-LT^{E76K}* telomere over-lengthening depends upon Cdc13p phosphorylation, then the *est2-LT^{E76K} cdc13^{T308A}* and/or *est2-LT^{E76K} cdc13$^{S249A, S255A, T308A}$* strains will have the same short telomeres as the Cdc13p phosphorylation mutants alone. The telomeres from all 4 strains will also be sequenced and analyzed to test if telomeres synthesized in either the *cdc13* or *est2-LT^{E76K} cdc13* mutant backgrounds have the same phenotypes.

To see if the phosphorylation of Cdc13p contributes to the *est2-up34* telomere length and sequence phenotypes, the same strategy discussed in the above paragraphs would be employed. I hypothesize that the *est2-up34* phenotypes will not be affected by lack of Cdc13p phosphorylation, as the lengthening phenotype of *est2-up34* is not *TEL1* dependent (Eugster et al., 2006). The telomere lengths and sequence phenotypes should be intermediate between *est2-up34* and Cdc13 phosphorylation single mutants.

Separating *est2-LT^{E76K}* telomere sequence and telomere length phenotypes

Elliot Kim, a past undergraduate student in the Friedman lab did a mini-project during which he mutated the E76 residue to alanine, aspartic acid, arginine, and lysine (as his positive control) He found all of the E76 mutants resulted in long telomeres. These data suggest loss of the negative charge is critical for generation of the long telomere phenotype. I hypothesize the charge is also important for the telomere sequence

generation, and can be tested by analyzing the telomere sequence phenotypes in these additional E76 mutants. If none of the other E76 mutations, E76R in particular, alter the telomere sequence, this would suggest something very special is happening with the *est2-LT^{E76K}* mutation. The over-lengthening and sequence phenotypes would not be due to a loss in the negative charge. Crystallographic analysis or structural modeling of full-length *EST2* from yeast to get better insight as to the spatial relationship of E76 with the rest of the protein may aid in explaining that phenomenon.

Processivity

Characterize *est2-LT^{E76K}* telomerase *in vivo* processivity at short telomeres

My published data shows for the first time that a gain-of-function mutant, *est2-LT^{E76K}*, has a modest increase in *in vivo* processivity during multiple cell cycles (Bairley et al., 2011). In yeast, the only other instance of *in vivo* processive synthesis has been demonstrated by wild-type telomerase on telomeres shorter than 125 base pairs in a single cell cycle (Chang, Arnerić and Lingner, 2007). The multiple cell cycle analysis I performed examined normal length telomeres. The single cell cycle analysis used a 2T-STEX (two-template single telomere extension) assay. In this assay, the short telomeres in a recipient *est1Δ* strain were rescued for growth by an *EST1* donor strain. One strain carried *TLC1* and the other *tlc1-tm*, the templates used to examine processivity. The resulting diploid was allowed to grow for a single cell cycle, the telomeres were isolated and repeat addition processivity was examined (Chang, Arnerić and Lingner, 2007). This method, while looking at conditions telomerase would not normally face (dramatic

shortening of all telomeres), is a great tool to assay whether the enzyme is processive or just has rapid turn-over at telomeres shorter than 125 base pairs.

To test whether *est2-LT^{E76K}* retains a selective increase in processivity on telomeres shorter than 125 bp or if this preference is eliminated, telomere addition by *est2-LT^{E76K}* and wild-type telomerase in Lingner's 2T-STEX assay (Chang, Arnerić and Lingner, 2007) will be done. This experiment will give a more accurate picture of the extent to which processivity is increased. I hypothesize there will be increased repeat addition processivity seen on telomeres longer than 125 base pairs given my multiple cell cycle analysis data due to the inherent nature of this mutant enzyme. For the telomeres shorter than 125 base pairs, there are three possible outcomes: *est2-LT^{E76K}* could add repeats to telomeres with (1) the same increased processivity as *EST2* telomerase, (2) decreased processivity, or (3) an even higher rate of processivity. If the rates were the same for the two enzymes, this would suggest that there is a limit to the elongation rate (in terms of repeat addition processivity) and that rate is not changed on the short telomeres by *est2-LT^{E76K}*. On the other hand, if the rate is decreased as compared to *EST2* enzymatic action, this would suggest Tel1p targeting to the shortest telomeres for rapid elongation is is somehow compromised in the *est2-LT^{E76K}* background. If however the rate were increased over that of *EST2* telomerase, that could suggest that the E76K mutation causes telomerase to be "stuck" in the highly processive mode and could give some important insight into how this difference is usually regulated.

Regardless of the results found in the first part, a kinase-dead allele of *TEL1* would be included in this analysis to see if the repeat addition processivity is due to Tel1p phosphorylating a target protein at the telomere. The Lingner lab did not address whether

the kinase function of Tel1p is required for the increased processivity at telomeres shorter than 125 base pairs in length (Chang, Arnerić and Lingner, 2007). Repeat addition processivity would be assayed using 2T-STEX in the kinase-dead TEL1 background. If the kinase function is required, mutating targets of Tel1p phosphorylation will be incorporated. To start teasing this apart, the *cdc13*^{T308A} and *cdc13*$^{S249A, S255A, T308A}$ mutants will be examined for their contributions. Also, mutations in the predicted Tel1p/Mec1p phosphorylation sites in Rif1p and Rpa1, discovered in a proteome wide screen of Tel1p kinase substrates that are phosphorylated independent of Rad53p in yeast (Smolka et al., 2007), will be included.

Anchor-site interactions

Length and sequence specificity

Through the design and implementation of my biotinylation pull-down assay, I have shown the first direct demonstration in yeast of a sequence-specific DNA binding activity that appears to be very similar to that previously studied in the human enzyme. The biotinylation pull-down assay could be extended to test the size and sequence of the oligonucleotide necessary for protein-DNA binding. I have tested TG28 and TG16 with MBP-Est2p^{TEN} and didn't see a difference in the binding enrichment when normalized to the AC control (Bairley et al., 2011), suggesting the minimum threshold for binding hasn't been reached. Telomeric primers of decreasing length can be tested. The minimum length I would include is 5 base pairs, as this is just under the preferred length of 7 base pairs that wild-type telomerase prefers for RNA/DNA binding (Förstemann and Lingner, 2005).

In their early studies that led to the discovery of telomerase, Grieder and Blackburn showed that ciliate telomerase was capable of recognizing and adding repeats to a yeast telomeric seed (Greider and Blackburn, 1987). *In vitro*, both *EST2* and *est2-LT^{E76K}* telomerase can utilize an *Oxytrica* sequence very efficiently in the telomerase activity assay (Lue and Li, 2007). Therefore, the telomeric sequences of different eukaryotes, up to 28-mer in length, would be tested in the biotinylation pull-down assay for MBP-Est2p^{TEN}, MBP-Est2 E76Kp^{TEN}, and MBP-Est2 R151Ap^{TEN}.

Anchor-site importance for Est3p – Est2p TEN domain binding

Dr. Ji showed that the E76K mutation does not disrupt the ability of Est2p to co-immunoprecipitate with Est1p and Est3p (Ji et al., 2005). Dr. Talley has shown in her recently published manuscript that isolated TEN domain protein directly interacts with Est3p *in vitro* (Talley et al., 2011). A similar finding has been recently reported for Est3p from two *Candida* yeast species (Yen et al., 2011). I want to know if an intact anchor-site is necessary for the Est3p- Est2p^{TEN} interaction. To start, *est2-R151A* would be assayed for the ability to co-immunoprecipitate with Est1p and Est3p. *TLC1* interaction is not disrupted by the R151A mutation (Lue and Li, 2007), so assembly may not be altered. To test the direct interaction, purified recombinant MBP-Est2p^{TEN} and His-Est3p would be mixed together and Western Blotting would detect the pull-down efficiency of Est3p to interact with the Est2 mutant TEN proteins. If the Est2 R151Ap^{TEN} mutant disrupts Est3p interaction with the TEN domain, and Est2 E76Kp^{TEN} does not, the double mutant Est2 E76K, R151Ap^{TEN} would be tested. If a functional anchor-site is part of the

requirement for Est3p interaction, then the R151A mutation should perturb this phenotype in the double mutant context.

RNA/DNA alignments

Specificity of the altered RNA/DNA alignment

I have shown the first evidence that one role of the anchor-site interaction may be to help align the template correctly with the DNA substrate, especially when the base pairing interaction is weak (Bairley et al., 2011). To see if the 3' alignment preference for *est2-LT*^{E76K} (with the *de novo* healing assay) is specific to the E76K allele, the assay can be conducted with *est2-LT*^{N95A}. The *est2-LT*^{N95A} allele is another *est2-LT* mutant that results in a similar telomere length increase and sequence change as *est2-LT*^{E76K} (Ji et al., 2008; Ji et al., 2005). If in the *de novo* healing assay both *est2-LT*^{N95A} and *est2-LT*^{E76K} gave similar 3' alignment preferences, then it would be prudent to test *est2-LT*^{N95A} for effects on *in vivo* repeat addition processivity as well as for protein-DNA interactions. The further study of *est2-LT*^{N95A} would also be of interest as a mutation of the corresponding asparagine residue in the human TERT protein results in shorter telomeres, reduced *in vitro* repeat addition processivity, telomerase activity, and DNA binding (Wyatt, Lobb and Beattie, 2007). If the previously discussed experiments show the change in telomere sequence is specific to the *est2-LT*^{E76K} telomerase (as opposed to say the *est2-LT*^{E76R} telomerase for example), then the other E76 mutant telomerases would also be assayed for their 3' alignment preference on the HO induced double stranded break.

Experimental approach to assay alignment *in vitro*

So far, all the *in vitro* activity and processivity assays I have done (using numerous yeast telomeric primers of differing sizes and 3' sequence) have not shown a difference in the activity of the wild-type and *est2-LT*^{E76K} enzymes (data not shown). These data imply either we haven't been able to do the correct experiment, or the differences that we observe in alignment are influenced in a way *in vivo* that cannot be recapitulated *in vitro*. Another experiment that could be done to see if the *est2-LT*^{E76K} enzyme directly influences the alignment of the RNA-DNA heteroduplex, is to assay the accessibility of the telomerase RNA, in the context of the *est2-LT*^{E76K} telomerase, to methylation in the presence or absence of a DNA substrate as has been previously demonstrated for *EST2* telomerase by the Lingner lab (Förstemann and Lingner, 2005).

In this assay, over-expressed telomerase was purified and the RNA template was probed for accessibility to dimethylsulfate (DMS). Before addition of a DNA substrate, the template was completely accessible for methylation. Addition of a primer with nucleotides complementary to the 3'- ^{484}ACACACACCC^{475} resulted in methylation protection only of the 3'- ^{481}CACACCC^{475} portion of the template (Förstemann and Lingner, 2005). This area of the template includes the preferred RNA/DNA alignment region shown in my *de novo* healing assay (Bairley et al., 2011). Providing dNTPs for the telomerase-substrate complex before DMS modification resulted in template protection at the 3' - ^{476}CCACACC^{470} positions that coincided with primer elongation. In both cases, the protected portion of the template was seven base pairs in length (Förstemann and Lingner, 2005). Analyzing the DMS protection of the RNA template with *est2-LT*^{E76K}

telomerase may show protection of the template by the primer at the extreme 3' end, which would support my *in vivo* data (see Chapter II).

Other possible *est2-LT^{E76K}* phenotypes

Telosome composition

In the Discussion section of this Chapter, I argued that telomerase has evolved specific telomeric sequence phenotypes to properly protect the ends from degradation by aiding in the creation of the telosome. Because *est2-LT^{E76K}* does not have any detrimental phenotypes that we know of [*e.g.* temperature sensitivity, increased single-stranded telomeric DNA, changes in TPE, etc.) (Ji et al., 2008; Ji et al., 2005)], there is no evidence that the overall integrity of the telosome is affected. However, the decrease in Rap1p association and subsequent increase in telomere length does suggest that the proteins making up the telosome could be altered in the *est2-LT^{E76K}* background. We have not done the right experiments to rule out that possibility.

To test this possibility, chromatin immunoprecipitation assays (ChIP) from the *est2-LT^{E76K}* and wild-type strains with G1 blocked and released cells would be tested for Rap1, Rif1p, Rif2p, Tel1p, Cdc13p, and Ku70p or Ku80p telomere binding. In this manner, the telosome composition can be monitored throughout the cell cycle. As a control for all the proposed experiments here, the *est2-up34* strain will be used because in this background, the expected increase in Rap1p bound to telomeres is seen (Ji et al., 2008). Rap1p also interacts with the Sir1-4 proteins (Taddei, Schober and Gasser, 2010). It is possible the levels of the Sir proteins are changed at *est2-LT^{E76K}* synthesized telomeres because there is a decreased amount of associated Rap1p molecules despite the

increase in telomere length. The amount of Sir1-4 proteins present can be assayed by conducting sequential ChIP using the DNA bound by Rap1p as the input.

Over-expression of either Rif1p or Rif2p leads to telomere shortening (Wotton and Shore, 1997). The Zakian lab has published a recent paper showing that as levels of Rif2p decrease, the affinity of Tel1p for shorter telomeres increases (McGee et al., 2010), suggesting that Rif2p is a sensing mechanism for Tel1p to aid in the recruitment of telomerase to the shorter telomeres. The *est2-LT*^{E76K} telomere length phenotype is dependent upon the presence of Tel1p, but *est2-LT*^{E76K} synthesized telomeres become synergistically longer when Rif2p or Rif1p is deleted. Therefore, it is possible that there is a decreased amount of Rif2p present at telomeres in the *est2-LT*^{E76K} background as compared to wild-type that may be detected by ChIP.

If protein levels by ChIP of Cdc13p are different in the *est2-LT*^{E76K} background as compared to wild-type, then immunoprecipitation for Stn1 and Ten1, using the Cdc13p ChIP DNA as the input, would need to be done because the CST complex is thought to play a similar role on the single stranded DNA as RPA (Bianchi, Negrini and Shore, 2004). ChIP analysis on the yKu heterodimer is also important as loss of yKu results in an increased amount of Cdc13p at the telomere, presumably due to the long ssDNA overhangs in a *yku*Δ background (Fisher, Taggart and Zakian, 2004). Because the *est2-LT*^{E76K} long telomere length phenotype is not yKu dependent (Ji et al., 2008), the levels of yKu at the telomere by ChIP should be the same for the *EST2* and *est2-LT*^{E76K} backgrounds. Also, there is no evidence of increased single-strandedness.

Potential alteration to the single stranded overhang

Dr. Ji already looked at the single stranded portion of bulk telomeres in a native gel and saw no evidence of long ssDNA (using a probe for G-rich ssDNA) by *est2-LT*^{E76K} telomerase (Ji et al., 2005). However, subtle changes to the 3' over-hang may not be detectible by native gel electrophoresis. If the *est2-LT*^{E76K} mutant does cause some defects in end-protection, then it might be synthetically lethal with a mutation that affects the single-stranded nature of the telomere. To test for synthethic lethality, growth assays on solid medium at 23°C, 25°C, 28°C, 30°C, 33°C and 37°C would be conducted. The mutants that would be included, alone and as double mutants with *est2-LT*^{E76K}, are *cdc13-1*^{ts}, *mre11-D56N* and *mre11-H125N*. The *cdc13-1*^{ts} allele results in loss of the CA-rich strand at the non-permissive temperature and a *RAD9* dependent cell cycle arrest (Garvik, Carson and Hartwell, 1995). The *mre11-D56N* and *mre11-H125N* would serve as negative controls for these experiments as they represent nuclease deficient *MRE11* (Moreau, Ferguson and Symington, 1999).

The above experiment stems from an idea that *est2-LT*^{E76K} telomerase could be indirectly affecting nucleolytic digestion, and goes as follows. The alignment restrictions by *est2-LT*^{E76K} telomerase contribute to the altered telomere sequences (Bairley et al., 2011). Decreased Rap1p molecules at *est2-LT*^{E76K} synthesized telomeres, due to the altered telomere sequences, shows that the *est2-LT*^{E76K} long-telomere phenotype is Rap1p dependent (Ji et al., 2008). The decrease in the expected Rap1p molecules, as a function of telomere length, could also mean there is a decrease in Rif2p and/or Rif1p at telomeres. Experiments have already been mentioned to test Rif2p and Rif1p abundance. One of the reported functions of the Rif proteins is to inhibit the MRX complex from

gaining access to telomere ends for nucleolytic processing (Bonetti et al., 2010). If the Rif2p and/or Rif1p levels are also decreased at *est2-LT*^{E76K} synthesized telomeres, there could be a slight increase in MRX action and subsequently, longer overhangs for telomerase to act upon. While this model is speculative at best, the experiments assaying synthetic lethality as well as the abundance of the Rif proteins are a good start in testing my theory.

CONCLUSIONS

The yeast TEN domain is a regulator of processivity, RNA/DNA alignments and anchor-site DNA binding. My data suggest that some or all of these functions could be related (Bairley et al., 2011). We know that the yeast TEN domain binds directly to Est3p (Talley et al., 2011) and that it also binds DNA (Bairley et al., 2011; Lue, 2005). The E76K mutation appears to increase the strength of the DNA interaction and may thereby influence processivity and primer/template alignment (although our evidence for an effect is still correlative). Whether the long-telomere phenotype generated by *est2-LT*^{E76K} is directly related to either of these basic functions (or perhaps represents a third function in Rap1 recruitment to the telomere) is unknown.

Functional telomerase in humans is responsible for the immortalization of approximately 85% of all cancers and telomerase deficiency is associated with accelerated aging illustrated by inherited conditions like dyskeratosis congenita (Aubert and Lansdorp, 2008; Stern and Bryan, 2008; Vulliamy and Dokal, 2008). Structural modeling of human TERT suggests that the TEN domain plays an important role in

advancing the RNA/DNA heteroduplex for subsequent rounds of telomere elongation (Steczkiewicz et al., 2011). As such, function of the TEN domain could be a potential therapeutic target. Understanding how the TEN domain contributes to telomerase activity, as a whole, is therefore important for the advancement of the field. Although my published manuscript has added mechanistic information on the consequences of the *est2-LT*^{E76K} mutation (see Chapter II), there are numerous projects, discussed in Chapter III that would add a substantial body of knowledge to the field. Given that the consequences of over-elongated telomeres are an avenue of telomere biology that is not well-studied, experimental potential is significant.

CHAPTER IV

REFERENCES

Abreu, E., E. Aritonovska, P. Reichenbach, G. Cristofari, B. Culp, R.M. Terns, J. Lingner, and M.P. Terns. "TIN2-tethered TPP1 recruits human telomerase to telomeres in vivo." Mol Cell Biol 30.12 (2010): 2971-82.

Allisopp, R.C., G.B. Morin, J.W. Horner, R. DePhino, C.B. Harley, and I.L. Weissman. "Letter to the Editor: Effect of TERT over-expression on the long-term transplantation capacity of hematopoietic stem cells." Nat Med 9.4 (2003): 369-71.

Armstrong, L., G. Saretzki, H. Peters, I. Wappler, J. Evans, N. Hole, T. von Zglinicki, and M. Lako. "Overexpression of telomerase confers growth advantage, stress resistance, and enhanced differentiation of ESCs toward the hematopoietic lineage." Stem Cells 23.4 (2005): 516-29.

Arnerić, M., and J. Lingner. "Tel1 kinase and subtelomere-bound Tbf1 mediate preferential elongation of short telomeres by telomerase in yeast." Embo J 8.11 (2007): 1080-85.

Askree, S.H., T. Yehuda, S. Smolikov, R. Gurevich, J. Hawk, C. Coker, A. Krauskopf, M. Kupiec, and M.J. McEachern. "A genome-wide screen for Saccharomyces cerevisiae deletion mutants that affect telomere length." Proc Natl Acad Sci U S A 101.23 (2004): 8658-63.

Aubert, G., and P.M. Lansdorp. "Telomeres and aging." Physiol Rev 88 (2008): 557-79.

Autexier, C., and N.F. Lue. "The structure and function of telomerase reverse transcriptase." Annu Rev Biochem 75 (2006): 493-517.

Bairley, R.C.B., G. Guillaume, L.R. Vega, and K.L. Friedman. "A mutation in the catalytic subunit of yeast telomerase alters primer/template alignment while promoting processivity and protein/DNA binding." J Cell Sci in press (2011).

Banerjee, S., S. Smith, J.H. Oum, H.J. Liaw, J.Y. Hwang, N. Sikdar, A. Motegi, S.E. Lee, and K. Myung. "Mph1p promotes gross chromosomal rearrangement through partial inhibition of homologous recombination." J Cell Biol 181.7 (2008): 1083-93.

Batista, L.F., M.F. Pech, F.L. Zhong, H.N. Nguyen, K.T. Xie, A.J. Zaug, S.M. Crary, J. Choi, V. Sebastiano, A. Cherry*, et al.* "Telomere shortening and loss of self-renewal in dyskeratosis congenita induced pluripotent stem cells." Nature 474.7351 (2011): 399-402.

Ben-Aroya, S., A. Koren, B. Liefshitz, R. Steinlauf, and M. Kupiec. "ELG1, a yeast gene required for genome stability, forms a complex related to replication factor C." Proc Natl Acad Sci U S A 100 (2003): 9906-11.

Bianchi, A., and D. Shore. "Early replication of short telomeres in budding yeast." Cell 128.6 (2007): 1051-62.

Bonetti, D., M. Clerici, S. Anbalagan, M. Martina, G. Lucchini, and M.P. Longhese. "Shelterin-like proteins and Yku inhibit nucleolytic processing of Saccharomyces cerevisiae telomeres." PLoS Genet 6.5 (2010): E pub. ahead of print.

Bosoy, D., and N.F. Lue. "Yeast telomerase is capable of limited repeat addition processivity." Nucleic Acids Res 32.1 (2004): 93-101.

Boulé, J.B., L.R. Vega, and V.A. Zakian. "The yeast Pif1p helicase removes telomerase from telomeric DNA." Nature 438.7064 (2005): 57-61.

Bryan, T.M., K.J. Goodrich, and T.R. Cech. "Telomerase RNA bound by protein motifs specific to telomerase reverse transcriptase." Mol Cell 6.2 (2000): 493-99.

Budd, M.E., C.C. Reis, S. Smith, K. Myung, and J.L. Campbell. "Evidence suggesting that Pif1 helicase functions in DNA replication with the Dna2 helicase/nuclease and DNA polymerase delta." Mol Cell Biol 26.7 (2006): 2490-500.

Chan, A., J.B. Boulé, and V.A. Zakian. "Two pathways recruit telomerase to Saccharomyces cerevisiae telomeres." PLoS One 4.10 (2008): 1-11.

Chan, S.R., and E.H. Blackburn. "Telomeres and telomerase." Philos Trans R Soc Lond B Biol Sci 359.1441 (2004): 109-21.

Chandra, A., T.R. Hughes, C.I. Nugent, and V. Lundblad. "Cdc13 both positively and negatively regulates telomere replication." Genes Dev 15.4 (2001): 404-14.

Chang, M., M. Arnerić, and J. Lingner. "Telomerase repeat addition processivity is increased at critically short telomeres in a Tel1-dependent manner in Saccharomyces cerevisiae." Genes Dev 21 (2007): 2485-94.

Chang, M., J.C. Dittmar, and R. Rothstein. "Long telomeres are preferentially extended during recombination-mediated telomere maintenance." Nat Struct Mol Biol 18.4 (2011): 451-57.

Chappell, A.S., and V. Lundblad. "Structural Elements Required for Association of the Saccharomyces cerevisiae Telomerase RNA with the Est2 Reverse Transcriptase." Mol Cell Biol 24.17 (2004): 7720-36.

Chen, J.L., and C.W. Greider. "Determinants in mammalian telomerase RNA that mediate enzyme processivity and cross-species incompatibility." Embo J 22.2 (2003): 304-14.

Cherry, J.M., C. Ball, S. Weng, G. Juvik, R. Schmidt, C. Adler, B. Dunn, S. Dwight, L. Riles, R.K. Mortimer*, et al.* "Genetic and physical maps of Saccharomyces cerevisiae.". 1997. Saccharomyces Genome Database. July 26, 2011. <http://www.yeastgenome.org/cgi-bin/protein/proteinPage.pl?dbid=S000002379>.

Cohn, M., and E.H. Blackburn. "Telomerase in yeast." Science 269 (1995): 396-400.

de Lange, T. "Shelterin: the protein complex that shapes and safeguards human telomeres." Genes Dev 19.18 (2005): 2100-10.

---. "How telomeres solve the end-protection problem." Science 326 (2009): 948-52.

de Lange, T., E.H. Blackburn, and V. Lundblad, eds. Telomeres. 2nd ed. Cold Spring Harbor, NY: Cold Spring Harbor Laboratory Press, 2006.

DeZwaan, D.C., O.A. Toogun, F.J. Echtenkamp, and B.C. Freeman. "The Hsp82 molecular chaperone promotes a switch between unextendable and extendable telomere states." Nat Struct Mol Biol 16.7 (2009): 711-16.

DeZwann, D.C., and B.C. Freeman. "The conserved Est1 protein stimulates telomerase DNA extension activity." Proc Natl Acad Sci U S A 106.41 (2009): 17337-42.

Diede, S.J., and D.E. Gottschling. "Exonuclease activity is required for sequence addition and Cdc13p loading at a de novo telomere." Curr Biol 11.17 (2001): 1336-40.

Dionne, I., and R.J. Wellinger. "Cell cycle-regulated generation of single-stranded G-rich DNA in the absence of telomerase." ProcNatlAcadSciUSA 93 (1996): 13902-07.

Eugster, A., C. Lanzuolo, M. Bonneton, P. Luciano, A. Pollice, J.F. Pulitzer, E. Stegberg, A.S. Berthiau, K. Forstemann, Y. Corda*, et al.* "The finger subdomain of yeast telomerase cooperates with Pif1p to limit telomere elongation." Nat Struct Mol Biol 13.8 (2006): 734-39.

Evans, S.K., and V. Lundblad. "Est1 and Cdc13 as comediators of telomerase access." Science 286.5437 (1999): 117-20.

Faure, V., S. Coulon, J. Hardy, and V. Géli. "Cdc13 and telomerase bind through different mechanisms at the lagging- and leading-strand telomeres." Mol Cell 38 (2010): 842-52.

Finger, S.N., and T.M. Bryan. "Multiple DNA-binding sites in Tetrahymena telomerase." Nucleic Acids Res 36.4 (2008): 1260-72.

Fisher, T.S., A.K. Taggart, and V.A. Zakian. "Cell cycle-dependent regulation of yeast telomerase by Ku." Nat Struct Mol Biol 11.12 (2004): 1198-205.

Fisher, T.S., and V.A. Zakian. "Ku: a multifunctional protein involved in telomere maintenance." DNA Repair (Amst) 504 (2005): 1-12.

Fitzgerald, M.S., K. Riha, F. Gao, S. Ren, T.D. McKnight, and D.E. Shippen. "Disruption of the telomerase catalytic subunit gene from Arabidopsis inactivates telomerase and leads to a slow loss of telomeric DNA." Proc Natl Acad Sci U S A 96.26 (1999): 14813-8.

Förstemann, K., M. Hoss, and J. Lingner. "Telomerase-dependent repeat divergence at the 3' ends of yeast telomeres." Nucleic Acids Res 28.14 (2000): 2690-94.

Förstemann, K., and J. Lingner. "Molecular basis for telomere repeat divergence in budding yeast." Mol Cell Biol 21.21 (2001): 7277-86.

---. "Telomerase limits the extent of base pairing between template RNA and telomeric DNA." Embo J 6.4 (2005): 361-66.

Förstemann, K., A.J. Zaug, T.R. Cech, and J. Lingner. "Yeast telomerase is specialized for C/A-rich RNA templates." Nucleic Acids Res 31 (2003): 1646-55.

Friedman, K.L., and T.R. Cech. "Essential functions of N-terminal domains in the yeast telomerase catalytic subunit revealed by selection for viable mutants." Genes Dev 13 (1999): 2863-74.

Friedman, K.L., J.J. Heit, D. Long, and T.R. Cech. "N-terminal domain of yeast telomerase reverse transcriptase: recruitment of Est3p to the telomerase complex." Mol Biol Cell 14 (2003): 1-13.

Gallardo, F., C. Olivier, A.T. Dandjinou, R.J. Wellinger, and P. Chartrand. "TLC1 RNA nucleo-cytoplasmic trafficking links telomerase biogenesis to its recruitment to telomeres." Embo J 27.5 (2008): 748-57.

Gao, H., T.B. Toro, M. Paschini, B. Braunstein-Ballew, R.B. Cervantes, and V. Lundblad. "Telomerase recruitment in Saccharomyces cerevisiae is not dependent on Tel1-mediated phosphorylation of Cdc13." Genetics 186.4 (2010): 1147-59.

Garber, P.M., G.M. Vidanes, and D.P. Toczyski. "Damage in Transition." Trends Biochem Sci 30.2 (2005): 63-66.

Garvik, B., M. Carson, and L. Hartwell. "Single-stranded DNA arising at telomeres in *cdc13* mutants may constitute a specific signal for the *RAD9* checkpoint." Mol Cell Biol 15 (1995): 6128-38.

Ghosal, G., and K. Muniyappa. "The characterization of Saccharomyces cerevisiae Mre11/Rad50/Xrs2 complex reveals that Rad50 negatively regulates Mre11 endonucleolytic but not the exonucleolytic activity." J Mol Biol 372.4 (2007): 864-82.

Gilley, D., M.S. Lee, and E.H. Blackburn. "Altering specific telomerase RNA template residues affects active site function." Genes Dev 9.18 (1995): 2214-26.

Gillis, A.J., A.P. Schuller, and E. Skordalakes. "Structure of the Tribolium castaneum telomerase catalytic subunit TERT." Nature 455.7213 (2008): 633-37.

Gottschling, D.E., and V.A. Zakian. "Telomere proteins: specific recognition and protection of the natural termini of Oxytricha macronuclear DNA." Cell 47.2 (1986): 1985-205.

Goudsouzian, L.K., C.T. Tuzon, and V.A. Zakian. "S. cerevisiae Tel1p and Mre11p are required for normal levels of Est1p and Est2p telomere association." Mol Cell 24.4 (2006): 603-10.

Grandin, N., C. Damon, and M. Charbonneau. "Ten1 functions in telomere end protection and length regulation in association with Stn1 and Cdc13." Embo J 20.5 (2001): 1173-83.

Grandin, N., S.I. Reed, and M. Charbonneau. "Stn1, a new Saccharomyces cerevisiae protein, is implicated in telomere size regulation in association with Cdc13." Genes Dev 11 (1997): 512-27.

Gravel, S., M. Larrivee, P. Labrecque, and R.J. Wellinger. "Yeast Ku as a regulator of chromosomal DNA end structure." Science 280.5364 (1998): 741-4.

Greider, C.W. "Telomerase is processive." Mol Cell Biol 11.9 (1991): 4572-80.

Greider, C.W., and E.H. Blackburn. "Identification of a specific telomere terminal transferase activity in *Tetrahymena* extracts." Cell 43 (1985): 405-13.

---. "The telomere terminal transferase of *Tetrahymena* is a ribonucleoprotein enzyme with two kinds of primer specificity." Cell 51 (1987): 887-98.

---. "A telomeric sequence in the RNA of *Tetrahymena* telomerase required for telomere repeat synthesis." Nature 337 (1989): 331-37.

Hammond, P.W., T.N. Lively, and T.R. Cech. "The anchor site of telomerase from *Euplotes aediculatus* revealed by photo-cross-linking to single- and double-stranded DNA primers." Mol Cell Biol 17 (1997): 296-308.

Hardy, C.F.J., L. Sussel, and D. Shore. "A *RAP1*-interacting protein involved in transcriptional silencing and telomere length regulation." Genes Dev 6 (1992): 801-14.

Hector, R.E., R.L. Shtofman, A. Ray, B.R. Chen, T. Nyun, K.L. Berkner, and K.W. Runge. "Tel1p preferentially associates with short telomeres to stimulate their elongation." Mol Cell 27.5 (2007): 851-58.

Hirano, Y., K. Fukunaga, and K. Sugimoto. "Rif1 and rif2 inhibit localization of tel1 to DNA ends." Mol Cell 33.3 (2009): 312-22.

Hirano, Y., and K. Sugimoto. "Cdc13 Telomere Capping Decreases Mec1 Association but Does Not Affect Tel1 Association with DNA Ends." Mol Biol Cell 18.6 (2007): 2026-36.

Horvath, M.P., and S.C. Schultz. "DNA G-quartets in a 1.86 A resolution structure of an Oxytricha nova telomeric protein-DNA complex." J Mol Biol 310.2 (2001): 367-77.

Horvath, M.P., V.L. Schweiker, J.M. Bevilacqua, J.A. Ruggles, and S.C. Schultz. "Crystal structure of the *Oxytricha nova* telomere end binding protein complexed with single strand DNA." Cell 95.7 (1998): 963-74.

Hossain, S., S. Singh, and N.F. Lue. "Functional analysis of the C-terminal extension of telomerase reverse transcriptase. A putative "thumb" domain." J Biol Chem 277.39 (2002): 36174-80.

Hug, N., and J. Lingner. "Telomere length homeostasis." Chromosoma 115 (2006): 413-25.

Hughes, T.R., S.K. Evans, R.G. Weilbaecher, and V. Lundblad. "The Est3 protein is a subunit of yeast telomerase." Curr Biol 10.13 (2000a): 809-12.

Hughes, T.R., R.G. Weilbaecher, M. Walterscheid, and V. Lundblad. "Identification of the single-strand telomeric DNA binding domain of the Saccharomyces cerevisiae Cdc13 protein." Proc Natl Acad Sci U S A 97.12 (2000b): 6457-62.

Jacobs, S.A., E.R. Podell, and T.R. Cech. "Crystal structure of the essential N-terminal domain of telomerase reverse transcriptase." Nat Struct Mol Biol 13.3 (2006): 218-25.

Jacobs, S.A., E.R. Podell, D.S. Wuttke, and T.R. Cech. "Soluble domains of telomerase reverse transcriptase identified by high-throughput screening." Protein Sci 14.8 (2005): 2051-8.

Ji, H., C.J. Adkins, B.R. Carthwright, and K.L. Friedman. "Yeast Est2p affects telomere length by influencing association of Rap1p with telomeric chromatin." Mol Cell Biol 28 (2008): 2380-90.

Ji, H., M.H. Platts, L.M. Dharamsi, and K.L. Friedman. "Regulation of telomere length by an N-terminal region of the yeast telomerase reverse transcriptase." Mol Cell Biol 25.20 (2005): 9103-14.

Jurczyluk, J., A.S. Nouwens, J.K. Holien, T.E. Adams, G.O. Lovrecz, M.W. Parker, S.B. Cohen, and T.M. Bryan. "Direct involvement of the TEN domain at the active site of human telomerase." Nucleic Acids Res 39.5 (2010): 1774-88.

Kiss, T. "Small Nucleolar RNAs: An Abundant Group of Noncoding RNAs with Diverse Cellular Functions." Cell 109.2 (2002): 145-48.

Kostriken, R., J.N. Strathern, A.J. Klar, J.B. Hicks, and F. Heffron. "A site-specific endonuclease essential for mating-type switching in Saccharomyces cerevisiae." Cell 35 (1983): 167-74.

Kramer, K.M., and J.E. Haber. "New telomeres in yeast are initiated with a highly selected subset of TG1-3 repeats." Genes Dev 7 (1993): 2345-56.

Kuchin, S., P. Yeghiayan, and M. Carlson. "Cyclin-dependent protein kinase and cyclin homologs SSN3 and SSN8 contribute to transcriptional control in yeast. ." Proc Natl Acad Sci U S A 92 (1995): 4006-10.

Lahaye, A., H. Stahl, D. Thines-Sempoux, and F. Foury. "PIF1: a DNA helicase in yeast mitrochondria." Embo J 10 (1991): 997-1007.

Landt, O., H.P. Grunert, and U. Hahn. "A general method for rapid site-directed mutagenesis using the polymerase chain reaction." Gene 96.1 (1990): 125-28.

Larose, S., N. Laterreur, G. Ghazal, J. Gagnon, R.J. Wellinger, and S.A. Elela. "RNase III-dependent regulation of yeast telomerase." J Biol Chem 282.7 (2007): 4373-81.

Larrivée, M., C. LeBel, and R.J. Wellinger. "The generation of proper constitutive G-tails on yeast telomeres is dependent on the MRX complex." Genes Dev 18.12 (2004): 1391-6.

Latrick, C.M., and T.R. Cech. "POT1-TPP1 enhances telomerase processivity by slowing primer dissociation and aiding translocation." Embo J 29.5 (2010): 924-33.

Lee, J., E.K. Mandell, T. Rao, D.S. Wuttke, and V. Lundblad. "Investigating the role of the Est3 protein in yeast telomere replication." Nucleic Acids Res 38.7 (2010): 2279-90.

Lee, J., E.K. Mandell, T.M. Tucey, D.K. Morris, and V. Lundblad. "The Est3 protein associates with yeast telomerase through an OB-fold domain." Nat Struct Mol Biol 15.9 (2008): 990-97.

Lee, M.S., and E.H. Blackburn. "Sequence-specific DNA primer effects on telomerase polymerization activity." Mol Cell Biol 13 (1993): 6586-99.

Lendvay, T.S., D.K. Morris, J. Sah, B. Balasubramanian, and V. Lundblad. "Senescence mutants of *Saccharomyces cerevisiae* with a defect in telomere replication identify three additional *EST* genes." Genetics 144 (1996): 1399-412.

Li, S., S. Makovets, T. Matsuguchi, J.D. Blethrow, K.M. Shokat, and E.H. Blackburn. "Cdk1-dependent phosphorylation of Cdc13 coordinates telomere elongation during cell-cycle progression." Cell 136.1 (2009): 50-61.

Lian, H.Y., E.D. Robertson, S. Hiraga, G.M. Alvino, D. Collingwood, H.J. McCune, A. Sridhar, B.J. Brewer, M.K. Raghuraman, and A.D. Donaldson. "The effect of Ku on

telomere replication time is mediated by telomere length but is independent of histone tail acetylation." Mol Biol Cell 22.10 (2011): 1753-65.

Lin, J.-J., and V.A. Zakian. "The *Saccharomyces CDC13* protein is a single-strand TG_{1-3} telomeric DNA-binding protein *in vitro* that affects telomere behavior *in vivo*." Proc Natl Acad Sci USA 93 (1996): 13760--65.

Lingner, J., and T.R. Cech. "Purification of telomerase from *Euplotes aediculatus*: Requirement of a primer 3' overhang." Proc Natl Acad Sci USA 93 (1996): 10712-17.

Lingner, J., T.R. Cech, T.R. Hughes, and V. Lundblad. "Three Ever Shorter Telomere (*EST*) genes are dispensable for *in vitro* yeast telomerase activity." Proc Natl Acad Sci USA 94.21 (1997a): 11190-95.

Lingner, J., T.R. Hughes, A. Shevchenko, M. Mann, V. Lundblad, and T.R. Cech. "Reverse transcriptase motifs in the catalytic subunit of telomerase." Science 276.5312 (1997b): 561-67.

Liu, C., X. Mao, and A.J. Lustig. "Mutational analysis defines a C-terminal tail domain of RAP1 essential for telomeric silencing in Saccharomyces cerevisiae." Genetics 138 (1994): 1025-40.

Livengood, A.J., A.J. Zaug, and T.R. Cech. "Essential regions of *Saccharomyces cerevisiae* telomerase RNA: Separate elements for Est1p and Est2p interaction." Mol Cell Biol 22.7 (2002): 2366-74.

Lue, N.F. "Adding to the ends: what makes telomerase processive and how important is it?" Bioessays 26.9 (2004): 955-62.

---. "A physical and functional constituent of telomerase anchor site." J Biol Chem 280.28 (2005): 26586-91.

Lue, N.F., and Z. Li. "Modeling and structure function analysis of the putative anchor site of yeast telomerase." Nucleic Acids Res 35.15 (2007): 5213-22.

Lue, N.F., Y.C. Lin, and I.S. Mian. "A conserved telomerase motif within the catalytic domain of telomerase reverse transcriptase is specifically required for repeat addition processivity." Mol Cell Biol 23.23 (2003): 8440-49.

Lundblad, V., and J.W. Szostak. "A mutant with a defect in telomere elongation leads to senescence in yeast." Cell 57.4 (1989): 633-43.

Malyavko, A.G., N.A. Logvina, M.E. Zvereva, and O.A. Dontsova. "In vitro dimerization of telomerase protein Est3p is stimulated by magnesium cations." Dokl Biochem Biophys 433 (2010): 152-54.

Mangahas, J.L., M.K. Alexander, L.L. Sandell, and V.A. Zakian. "Repair of chromosome ends after telomere loss in Saccharomyces." Mol Biol Cell 12.12 (2001): 4078-89.

Marcand, S., V. Brevet, and E. Gilson. "Progressive *cis*-inhibition of telomerase upon telomere elongation." Embo J 18.12 (1999): 3509-19.

Marcand, S., V. Brevet, C. Mann, and E. Gilson. "Cell cycle restriction of telomere elongation." Curr Biol 10.8 (2000): 487-90.

Marcand, S., E. Gilson, and D. Shore. "A protein-counting mechanism for telomere length regulation in yeast." Science 275 (1997): 986-90.

McCarroll, R.M., and W.L. Fangman. "Time of replication of yeast centromeres and telomeres." Cell 54 (1988): 505-13.

McClintock, B. "The Stability of Broken Ends of Chromosomes in Zea Mays." Genetics 26.2 (1941): 234-82.

McElligott, R., and R.J. Wellinger. "The terminal DNA structure of mammalian chromosome." Embo J 16.12 (1997): 3705-14.

McGee, J.S., J.A. Phillips, A. Chan, M. Sabourin, P. K., and V.A. Zakian. "Reduced Rif2 and lack of Mec1 target short telomeres for elongation rather than double-strand break repair." Nat Struct Mol Biol 17.12 (2010): 1438-45.

Mitchell, M., A. Gillis, M. Futahashi, H. Fujiwara, and E. Skordalakes. "Structural basis for telomerase catalytic subunit TERT binding to RNA template and telomeric DNA." Nat Struct Mol Biol 17.4 (2010): 513-18.

Mitton-Fry, R.M., E.M. Anderson, T.R. Hughes, V. Lundblad, and D.S. Wuttke. "Conserved structure for single-stranded telomeric DNA recognition." Science 296.5565 (2002): 145-47.

Moreau, S., J.R. Ferguson, and L.S. Symington. "The nuclease activity of mre11 is required for meiosis but not for mating type switching, end joining, or telomere maintenance." Mol Cell Biol 19.1 (1999): 556-66.

Moriarty, T.J., R.J. Ward, M.A. Taboski, and C. Autexier. "An anchor site-type defect in human telomerase that disrupts telomere length maintenance and cellular immortalization." Mol Biol Cell 16.7 (2005): 3152-61.

Morin, G.B. "The human telomere terminal transferase enzyme is a ribonucleoprotein that synthesizes TTAGGG repeats." Cell 59 (1989): 521-29.

Morris, D.K., and V. Lundblad. "Programmed translational frameshifting in a gene required for yeast telomere replication." Curr Biol 7.12 (1997): 969-76.

Mozdy, A.D., and T.R. Cech. "Low abundance of telomerase in yeast: implications for telomerase haploinsufficiency." Rna 12.9 (2006): 1721-37.

Mozdy, A.D., E.R. Podell, and T.R. Cech. "Multiple yeast genes, including Paf1 complex genes, affect telomere length via telomerase RNA abundance." Mol Cell Biol 28.12 (2008): 4152-61.

Nakada, D., T. Shimomura, K. Matsumoto, and K. Sugimoto. "The ATM-related Tel1 protein of Saccharomyces cerevisiae controls a checkpoint response following phleomycin treatment." Nucleic Acids Res 31 (2003): 1715-24.

Nakamura, T.M., G.B. Morin, K.B. Chapman, S.L. Weinrich, W.H. Andrews, J. Lingner, C.B. Harley, and T.R. Cech. "Telomerase catalytic subunit homologs from fission yeast and human." Science 277.5328 (1997): 955-59.

Negrini, S., V. Ribaud, A. Bianchi, and D. Shore. "DNA breaks are masked by multiple Rap1 binding in yeast: implications for telomere capping and telomerase regulation." Genes Dev 21.3 (2007): 292-302.

Nugent, C.I., T.R. Hughes, N.F. Lue, and V. Lundblad. "Cdc13p: A single-strand telomeric DNA binding protein with a dual role in yeast telomere maintenance." Science 274 (1996): 249-52.

O'Connor, C.M., C.K. Lai, and K. Collins. "Telomerase RNA mutations in Saccharomyces cerevisae alter telomerase action and reveal nonprocessivity in vivo and in vitro." Genes Dev 11 (2005): 528-40.

Orr-Weaver, T.L., J.W. Szostak, and R.J. Rothenstein. "Yeast transformation: a model system for the study of recombination." Proc Natl Acad Sci U S A 78.10 (1981): 6354-58.

Osterhage, J.L., J.M. Talley, and K.L. Friedman. "Proteasome-dependent dergradation of Est1p regulates the cell cycle restricted assembly of telomerase in *Saccharomyces cerevisiae*." Nat Struct Mol Biol (2006).

Palm, W., and T. de Lange. "How sheltrine protects mammalian telomeres." Annu Rev Genet 42 (2008): 301-34.

Parenteau, J., and R.J. Wellinger. "Accumulation of single-stranded DNA and destabilization of telomeric repeats in yeast mutant strains carrying a deletion of RAD27." Mol Cell Biol 19.6 (1999): 4143-52.

---. "Differential processing of leading- and lagging-strand ends at Saccharomyces cerevisiae telomeres revealed by the absence of Rad27p nuclease." Genetics 162.4 (2002): 1583-94.

Pennock, E., K. Buckley, and V. Lundblad. "Cdc13 delivers separate complexes to the telomere for end protection and replication." Cell 104.3 (2001): 387-96.

Peterson, S.E., A.E. Stellwagen, S.J. Diede, M.S. Singer, Z.W. Haimberger, C.O. Johnson, M. Tzoneva, and D.E. Gottschling. "The function of a stem-loop in telomerase RNA is linked to the DNA repair protein Ku." Nat Genet 27.1 (2001): 64-7.

Petreaca, R.C., H.C. Chiu, H.A. Eckelhoefer, C. Chuang, L. Xu, and C.I. Nugent. "Chromosome end protection plasticity revealed by Stn1p and Ten1p bypass of Cdc13p." Nat Cell Biol 8.7 (2006): 748-55.

Prescott, J., and E.H. Blackburn. "Functionally interacting telomerase RNAs in the yeast telomerase complex." Genes Dev 11.21 (1997a): 2790-800.

---. "Telomerase RNA mutations in *Saccharomyces cerevisiae* alter telomerase action and reveal nonprocessivity *in vivo* and *in vitro*." Genes Dev 11.4 (1997b): 528-40.

Price, C.M. "Telomere structure in Euplotes crassus: characterization of DNA-protein interactions and isolation of a telomere-binding protein." Mol Cell Biol 10.7 (1990): 3421-31.

Price, C.M., K.A. Boltz, M.F. Chaiken, J.A. Stewart, M.A. Beilstein, and D.E. Shippen. "Evolution of CST function in telomere maintenance." Cell Cycle 9.16 (2010): 3157-65.

Qiao, F., and T.R. Cech. "Triple-helix structure in telomerase RNA contributes to catalysis." Nat Struct Mol Biol 15.6 (2008): 634-40.

Romi, E., N. Baran, M. Gantman, M. Shmoish, B. Min, K. Collins, and H. Manor. "High-resolution physical and functional mapping of the template adjacent DNA binding site in catalytically active telomerase." Proc Natl Acad Sci U S A 104.21 (2007): 8791-99.

Rouda, S., and E. Skordalakes. "Structure of the RNA-binding domain of telomerase: implications for RNA recognition and binding." Structure 15.11 (2007): 1403-12.

Rusche, L.N., A.L. Kirchmaier, and J. Rine. "The establishment, inheritance, and function of silenced chromatin in Saccharomyces cerevisiae." Annu Rev Biochem 72 (2003): 481-16.

Sabourin, M., C.T. Tuzon, and V.A. Zakian. "Telomerase and Tel1p preferentially associate with short telomeres in S. cerevisiae." Mol Cell 27.4 (2007): 550-61.

Schramke, V., P. Luciano, V. Brevet, S. Guillot, Y. Corda, M.P. Longhese, E. Gilson, and V. Geli. "RPA regulates telomerase action by providing Est1p access to chromosome ends." Nat Genet 36.1 (2004): 46-54.

Schulz, V.P., and V.A. Zakian. "The Saccharomyces *PIF1* DNA helicase inhibits telomere elongation and *de novo* telomere formation." Cell 76 (1994): 145-55.

Sealey, D.C.F., L. Zheng, M.A.S. Taboski, J. Cruickshank, M. Ikura, and L.A. Harrington. "The N-terminus of hTERT contains a DNA-binding domain and is required

for telomerase activity and cellular immortalization." Nucleic Acids Res 38 (2010): 2019-35.

Seto, A.G., A.J. Livengood, Y. Tzfati, E.H. Blackburn, and T.R. Cech. "A Bulged Stem Tethers Est1p to Telomerase RNA in Budding Yeast." Genes Dev 16 (2002): 2800-12.

Seto, A.G., A.J. Zaug, S.G. Sabel, S.L. Wolin, and T.R. Cech. "*Saccharomyces cerevisiae* telomerase is an Sm small nuclear ribonucleoprotein particle." Nature 401 (1999): 177-80.

Shampay, J., J.W. Szostak, and E.H. Blackburn. "DNA sequences of telomeres maintained in yeast." Nature 310.5973 (1984): 154-57.

Sharanov, Y.S., M.I. Zvereva, and O.A. Dontsova. "Saccharomyces cerevisiae telomerase subunit Est3p binds DNA and RNA and stimulates unwinding of RNA/DNA heteroduplexes." FEBS Lett 580.19 (2006): 4683-90.

Shore, D., and A. Bianchi. "Telomere length regulation: coupliing DNA end processing to feedback regulation of telomerase." Embo J Focus Review (2009): 1-14.

Sikorski, R.S., and P. Hieter. "A system of shuttle vectors and yeast host strains designed for efficient manipulation of DNA in *Saccharomyces cerevisiae*." Genetics 122.1 (1989): 19-27.

Singer, M.S., and D.E. Gottschling. "*TLC1*: Template RNA component of *Saccharomyces cerevisiae* telomerase." Science 266 (1994): 404-09.

Smolikov, S., Y. Mazor, and A. Krauskopf. "ELG1, a regulator of genome stability, has a role in telomere length regulation and in silencing." Proc Natl Acad Sci U S A 101 (2004): 1656-61.

Smolka, M.B., C.P. Albuquerque, S.H. Chen, and H. Zhou. "Proteome-wide identification of in vivo targets of DNA damage checkpoint kinases." Proc Natl Acad Sci U S A 104.25 (2007): 10364-69.

Steczkiewicz, K., M.T. Zimmermann, M. Kurcinski, B.A. Lewis, D. Dobbs, A. Kloczkowski, R.L. Jernigan, A. Lolinski, and K. Ginalski. "Human telomerase model shows the role of the TEN domain in advancing the double helix for the next polymerization step." Proc Natl Acad Sci U S A 108.23 (2011): 9443-8.

Stellwagen, A.E., Z.W. Haimberger, J.R. Veatch, and D.E. Gottschling. "Ku interacts with telomerase RNA to promote telomere addition at native and broken chromosome ends." Genes Dev 17.19 (2003): 2384-95.

Stern, J.L., and T.M. Bryan. "Telomerase recruitment to telomeres." Cytogenet Genome Res 122 (2008): 243-54.

Szostak, J.W., and E.H. Blackburn. "Cloning yeast telomeres on linear plasmid vectors." Cell 29.1 (1982): 245-55.

Taddei, A., H. Schober, and S.M. Gasser. "The budding yeast nucleus." Cold Spring Harb Perspect Biol 2.8 (2010): a000612.

Taggart, A.K.P., S.-C. Teng, and V.A. Zakian. "Est1p as a cell cycle-regulated activator of telomere-bound telomerase." Science 297.5583 (2002): 1023-26.

Talley, J.M., D.C. DeZwann, L.D. Maness, B.C. Freeman, and K.L. Friedman. "Stimulation of yeast telomerase activity by the Ever Shorter Telomeres 3 (Est3) subunit is dependent on direct interaction with the catalytic protein Est2." J Biol Chem 286.30 (2011): 26431-9.

Teixeira, M.T., K. Förstemann, S.M. Gasser, and J. Lingner. "Intracellular trafficking of yeast telomerase components." Embo J 3.7 (2002): 652-9.

Teixeira, M.T., M. Arneric, P. Sperisen, and J. Lingner. "Telomere length homeostasis is achieved via a switch between telomerase-extendible and -nonextendible states." Cell 117.3 (2004): 323-35.

Tseng, S.F., J.J. Lin, and S.C. Teng. "The telomerase-recruitment domain of the telomere binding protein Cdc13 is regulated by Mec1p/Tel1p-dependent phosphorylation." Nucleic Acids Res 34.21 (2006): 6327-36.

Tuzon, C.T., Y. Wu, A. Chan, and V.A. Zakian. "The Saccharomyces cerevisiae Telomerase Subunit Est3 Binds Telomeres in a Cell Cycle- and Est1-Dependent Manner and Interacts Directly with Est1 In Vitro." PLoS One 7.5 (2011): e1002060.

Vega, L.R., J.A. Phillips, B.R. Thornton, J.A. Benanti, M.T. Onigbanjo, D.P. Toczyski, and V.A. Zakian. "Sensitivity of yeast strains with long G-tails to levels of telomere-bound telomerase." PLoS One 3.6 (2007): e105.

Vodenicharov, M.D., and R.J. Wellinger. "DNA degradation at unprotected telomeres in yeast is regulated by the CDK1 (Cdc28/Clb) cell-cycle kinase." Mol Cell 24.1 (2006): 127-37.

Vulliamy, T., and I. Dokal. "Dyskeratosis congenita: the diverse clinical presentation of mutation in the telomerase complex." Biochimie Review (2008): 122-30.

Walmsley, R.M., and T.D. Petes. "Genetic control of chromosome length in yeast." PNAS 82 (1985): 506-10.

Wang, S.-S., and V.A. Zakian. "Telomere-telomere recombination provides an express pathway for telomere acquisition." Nature 345 (1990): 456-58.

Wellinger, R.J., K. Ethier, P. Labrecque, and V.A. Zakian. "Evidence for a new step in telomere maintenance." Cell 85 (1996): 423-33.

Wellinger, R.J., A.J. Wolf, and V.A. Zakian. "Origin activation and formation of single-strand TG1-3 tails occur sequentially in late S phase on a yeast linear plasmid." Mol Cell Biol 13.7 (1993): 4057-65.

Wotton, D., and D. Shore. "A novel Rap1p-interacting factor, Rif2p, cooperates with Rif1p to regulate telomere length in *Saccharomyces cerevisiae*." Genes Dev 11.6 (1997): 748-60.

Wright, W.E., V.M. Tesmer, K.E. Huffman, S.D. Levene, and J.W. Shay. "Normal human chromosomes have long G-rich telomeric overhangs at one end." Genes Dev 11.21 (1997): 2801-09.

Wyatt, H.D.M., D.A. Lobb, and T.L. Beattie. "Characterization of physical and functional anchor site interactions in human telomerase." Mol Cell Biol 27.8 (2007): 3226-40.

Wyatt, H.D.M., A.R. Tsang, D.A. Lobb, and T.L. Beattie. "Human telomerase reverse transcriptase (hTERT) Q169 is essential for telomerase function in vitro and in vivo." PLoS One 4 (2009): 1-15.

Xia, J., Y. Peng, I.S. Mian, and N.F. Lue. "Identification of functionally important domains in the N-terminal region of telomerase reverse transcriptase." Mol Cell Biol 20.14 (2000): 5196-207.

Xie, M., J.D. Podlevsky, X. Qi, C.J. Bley, and J.J. Chen. "A novel motif in telomerase reverse transcriptase regulates telomere repeat addition rate and processivity." Nucleic Acids Res 38.6 (2010): 1982-96.

Yang, C.P., Y.B. Chen, F.L. Meng, and J.Q. Zhou. "Saccharomyces cerevisiae Est3p dimerizes in vitro and dimerization contributes to efficient telomere replication in vivo." Nucleic Acids Res 34.2 (2006): 407-16.

Yen, W.F., L. Chico, M. Lei, and N.F. Lue. "Telomerase and Retrotransposons: Reverse Transcriptases That Shaped Genomes Sackler Special Feature: Telomerase regulatory subunit Est3 in two Candida species physically interacts with the TEN domain of TERT and telomeric DNA." Proc Natl Acad Sci U S A In press (2011).

Yu, G.L., and E.H. Blackburn. "Amplification of tandemly repeated origin control sequences confers a replication advantage on rDNA replicons in Tetrahymena thermophila." Mol Cell Biol 10.5 (1990): 2070-80.

Zappulla, D.C., K. Goodrich, and T.R. Cech. "A miniature yeast telomerase RNA functions in vivo and reconstitutes activity in vitro." Nat Struct Mol Biol 12.12 (2005): 1072-77.

Zaug, A.J., E.R. Podell, and T.R. Cech. "Mutation in TERT separates processivity from anchor-site function." Nat Struct Mol Biol 15.8 (2008): 870-72.

Zheng, L., and B. Shen. "Okazaki fragment maturation: nucleases take centre stage." Mol Cell Biol 3.1 (2011): 23-30.

Zhong, F., S.A. Savage, M. Shkreli, N. Giri, L. Jessop, T. Myers, R. Chen, B.P. Alter, and S.E. Artandi. "isruption of telomerase trafficking by TCAB1 mutation causes dyskeratosis congenita." Genes Dev 25.1 (2011): 11-16.

Zhou, J., E.K. Monson, S. Teng, V.P. Schulz, and V.A. Zakian. "Pif1p helicase, a catalytic inhibitor of telomerase in yeast." Science 289.5480 (2000): 771-74.